

DISCOVERY OF INDUSTRIALLY RELEVANT OXIDOREDUCTASES

Thesis Submitted for the Degree of

Master of Science

by

Kezia Rajan, B.Sc.

Supervised by

Dr. Ciaran Fagan

School of Biotechnology

Dublin City University

Ireland

Dr. Andrew Dowd

MBio

Monaghan

Ireland

January 2020

Declaration

I hereby certify that this material, which I now submit for assessment on the programme of study leading to the award of Master of Science, is entirely my own work, and that I have exercised reasonable care to ensure that the work is original, and does not to the best of my knowledge breach any law of copyright, and has not been taken from the work of others save and to the extent that such work has been cited and acknowledged within the text of my work.

Signed: 

Kezia Rajan

ID No.: 17212904

Date: 03rd January 2020

Acknowledgements

I would like to thank the following:

God, for sending me angels in the form of wonderful human beings over the last two years to help me with any- and everything related to my project.

Dr. Ciaran Fagan and Dr. Andrew Dowd, for guiding me and always going out of their way to help me. Thank you for your patience, your advice, and thank you for constantly believing in me. I feel extremely privileged to have gotten an opportunity to work alongside both of you. Everything I've learnt and the passion for research that this project has sparked in me, I owe it all to you both. Although I know that words will never be enough to express my gratitude, I still want to say a huge thank you from the bottom of my heart. I couldn't have come this far without the two of you.

The IRC, for funding this project and giving me a wonderful research opportunity.

MBio and all of its staff, for accommodating me and helping me with any and everything over the last two years.

Dr. Linda Holland, Graham Dodrill, David Cunningham, and Janice Cunningham, for accommodating me in your labs at DCU. Thank you for your kindness and help.

My late grandad, for always being my biggest motivator. I miss you every day and I wish you were here to see how far I've come, but, I hope I've made you proud. Thank you for your words of encouragement and sound advice. They're what got me this far.

My parents, for giving me an education. You're the reason I'm here today. Thank you for all your hard work and constant advice. Thank you for constantly encouraging me and supporting me.

My sisters, for begrudgingly listening to all my 'science talk' despite your lack of scientific interest. Thank you for keeping me sane and grounded. Thank you for partaking in my highs and lows over the last two years as if my troubles were your very own.

Navya, for going above and beyond when I couldn't go any further without a helping hand. Thank you for your time, effort, and kindness. I am indebted to you.

My best friends, for constantly checking up on me and making me forget my worries and fears.

My fiancé, for his limitless patience. Thank you for all your help with the 'fixing up'. Thank you for patiently listening to my constant moans and whines about giving up. You're godsent and I'm grateful for you every day.

Contents

Abbreviations	vii
List of Figures.....	ix
List of Tables	xiii
Abstract.....	xvi
CHAPTER 1: OXIDOREDUCTASES: OCCURRENCE, ANALYSIS, AND USES	17
1.0 Introduction.....	18
1.1 Oxidoreductases	19
1.2 Laccase	23
1.2.1 Enzyme assays for the detection of laccase	27
1.3 Catalase	30
1.3.1 Enzyme assays for the detection of catalase	32
1.4 Dehydrogenase	32
1.4.1 Enzyme assays for the detection of dehydrogenase	34
1.5 Lytic Polysaccharide Monooxygenase.....	36
1.5.1 Enzyme assays for the detection of LPMO.....	39
1.6 Applications of Oxidoreductases	44
1.7 Conclusion.....	46
1.8 Project Aims and Plans.....	47
CHAPTER 2: MATERIALS & METHODS	49
2.1 Equipment.....	50
2.2 Consumables.....	52
2.3 Reagents	53
2.4 Buffer Preparations	55
2.4.1 Preparation of 0.1 M Acetate Buffer (pH 3.6, pH 4.0, and pH 5.0).....	55
2.4.2 Preparation of 0.1 M Sodium Phosphate Buffer (pH 6.2, pH 7.0, and pH 8.0)	55
2.4.3 Preparation of 0.1 M Citrate Buffer (pH 3.0, pH 4.0, and pH 5.0)	56
2.4.4 Preparation of 0.1 M Potassium Phosphate Buffer (pH 6.0, pH 7.0, and pH 8.0)	56
2.4.5 Preparation of 0.1 M and 20 mM Potassium Phosphate Buffer (pH 6.4)	57
2.4.6 Preparation of 150 mM Potassium Phosphate Buffer, pH 7.0	57
2.5 Preparation of Reagents and Solutions	57
2.5.1 Preparation of 1 M HCl.....	57
2.5.2 Preparation of 5 M and 1 M Potassium Hydroxide.....	58
2.5.3 Preparation of 0.5 M Copper Sulphate solution.....	58
2.5.4 Preparation of 0.5 M Sulphuric Acid solution	58
2.5.5 Preparation of 4% (v/v) Antifoam SE-15.....	58
2.5.6 Preparation of 25% (v/v) Ammonium Hydroxide base	58

2.6 Culture Preparation.....	59
2.6.1 Preparation of PDA.....	59
2.6.2 Preparation of Glycerol stocks.....	59
2.6.3 Fermentation of <i>Talaromyces emersonii</i> in Shake Flasks or Fermenters.....	59
2.7 Enzyme Cocktail Clean-up.....	60
2.7.1 Concentration and Buffer Exchange.....	60
2.8 Assays.....	61
2.8.1 Bradford Assay Method for Protein Concentration.....	61
2.8.2 Laccase Assay using ABTS as the substrate.....	61
2.8.3 Laccase assay using Amplex Red as the substrate.....	62
2.8.4 Catalase Assay using the Megazyme Assay Kit.....	63
2.8.5 Sodium Dodecyl Sulphate Gel Electrophoresis (SDS-PAGE).....	65
2.9 Protein Purification.....	66
2.9.1 Preparation of 2 M Sodium Hydroxide.....	67
2.9.2 Preparation of 50 mM Sodium Phosphate/1.2 M Ammonium Sulphate, pH 7.0.....	67
2.9.3 Preparation of 50 mM Sodium Phosphate, pH 7.0.....	67
2.9.4 Sample Preparation.....	67
2.9.5 Sample Application.....	68
2.10 Proteomics Analysis.....	68
2.10.1 Sample Preparation.....	68
2.10.2 Label-free Liquid Chromatography Spectrometry.....	69
2.10.3 Protein Identification and Quantification.....	70
CHAPTER 3: RESULTS & DISCUSSION – BIOINFORMATICS ANALYSES.....	72
3.1 Organism of Choice.....	73
3.2 Bioinformatics Analysis Procedure.....	74
3.3 Discussion.....	80
CHAPTER 4: RESULTS & DISCUSSION - LACCASE.....	81
4.1 Introduction.....	82
4.2 Preliminary Results from the in-house <i>T. emersonii</i> cocktail.....	82
4.3 Preliminary Results from HIC of the in-house <i>T. emersonii</i> cocktail.....	83
4.4 Shake Flask Analyses.....	85
4.5 Induction of Laccase Activity in Shake Flasks.....	90
4.6 Scale-up of <i>T. emersonii</i> Production.....	96
4.7 Hydrophobic Interaction Chromatography of MBL191L054.....	102
4.8 Characterisation of Laccase.....	103
CHAPTER 5: RESULTS & DISCUSSION - CATALASE.....	107
5.1 Introduction.....	108

5.2 Preliminary Results from the in-house <i>T. emersonii</i> cocktail.....	109
5.3 Preliminary Results from HIC of the in-house <i>T. emersonii</i> cocktail.....	110
5.4 Shake Flask Analyses.....	111
5.5 Scale-up of <i>T. emersonii</i> Production.....	114
5.6 HIC of MBL195L01 and MBL191L053.....	117
5.7 Characterisation of Catalase.....	122
CHAPTER 6: RESULTS & DISCUSSION - PROTEOMICS ANALYSIS	130
6.1 Protein Analysis.....	131
6.2 Proteomics Analysis – Control vs. Copper Sulphate vs. Titanium Silicate	134
CHAPTER 7: DISCUSSION & CONCLUSION.....	142
7.1 Bioinformatics Analyses.....	143
7.2 Laccase.....	143
7.3 Catalase.....	145
7.4 Proteomics Analysis.....	147
7.5 Conclusion	148
8.0 References	149
9.0 Appendix.....	158

Abbreviations

AA	Auxiliary activity
ABTS	2,2'-Azino-bis (3-ethylbenzothiazoline-6-sulphonic acid)
BE	Buffer Exchange
BSA	Bovine serum albumin
CV	Column volumes
cAMP	Cyclic adenosine 3',5'-monophosphate
2,6-DCPIP	2,6-Dichlorophenol-indophenol
DHBS	3,5-Dichloro-2-hydroxybenzenesulphonate
DMP	Dimethoxyphenol
DMSO	Dimethyl sulphoxide
EPR	Electron paramagnetic resonance
FAD	Flavin adenine dinucleotide
FMN	Flavin mononucleotide
GRAS	Generally regarded as safe
H ₂ O ₂	Hydrogen peroxide
HCl	Hydrochloric acid
HIC	Hydrophobic Interaction Chromatography
HRP	Horseradish peroxidase
I.U.B.	International Union of Biochemistry
KOH	Potassium hydroxide
LDS	Lithium Dodecyl Sulphate
<LoQ	Below Limit of Quantitation
LPMO(s)	Lytic polysaccharide monoxygenase(s)
Meldola's Blue	8-Di-methylamino-2-benzophenoxazine
MWCO	Molecular weight cut-off
NAD(P) ⁺	Nicotinamide adenine dinucleotide (phosphate)
NAD(P)H	Reduced form of nicotinamide adenine dinucleotide phosphate
NBT	Nitroblue tetrazolium
NCBI	National Center for Biotechnology Information
nd	not determined
NHA	N-hydroxy-acetanilide
pBLAST	Protein Basic Local Alignment Search Tool
PDA	Potato dextrose agar
PMS	Phenazine methosulphate
PQQ	Pyrroloquinoline quinone

SD	Standard Deviation
SDS-PAGE	Sodium dodecyl sulphate polyacrylamide gel electrophoresis
SOPs	Standard Operating Procedures
TGS	Tris/Glycine/SDS
TIC	Total ion chromatogram
TiSiO ₄	Titanium silicate
UPO(s)	Unspecific peroxygenase(s)

List of Figures

Introduction

Figure 1.0. 1: A diagram summarising the six major classes of enzyme families and their functions (Karigar and Rao, 2011)..... 18

Figure 1.2. 1: An image of the three steps involved in laccase-mediated catalysis (Brijwani et al., 2010). 25

Figure 1.2. 2: A diagram summarising the different types of fungi based on their wood decay patterns (Goodell et al., 2008, pp. 9-31). 26

Figure 1.2.3: An image of the predicted structure of laccase in *Thielavia arenaria* (MW: 80 kDa) as generated using Phyre2 protein fold recognition server. Model dimensions (Å): X: 63.859, Y: 61.753, Z: 67.394. Rainbow-colour-code indicates the protein chain from blue at the N-terminus to red at the C-terminus. The sequence for multicopper oxidase was obtained from NCBI pBLAST and entered into the Phyre2 server (GenBank: ORY61466.1). 27

Figure 1.2.1. 1: A schematic representation of the reaction mechanism of the ABTS Assay (Christopher et al., 2014). 28

Figure 1.2.1. 2: A schematic representation of the reaction mechanism of the Amplex Red Assay (Wang et al., 2017a)..... 29

Figure 1.3. 1: The equation of chemical reaction depicting the decomposition of hydrogen peroxide into water and oxygen in the presence of catalase 30

Figure 1.3. 2: An image of the predicted structure of catalase in *Neurospora crassa* (MW: 82 kDa) as generated using Phyre2 protein fold recognition server. Model dimensions (Å): X: 109.210, Y: 73.056, Z: 83.151. Rainbow-colour-code indicates the protein chain from blue at the N-terminus to red at the C-terminus. The sequence for catalase was obtained from NCBI pBLAST and entered into the Phyre2 server (ID: 3872372). 31

Figure 1.4. 1: An image of the predicted structure of FAD-linked dehydrogenase enzyme in *Phanerochaete chrysosporium* (81 914 Da) as generated using Phyre2 protein fold recognition server. Model dimensions (Å): X: 62.498, Y: 63.241, Z: 68.752. Rainbow-colour-code indicates the protein chain from blue at the N-terminus to red at the C-terminus. The sequence for choline dehydrogenase was obtained from NCBI pBLAST and entered into the Phyre2 server (ID: 41989250). There is no clear biochemical evidence indicating the presence of FAD as a cofactor (Gadda and McAllister-Wilkins 2003)..... 34

Figure 1.5. 1: An image summarising the three main families of LPMOs in the auxiliary activity enzyme class (Villares et al., 2017). 38

Figure 1.5.2: An image of the predicted structure of a copper-dependent polysaccharide monooxygenase enzyme in *Aspergillus oryzae* (~23 kDa) as generated using Phyre2 protein fold recognition server. Model dimensions (Å): X: 42.279, Y: 46.686, Z: 54.700. Rainbow-colour-code indicates the protein chain from blue at the N-terminus to red at the C-terminus (ID: 30972848). 38

Figure 1.5.1. 1: Schematic representation of the PMO Activity Assay (Kittl et al., 2012)..... 40

Figure 1.5.1. 2: A diagram summarising the different assay methods currently available for the four different oxidoreductases discussed in this review..... 41

Materials & Methods

Figure 2.9.5. 1: Hydrophobic Interaction Chromatography separation showing a linear gradient 68

Results & Discussion – Bioinformatics Analyses

Figure 3.1. 1: An image of *T. emersonii* grown on PDA plate 74

Figure 3.2. 1: The workflow for the identification of oxidoreductases of interest using data obtained from Mass Spectrometry, Geneious, and pBLAST 75

Figure 3.2. 2: A snapshot of the Talem codes generated for the various proteins identified from mass spectrometry..... 76

Figure 3.2. 3: An image of the complete amino acid sequences of proteins obtained by entering the Talem codes on Geneious. The sequences highlighted in yellow refer to the peptide sequences obtained from mass spectrometry analysis. Alternatively, entering the peptide sequences obtained through mass spectrometry in Geneious could also be used to generate complete amino acid sequences of the proteins of interest. 77

Figure 3.2. 4: A snapshot of the results obtained in pBLAST that confirmed the identity of the protein as a catalase as was indicated in the mass spectrometry results. After entering the Talem code of the unknown proteins in Geneious, complete amino acid sequence of the protein was obtained. The amino acid sequence was entered on pBLAST as a query sequence in order to identify the protein. 78

Figure 3.2. 5: A snapshot of the results obtained in pBLAST that confirmed the identity of the protein as laccase as was indicated in the mass spectrometry results. After entering the Talem code of the unknown proteins in Geneious, complete amino acid sequence of the protein was obtained. The amino acid sequence was entered on pBLAST as a query sequence in order to identify the protein. 79

Results & Discussion – Laccase

Figure 4.3. 1: An image of the HIC UV profile with linear gradient [1.2 M ammonium sulphate in 50 mM sodium phosphate, pH 7.0] in for the in-house *T. emersonii* cocktail. The UV chromatogram is depicted in blue, the eluted fractions are depicted in red. The image is a screenshot from the ÄKTA Pure 25 Chromatography System software. The fractions that were selected for buffer-exchange are indicated in the figure. The fractions in which laccase activity was detected after buffer-exchange are outlined with a blue frame..... 83

Figure 4.4. 1: SDS-PAGE analysis displaying the typical profile of *T. emersonii* proteins from Shake Flask 3C fractions before and after buffer exchange. The arrow corresponds to the protein bands formed by Cellobiohydrolase isoforms (~30-42 kDa). 87

Figure 4.4. 2: Net fluorescence intensity of Shake Flask 3C Fractions (Pre- and Post- Buffer Exchange). A graph showing the difference in the net fluorescence intensity of the Shake Flask 3C fractions before and after buffer exchange at 0, 96, 120, and 144 hours. The blue and orange represent net fluorescence intensity before and after buffer exchange respectively. The net fluorescence intensity refers to the blank adjusted fluorescence intensity values. 88

Figure 4.5. 1: SDS-PAGE analysis displaying the typical profile of *T. emersonii* proteins from of Shake Flask 4A and 4D fractions. The arrows correspond to the protein bands formed by β -Glucosidase (~ 90 kDa), Cellobiohydrolase isoforms (~ 30-42 kDa), and Endoglucanase (~ 27 kDa)..... 92

Figure 4.5. 2: SDS-PAGE analysis displaying the typical profile of *T. emersonii* proteins from Shake Flask 5A and 5B fractions. Shake Flask 5 A samples were not induced with 1 mM CuSO₄. Shake Flask 5B fractions were induced with 1 mM CuSO₄ at 24 hours of culture. The arrows correspond to the protein bands formed by β -Glucosidase (~ 90 kDa), Cellobiohydrolase isoforms (~ 30-42 kDa), and Endoglucanase (~ 27 kDa). 93

Figure 4.5. 3: Net Fluorescence Intensity of Shake Flask Batches (Pre- and Post- Buffer Exchange). A graph showing the difference in the net fluorescence intensity of the Shake Flasks 4A, 4D, 5A, and 5B fractions, at 120 hours, before and after 2 X Concentration and Buffer Exchange (BE). Shake Flask 4A and 5A are the control fractions while Shake Flask 4D and 5B

contains copper sulphate. The blue and orange represent net fluorescence intensity before and after buffer exchange respectively. The net fluorescence intensity refers to the blank adjusted fluorescence intensity values..... 94

Figure 4.6. 1: SDS-PAGE analyses displaying the typical profile of *T. emersonii* proteins from MBL195L01, MBL195L03 5 L culture fractions. All fractions were control fractions except for MBL195L03 140 Hrs 1 X which was induced with 1 mM CuSO₄ at 24 hours. The approximate location of the three main glycosyl hydrolase enzymes is indicated by letters A, B, and C. A: β -Glucosidase (~90 kDa), B: Cellobiohydrolase isoforms (~ 30-42 kDa), and C: Endoglucanase (~ 27 kDa)..... 98

Figure 4.6. 2: SDS-PAGE analysis displaying the typical profile of *T. emersonii* proteins from 1 L fermenter fractions at 0, 24, and 140 hours. Copper sulphate was added at 24 hours to MBL191L052 and MBL191L054 only. The arrow corresponds to the protein bands formed by Cellobiohydrolase isoforms (~ 30-42 kDa)..... 99

Figure 4.6. 3: Net A₄₀₅ of *T. emersonii* cocktail from 5 L and 1 L fermenter batches using ABTS assay for laccase activity. A bar chart showing the net absorbance of the in-house *T. emersonii* cocktail obtained from 5 L and 1 L fermenter batches. The 1 L fractions were not buffer-exchanged..... 99

Figure 4.7. 1: An image of the HIC UV profile with linear gradient [1.2 M ammonium sulphate in 50 mM sodium phosphate, pH 7.0] in for MBL191L054. The orange displays the buffer gradient, the blue displays the absorbance of the fractions at 280 nm, and the grey displays the net absorbance of the HIC fractions at 405 nm when screened for laccase activity using ABTS. 102

Figure 4.8. 1: A graph of pH vs. Relative Activity (%) of the pooled, 2 X concentrated and buffer-exchanged HIC Fractions (Fractions 37, 38, 39) and 2 X concentrated and buffer-exchanged enzyme cocktail (MBL191L054). The orange refers to the pooled, 2 X concentrated and buffer-exchanged HIC Fractions (Fractions 37, 38, 39) and blue refers to the 2 X concentrated and buffer-exchanged enzyme cocktail MBL191L054. 103

Figure 4.8. 2: A graph of Temperature vs. Relative Activity (%) of the pooled, 2 X concentrated, and buffer-exchanged HIC Fractions (Fractions 37, 38, 39)..... 104

Results & Discussion - Catalase

Figure 5.3. 1: An image of the HIC UV profile with linear gradient [1.2 M ammonium sulphate in 50 mM sodium phosphate, pH 7.0] for the in-house *T. emersonii* cocktail. The UV chromatogram is depicted in blue, the eluted fractions are depicted in red. The image is a screenshot from the ÄKTA Pure 25 Chromatography System software. The fractions that were selected for buffer-exchange are indicated in the figure. Fractions in which catalase activity was detected after buffer-exchange are outlined with a blue frame. 110

Figure 5.5. 1: SDS-PAGE analysis displaying the typical profile of *T. emersonii* proteins from 10 L fermenter fractions at 0, 24, 96, 120 and 140 hours. The arrows correspond to the protein bands formed by β -Glucosidase (~ 90 kDa), Cellobiohydrolase isoforms (~ 30-42 kDa), and Endoglucanase (~27 kDa). 115

Figure 5.6. 1: An image of the HIC UV profile with linear gradient [1.2 M ammonium sulphate in 50 mM sodium phosphate, pH 7.0] in for MBL195L01 (5 L culture), 10 X concentrated. The UV chromatogram is depicted in blue, the eluted fractions are depicted in red, and the salt concentration is depicted in green. The image is a screenshot from the ÄKTA Pure 25 Chromatography System software. The fractions that were selected for buffer-exchange are indicated in the figure. The vertical dotted red lines show the boundaries between the pools (1-6) of fractions from the column..... 117

Figure 5.6. 2: An image of the HIC UV profile with linear gradient [1.2 M ammonium sulphate in 50 mM sodium phosphate, pH 7.0] for MBL191L053 (1 L culture) 20 X concentrated. The grey displays the buffer gradient and the orange displays the absorbance of the fractions at 280 nm. The vertical dotted red lines show the boundaries between the pools (1-6) of fractions from the column. 118

Figure 5.6. 3: SDS-PAGE analysis displaying the typical profile of *T. emersonii* proteins from the HIC Fractions. 2 X concentrated and pooled HIC fractions from MBL195L01 (5 L culture) 10 X concentrated and MBL191L053 (1 L culture) 20 X concentrated. The arrows correspond to the protein bands formed by β -Glucosidase (~90 kDa), Cellobiohydrolase isoforms (~ 30-42 kDa), and Endoglucanase (~27 kDa). The orange line after Lane 4 is to indicate that bands in Lanes 2, 3, and 4 come from the 5 L culture while Lanes 5, 6, and 7 come from a 1 L culture. 120

Figure 5.7. 1: A graph depicting the optimum pH of catalase in the Pooled, 2 X concentrated & Buffer-Exchanged Pool 1 (Catalase 1) fractions from MBL195L01 (5 L culture) 10 X concentrated and MBL191L053 (1 L culture) 20 X concentrated. MBL195L01 10 X was assayed once in triplicates while MBL191L053 20 X was assayed twice in triplicates each time. 122

Figure 5.7. 2: A graph depicting the optimum pH of catalase in the Pooled, 2 X concentrated & Buffer-Exchanged Pool 3 (Catalase 3) fractions from MBL195L01 (5 L culture) 10 X concentrated. 122

Figure 5.7. 3: A graph depicting the optimum pH of catalase in the Pooled, 2 X concentrated & Buffer-Exchanged Pool 3 (Catalase 3) fractions from MBL191L053 (1 L culture) 20 X concentrated. 123

Figure 5.7. 4: A graph depicting the optimum pH of catalase in the Pooled, 2 X concentrated & Buffer-Exchanged Pool 4 fractions from MBL195L01 10 X and MBL191L053 20 X. 123

Figure 5.7. 5: A graph highlighting the different pH optima values of Catalase 1, Catalase 3, and Catalase 4 from the 5 L (MBL191L01 10 X concentrated) and 1 L (MBL191L053 20 X concentrated) fractions. The pH optimum graphs are shown individually in figures above (see figures 5.7.1 – 5.7.4). 124

Figure 5.7. 6: A graph depicting the optimum temperature of catalase in the Pooled, 2 X concentrated & Buffer-Exchanged Pool 1 fractions from MBL195L01 (5 L culture) 10 X concentrated and MBL191L053 (1 L culture) 20 X concentrated. 124

Figure 5.7. 7: A graph depicting the optimum temperature of catalase in the Pooled, 2 X concentrated & Buffer-Exchanged Pool 3 fractions from MBL195L01 (5 L culture) 10 X concentrated and MBL191L053 (1 L culture) 20 X concentrated. 125

Figure 5.7. 8: A graph depicting the optimum temperature of catalase in the Pooled, 2 X concentrated & Buffer-Exchanged Pool 4 fractions from MBL191L053 (1 L culture) 20 X concentrated. 125

Figure 5.7. 9: A graph highlighting the different temperature optima values of Catalase 1, Catalase 3, and Catalase 4 from the 5 L (MBL191L01 10 X concentrated) and 1 L (MBL191L053 20 X concentrated) fractions. The temperature optimum graphs are shown individually in figures above (see figures 5.7.6 – 5.7.8). 126

Results & Discussion - Proteomics Analysis

Figure 6.1. 1: SDS-PAGE analysis displaying the typical profile of *T. emersonii* proteins from the 12 Shake Flask Fractions at 120 hours. The 12 Shake Flask fractions included 4 control fractions (Lanes 2-5), Copper Sulphate induced fractions (Lanes 6-9) and Titanium Silicate induced fractions (Lanes 10-13). The arrows correspond to the protein bands formed by β -Glucosidase (~90 kDa), Cellobiohydrolase isoforms (~ 30-42 kDa), and Endoglucanase (~27 kDa). 132

Figure 6.2. 1: Total Ion Chromatogram (TIC) trace of Shake Flask 4 (Control) at 120 hours 134

Figure 6.2. 2: TIC trace of Shake Flask 5 (copper sulphate) at 120 hours 134

Figure 6.2. 3: TIC trace of Shake Flask 11 (titanium silicate) at 120 hours 135

List of Tables

Introduction

Table 1.0. 1: A table summarising some of the important subclasses of enzymes from the six major enzyme families. Examples of each of the subclasses are also displayed (Jain et al. 2005, p. 340). 19

Table 1.1. 1: A table displaying all of the twenty-two subclasses of oxidoreductases along with examples of enzymes from each subclass. The enzyme subclasses of interest in this review are highlighted (Nomenclature Committee of the International Union of Biochemistry and Molecular Biology, 2010). 21

Table 1.2. 1: A table summarising the types of copper atoms present in the active site of laccase (Rodríguez-Delgado et al., 2015). 24

Table 1.2. 2: A table summarising the function of laccases in insects, bacteria, and fungi (Riviera-Hoyos et al., 2013). 25

Table 1.5.1. 1: A table summarising some of the assays that are currently in place for the enzymes discussed in this review. The advantages and disadvantages of each of the assay methods are also listed. 42

Materials & Methods

Table 2.4.1. 1: A table displaying the volumes (mL) of 0.1 M Acetic Acid and 0.1M Sodium Acetate required for the preparation of 0.1 M Acetate Buffer at pH 3.6, 4.0, and 5.0. 55

Table 2.4.2. 1: A Table displaying the volumes (mL) of 0.1 M Sodium Phosphate Monobasic and 0.1 M Sodium Phosphate Dibasic required for the preparation of 0.1 M Sodium Phosphate buffer at pH 6.2, 7.0, and 8.0. 56

Table 2.4.3. 1: A Table displaying the volume (mL) of 0.1 M Citric Acid and 0.1 M Sodium Citrate required for the preparation of 0.1 M Citrate Buffer at pH 3.0, 4.0, and 5.0. 56

Table 2.4.4. 1: A Table listing the volume (mL) of 1 M Potassium Phosphate Dibasic and 1 M Potassium Phosphate Monobasic for the preparation of 0.1 M Potassium Phosphate Buffer at pH 6.0, 7.0, and 8.0. 57

Table 2.8.2. 1: A Table displaying the volumes (μ L) of laccase standard solution and ultrapure water required for the preparation of specific Units/mL of laccase for the laccase standard curve. 62

Table 2.8.4. 1: A Table displaying the volumes (μ L) of catalase standard solution and ultrapure water required for the preparation of specific Units/mL of catalase for the catalase standard curve. 65

Results & Discussion - Laccase

Table 4.2. 1: A table displaying the mg/mL (\pm SD), U/mL of laccase (\pm SD), and specific activity (U/mg) in the buffer exchanged in-house *T. emersonii* cocktail. SD = Standard Deviation. 82

Table 4.4. 1: A table listing the protein concentration (mg/mL) of the shake flask cultures that were set up to obtain fresh enzyme cocktail for assays. nd = not determined. 85

Table 4.4. 2: A table listing the protein concentration (mg/mL) of the shake flask cultures that were set up to obtain fresh enzyme cocktail for assays. 85

Table 4.4. 3: A table listing the protein concentration (mg/mL) of the shake flask cultures that were set up to obtain fresh enzyme cocktail for assays. There are two values for protein concentration for Shake Flask 3C. The values in italics refer to the protein concentration estimated following buffer exchange. 86

Table 4.5. 1: A table listing the protein concentration (mg/mL) of the shake flask cultures that were set up to obtain fresh enzyme cocktail for assays. Four shake flasks were set up: two were controls and two contained 1 mM copper sulphate added after 24 hours of culture. The values in italics beside Shake Flasks 4A and 4D refer to the protein concentration after 2 X concentration and buffer-exchange. 90

Table 4.5. 2: A table listing the protein concentration (mg/mL) of the shake flask cultures set up to obtain fresh enzyme cocktail for assays. Four shake flasks were set up: two were controls and two contained 1 mM copper sulphate after 24 hours of culture. The values in italics beside Shake Flasks 5A and 5B refer to the protein concentration after 2 X concentration and buffer-exchange. The protein concentration for one of the two of the control Shake Flasks could not be quantified as a result of breakage of the flask during culture due to technical difficulties. 91

Table 4.5. 3: A table listing the protein concentration (mg/mL), U/mL of laccase, U/mg of laccase specific activity, IU/mL of β -Glucosidase, Glucanase, and Cellobiohydrolase in Shake Flasks 4A, 4D, 5A, and 5B at 120 hours with copper added at 24 hours. The values in italics refer to the IU/mL of each of the enzymes after 2X concentration and buffer exchange. <LoQ = Below limit of quantitation. 91

Table 4.6. 1: A table listing the protein concentration (mg/mL), U/mL of Laccase, U/mg of Laccase Specific Activity, IU/mL of β -Glucosidase, Endoglucanase, Cellobiohydrolase and U/mL of Xylanase in the various fermentation batches of *T. emersonii* cultured for 140 hours in 5 L and 1 L benchtop bioreactors. The values in italics refer to the protein concentration in the 10 X concentrated fraction of MBL195L01, 6 X concentrated fraction of MBL195L02, 6 X concentrated and buffer exchanged fraction of MBL191L053, and 20 X concentrated fraction of MBL191L054. 97

Table 4.7. 1: A table listing the protein concentration, laccase activity (U/mL), and laccase specific activity (U/mg) in HIC Fractions that were 2 X concentrated and buffer-exchanged. 102

Results & Discussion - Catalase

Table 5.4. 1: A table listing the protein concentration (mg/mL), U/mL of catalase, and catalase specific activity (U/mg) in the various Shake Flask 1 batches (A, B, and D) at 120 hours. Detailed protein concentration (mg/mL) at 0, 24, 96, and 120 hours can be seen in Table 4.4.1. (Only single assays were performed, not duplicates or triplicates) (nd = not determined)..... 111

Table 5.4. 2: A table listing the protein concentration (mg/mL), U/mL of catalase, and catalase specific activity (U/mg) in Shake Flask 4 batches (A and D) at 120 hours. The values in italics are those obtained after 2 X concentration and buffer-exchange. Detailed protein concentrations (mg/mL) at 0, 24, 96, and 120 hours can be seen in Table 4.5.1. Catalase activity (U/mL) and catalase specific activity (U/mg) in batches 4B and 4C were not determined as the flasks with the highest protein concentration in the control and copper sulphate induced fractions were selected. (nd = not determined)..... 112

Table 5.4. 3: A table listing the protein concentration (mg/mL), U/mL of catalase, and catalase specific activity (U/mg) in the Shake Flask 5 batches (A and B). The values in italics are those obtained after 2 X concentration and buffer-exchange. Detailed protein concentration (mg/mL) at 0, 24, and 120 hours can be seen in Table 4.5.2. Catalase activity (U/mL) and catalase specific activity (U/mg) was not determined for Shake Flask fraction 5C. 112

Table 5.5. 1: A table listing the protein concentration (mg/mL), catalase (U/mL), and catalase specific activity (U/mg) in the 5 L, 10 L, and 1 L bioreactor batch cultures of *T. emersonii* at 140 hours..... 114

Table 5.5. 2: A table displaying the U/mL of β -Glucosidase, Endoglucanase, Cellobiohydrolase, and Xylanase as well as U/mL of catalase and catalase specific activity (U/mg) at 140 hours in the 10 L bioreactor run carried out at DCU. 114

Table 5.6. 1: A table indicating the U/mL of Catalase Activity in the buffer-exchanged HIC fractions of MBL195L01 (5 L culture) 10 X concentrated. The two columns showing values for catalase activity (U/mL) obtained were repetition of the assay (in triplicates each time) on two consecutive days. 117

Table 5.6. 2: A table listing the protein concentration (mg/mL), catalase activity (U/mL), and catalase specific activity in the pooled HIC fractions of MBL195L01 (5 L culture) 10 X concentrated that had been 2 X concentrated and buffer-exchanged after pooling together. ... 118

Table 5.6. 3: A table listing the catalase activity (U/mL) in the HIC fractions from MBL191L053 (1 L culture) 20 X concentrated. The assay was repeated twice (in triplicates each time) on two consecutive days. 119

Table 5.6. 4: A table listing the protein concentration (mg/mL), catalase activity (U/mL), and catalase specific activity in the pooled HIC fractions of MBL191L053 (1 L culture) 20 X concentrate that had been 2 X concentrated and buffer-exchanged after pooling. 119

Table 5.7. 1: A table summarising the pH and temperature optima values of catalase 1, catalase 3, and catalase 4 in the 5 L (MBL195L01 10 X concentrated) and 1 L (MBL191L053 20 X concentrated) fractions. The values in italics refer to the optimum pH and temperature values for the 1 L fractions. 126

Results & Discussion – Proteomics Analysis

Table 6.1. 1: A table displaying the protein concentration (mg/mL) in the 12 shake flasks at 0 and 120 hours of culture..... 131

Table 6.2. 1: A table displaying the list of proteins that were only found in the control shake flasks vs. copper sulphate induced flasks and control shake flasks vs. titanium silicate induced flasks. The proteins in italics refer to those that were upregulated in the copper sulphate and titanium silicate induced-shake flasks..... 135

Discovery of Industrially Relevant Oxidoreductases - Kezia Rajan

Abstract

Oxidoreductases are a family of enzymes that have a role in various reduction, oxidation, and oxyfunctionalization reactions. They cleave chemical bonds to facilitate electron transfer from a reduced organic substrate (donor) to another chemical compound (acceptor). There are twenty-two subclasses of oxidoreductases including dehydrogenases, oxidases, mono- and di-oxygenases, peroxidases, laccases, reductases, and hydroxylases. The literature survey reviews recent discoveries and developments in the field of oxidoreductases, with particular emphasis on laccases, catalases, dehydrogenases, and lytic polysaccharide monooxygenases, during the past decade. The review also focuses on some of the common assay methods that are in use for their detection as well as some of their biotechnological applications. Experimental studies were carried out to understand the properties of laccase and catalase present in *T. emersonii*. Studies of laccase in *T. emersonii* indicated that there was only laccase present with an acidic pH optimum of pH 3.0 and temperature optimum of 40 °C. Studies of catalase in *T. emersonii* indicated that multiple catalase isoforms were present with pH optima of 4.0, 5.0, 7.0, and 8.0 and a temperature optimum of 50 °C. Furthermore, the use of copper sulphate was advantageous to increasing laccase production in fermentation culture. However, from the experiments conducted, it was also observed that copper sulphate had a negative impact on catalase activity. Mass spectrometry analyses were also carried out to investigate the impact of copper sulphate on protein expression, protein interaction, and protein modification.

**CHAPTER 1: OXIDOREDUCTASES: OCCURRENCE, ANALYSIS,
AND USES**

1.0 Introduction

The International Union of Biochemistry (I.U.B.) has categorised the known enzymes into six major families namely, the oxidoreductases, transferases, hydrolases, lyases (synthases), isomerases, and ligases (synthetases) (Karigar and Rao, 2011; May and Padgette, 1983). Oxidoreductases are involved in the transfer of protons and electrons from a donor to an acceptor. The catalysis of the transfer of a functional group from a donor to an acceptor is carried out by transferases. The cleavage of C-C, C-O, C-N and other bonds by water is catalysed by hydrolases. These same bonds are cleaved by elimination, leaving double bonds through the action of lyases. In reverse mode, lyases catalyse the addition of groups across double bonds. Isomerisation or structural or geometric rearrangements are facilitated by isomerases. Lastly, the joining of two molecules is catalysed by ligases (Karigar and Rao, 2011). The enzyme category of interest in this introduction is the oxidoreductases. This introduction highlights four types of fungal oxidoreductases in particular and the assay methods for their detection.

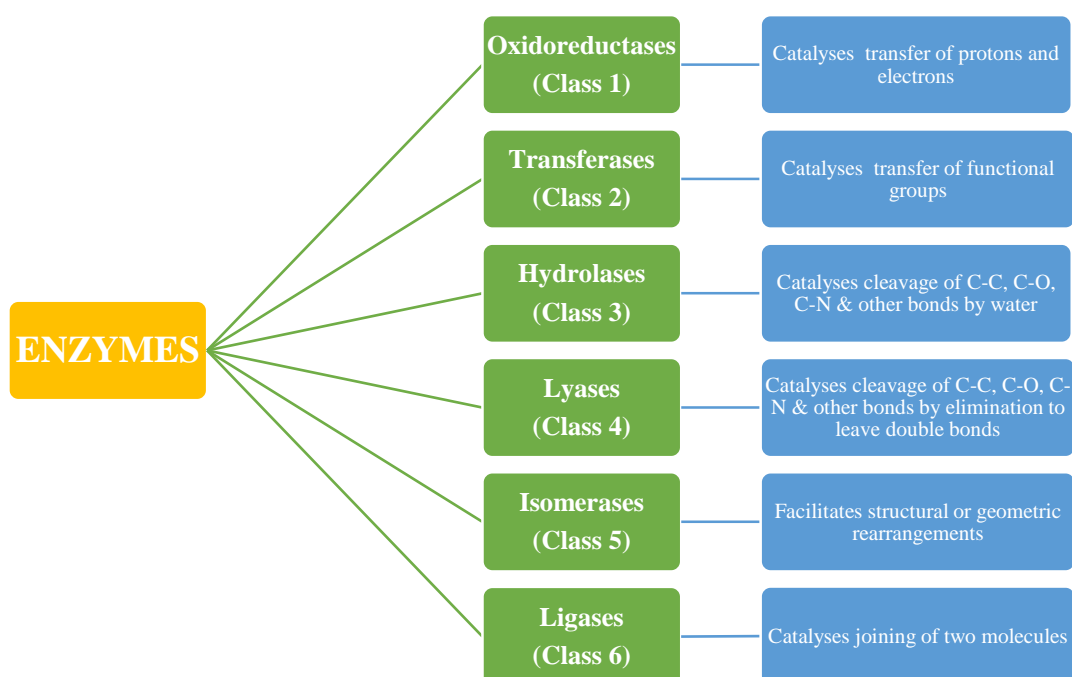


Figure 1.0. 1: A diagram summarising the six major classes of enzyme families and their functions (Karigar and Rao, 2011).

Table 1.0. 1: A table summarising some of the important subclasses of enzymes from the six major enzyme families. Examples of each of the subclasses are also displayed (Jain et al. 2005, p. 340).

ENZYME CLASS	SUBCLASS	EXAMPLE
<u>Oxidoreductases</u> (Class 1)	1.1 Enzymes acting on CH-OH group of electron donors	1.1.1.1 Alcohol : NAD oxidoreductase
	1.2 Enzymes acting on CH-CH group of electron donors	1.3.2.2 Acyl-CoA : cytochrome c oxidoreductase
	1.9 Enzymes acting on the heme groups of electron donors	1.9.3.1 Cytochrome c : O ₂ oxidoreductase
	1.11 Enzymes acting on H ₂ O ₂ as electron acceptor	1.11.1.6 H ₂ O ₂ : H ₂ O ₂ oxidoreductase
<u>Transferases</u> (Class 2)	2.3 Acyltransferases	2.3.1.6 Acetyl-CoA : choline O-acetyltransferase
	2.4 Glycosyltransferases	2.4.1.1 α-1,4-Glucan : orthophosphate glycosyl transferase
	2.7 Enzymes catalysing the transfer of phosphorous-containing groups	2.7.1.1 ATP : D-hexose-6-phosphotransferase
<u>Hydrolases</u> (Class 3)	3.1 Enzymes acting on ester bonds	3.1.1.3 Glycerol ester hydrolase
	3.2 Enzymes acting on glycosyl compounds	3.2.1.23 β-D-galactoside galactohydrolase
	3.4 Enzymes acting on peptide bonds	Pepsin, thrombin, plasmin
	3.5 Enzymes acting on C-N bonds, other than peptide bonds	3.5.3.1 L-arginine ureohydrolase
<u>Lyases</u> (Class 4)	4.1 C-C lyases	4.1.2.7 Ketose-1-phosphate aldehyde-lyase
	4.2 C-O lyases	4.2.1.2 L-malate hydro-lyase
	4.3 C-N lyases	4.3.1.3 L-histidine ammonia-lyase
<u>Isomerases</u> (Class 5)	5.1 Racemases and epimerases	5.1.1.1 Alanine racemase
	5.2 <i>Cis-trans</i> isomerases	5.2.1.3 <i>All trans</i> -retinene 11- <i>cis-trans</i> isomerase
	5.3 Intramolecular oxidoreductases	5.3.1.9 D-glucose-6-phosphate keto-isomerase
<u>Ligases</u> (Class 6)	6.2 Enzymes catalysing formation of C-S bonds	6.2.1.1 Acetate : CoA ligase (AMP)
	6.3 Enzymes catalysing formation of C-N bonds	6.3.1.2 L-glutamate : ammonia ligase (ADP)
	6.4 Enzymes catalysing the formation of C-C bonds	6.4.1.2 Acetyl-CoA : CO ₂ ligase (ADP)

1.1 Oxidoreductases

Oxidoreductases are one of the largest classes of enzymes as they make up approximately 25% of all enzymes (Wang et al., 2017b). They are highly versatile enzymes that have a role in specific oxidation, oxyfunctionalization, and reduction reactions (Johannes et al.,

2006, pp. 77-93). They are further divided into twenty-two subclasses which include dehydrogenases (e.g. flavin and nicotinamide dehydrogenases), oxidases, mono- and di-oxygenases, peroxidases, laccases, reductases, and hydroxylases (Khatoon, et al., 2017; May and Padgett 1983). Oxidoreductases also include hydrogenases, demethylases, nitrogenases, denitrases, dehalogenases, dechlorinases and others (Shah et al., 2012, pp. 221-247). Oxidoreductases require cofactors for catalytic activity such as nicotinamide adenine dinucleotide (phosphate) (NAD(P)^+), flavin adenine dinucleotide (FAD), heme, and metal ions (Martínez et al., 2017; Johannes et al., 2006, pp.77-93; May and Padgett 1983). Eighty percent of known oxidoreductases require NADH and 10% require NADPH (Wang et al., 2017b). These cofactors are expensive, limiting these enzymes' industrial applications (Jiang et al. 2012; Johannes et al., 2006, pp.77-93). For example, the bulk price per mol of NADH and NADPH is \$3000 and \$215 000 respectively (Wang et al., 2017b). Therefore, oxidoreductases are generally employed in fermentation-based processes or whole-cell biotransformations (Johannes et al., 2006, pp.77-93). Moreover, strategies such as the establishment of cofactor regeneration systems, metabolic engineering to improve endogenous cofactor availability, and the replacement of cofactors with biomimetic factors have been proposed and implemented to solve the cofactor issues (Jiang et al., 2012).

Oxidoreductases cleave chemical bonds to facilitate electron transfer from a reduced organic substrate (donor) to another chemical compound (acceptor) (Karigar and Rao, 2011). Since a vast number of oxidation/reduction reactions are involved in industrial chemistry, oxidoreductases have a variety of biotechnological applications (May and Padgett, 1983). They mediate oxidative coupling in the detoxification of organic compounds by various bacteria, fungi, and higher plants. The toxic substances are oxidised to harmless compounds during the oxidation-reduction reactions (Karigar and Rao, 2011). Additionally, di-oxygenases, peroxidases, and laccases have a role in the biodegradation of polymeric compounds. Highly active oxidoreductase enzymes for biodegradation have been reported from white rot fungi (Khatoon et al., 2017).

Table 1.1. 1: A table displaying all of the twenty-two subclasses of oxidoreductases along with examples of enzymes from each subclass. The enzyme subclasses of interest in this review are highlighted (Nomenclature Committee of the International Union of Biochemistry and Molecular Biology, 2010).

EC 1	Oxidoreductases Subclasses	Examples
EC 1.1	Acting on the CH-OH group of donors	alcohol dehydrogenase, choline dehydrogenase, glycerol dehydrogenase, D-xylulose reductase, L-xylulose reductase
EC 1.2	Acting on the aldehyde or oxo group of donors	Formate dehydrogenase, aldehyde dehydrogenase, benzaldehyde dehydrogenase, betaine-aldehyde dehydrogenase
EC 1.3	Acting on the CH-CH group of donors	Dihydrouracil dehydrogenase, dihydropyrimidine dehydrogenase, fumarate reductase, 2-coumarate reductase
EC 1.4	Acting on the CH-NH ₂ group of donors	Alanine dehydrogenase, glutamate dehydrogenase, glutamate synthase, D-aspartate oxidase, aspartate dehydrogenase, monoamine oxidase
EC 1.5	Acting on the CH-NH group of donors	Dihydrofolate reductase, methylenetetrahydrofolate dehydrogenase, formyltetrahydrofolate dehydrogenase, alanopine dehydrogenase
EC 1.6	Acting on NADH or NADPH	Leghemoglobin reductase, NADPH dehydrogenase, NADH dehydrogenase, nitrate reductase, nitrite reductase
EC 1.7	Acting on other nitrogenous compounds as donors	Nitrite reductase, hyponitrite reductase, azobenzene reductase, hydroxylamine reductase, nitroalkane oxidase, hydroxylamine oxidase
EC 1.8	Acting on a sulphur group of donors	Sulphite reductase, hypotaurine dehydrogenase, dihydrolipoyl dehydrogenase, cysteine reductase, sulphite dehydrogenase
EC 1.9	Acting on a heme group of donors	Cytochrome- <i>c</i> oxidase, iron-cytochrome- <i>c</i> reductase
EC 1.10	Acting on diphenols and related substances as donors	Ubiquinol-cytochrome- <i>c</i> reductase, catechol oxidase, laccase, L-ascorbate oxidase, rifamycin-B oxidase
EC 1.11	Acting on a peroxide as acceptor	NADH peroxidase, NADPH peroxidase, fatty-acid peroxidase, catalase, peroxidase, iodide peroxidase, glutathione peroxidase
EC 1.12	Acting on hydrogen as donor	Hydrogen dehydrogenase, ferredoxin hydrogenase, hydrogenase (acceptor)
EC 1.13	Acting on single donors with incorporation of molecular oxygen (oxygenases)	Lipoxygenase, sulphur dioxygenase, cysteamine dioxygenase, cysteine dioxygenase, stizolobate synthase, stizolobinate synthase

EC 1.14	Acting on paired donors, with incorporation or reduction of molecular oxygen	Procollagen-proline dioxygenase, thymine dioxygenase, trimethyllysine dioxygenase, leucocyanidin oxygenase
EC 1.15	Acting on superoxide radicals as acceptor	Superoxide dismutase, superoxide reductase
EC 1.16	Oxidising metal ions	Ferric-chelate reductase, ferroxidase, xanthine dehydrogenase, pteridine oxidase, xanthine oxidase, ribonucleoside-triphosphate reductase
EC 1.17	Acting on CH or CH ₂ groups	Phenylacetyl-CoA dehydrogenase, ethylbenzene hydroxylase, uracil/thymine dehydrogenase
EC 1.18	Acting on iron-sulphur proteins as donors	Nitrogenase, ferredoxin-NAD ⁺ reductase
EC 1.19	Acting on reduced flavodoxin as donor	Nitrogenase (flavodoxin)
EC 1.20	Acting on phosphorous or arsenic in donors	Phosphonate dehydrogenase, methylarsonate reductase, mycoredoxin, arsenate reductase
EC 1.21	Acting on X-H and Y-H to form an X-Y bond	Columbamine oxidase, reticuline oxidase, glycine reductase, betaine reductase
EC 1.97	Other oxidoreductases	chlorate reductase, sulphur reductase, selenate reductase

1.2 Laccase

Laccase was first identified in latex obtained from the Japanese lacquer tree *Rhus vernicifera* tree in 1883 (Loginov et al., 2014; Dashtban et al., 2010). The enzyme was isolated and purified and its mechanism of action reported in 1894. Although laccase activity was thought to be exclusive to higher plants and fungi, it is now understood that laccases are almost ubiquitous enzymes as they have been isolated from arthropods, prokaryotes, plants, and fungi (*Ascomycetes*, *Basidiomycetes*, and *Deuteromycetes*) (Loginov et al., 2014). Laccases, also known as p-diphenol: dioxygen oxidoreductases, are multi-copper oxidase enzymes (Jaber et al., 2017; Riviera-Hoyos et al., 2013). The laccase family (EC 1.10.3.2) is the largest subgroup of the blue multi-copper oxidases (Loginov et al., 2014). Multicopper oxidases contain copper atom in the catalytic centre (Baldrian, 2006). A cluster of four copper atoms (type I copper, type II copper, and two type III copper atoms) forms the active site of the enzyme. Characteristics obtained by UV/visible and electron paramagnetic resonance (EPR) spectroscopy are used to classify the copper atoms into three groups. Type I copper atom is ligated by at least one cysteine and two histidines. It is responsible for the intense blue colour of the enzyme and has strong electronic absorption at ~600 nm. It is also detectable by EPR (Rodríguez-Delgado et al., 2015). There are also white or yellow laccases that lack a blue copper atom (Brijwani et al., 2010). Type II copper atom is ligated by two histidines. It shows no absorption in the visible spectrum and remains colourless. However, it reveals detectable EPR properties. Type III copper atoms consist of a pair of anti-ferromagnetically coupled copper atoms. Each pair is ligated by three histidines. The oxidized form of the copper atom is characterised spectroscopically by a weak adsorption at 330 nm and by the absence of an EPR signal (Rodríguez-Delgado et al., 2015).

Table 1.2. 1: A table summarising the types of copper atoms present in the active site of laccase (Rodríguez-Delgado et al., 2015).

Copper Atom Type	Characteristics
Type I Copper	<ul style="list-style-type: none"> • Ligated by at least 1 cysteine and 2 histidines • Responsible for blue colour of enzyme • Strong electronic absorption at ~600 nm • Detectable by EPR
Type II Copper	<ul style="list-style-type: none"> • Ligated by two histidines • No absorption in the visible spectrum and remains colourless • Detectable EPR properties
Type III Copper	<ul style="list-style-type: none"> • A pair of anti-ferromagnetically coupled copper atoms • Each pair is ligated by 3 histidines • Oxidized form of the copper atom is characterised spectroscopically by a weak adsorption at 330 nm and by the absence of an EPR signal

Laccases have broad substrate specificity and can catalyse the oxidation of a wide range of phenolic compounds and organic aromatic amines into their free radicals (Jaber et al., 2017). Concomitantly, molecular oxygen is reduced to water in the reaction (Riviera-Hoyos et al., 2013). There are three steps in laccase-mediated catalysis. Firstly, the type I copper atom is reduced by the substrate. Secondly, electron transfer occurs from the type I copper atom to the type II and type III copper trinuclear cluster. Thirdly, oxygen is reduced to water at the trinuclear cluster. Furthermore, the inclusion of mediators can extend laccase-mediated catalysis to non-phenolic substrates. Mediators are low molecular weight non-phenolic organic compounds. These are oxidised by laccase to form highly active cation radicals which can, in turn, oxidise non-phenolic compounds that cannot be oxidised by laccase alone (Brijwani et al., 2010).

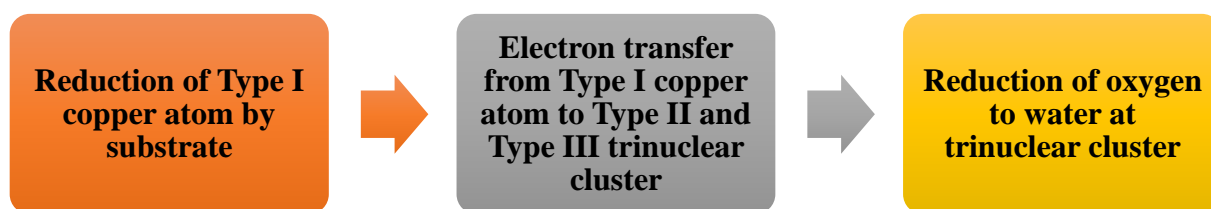


Figure 1.2. 1: An image of the three steps involved in laccase-mediated catalysis (Brijwani et al., 2010).

The main function of laccase-type proteins in insects is for the sclerotization of epidermal cuticle (Riviera-Hoyos et al., 2013). It has been observed that the enzyme has oxidative activity for various catecholic substrates. These enzymes are mainly distributed in the epidermis of the insect. Furthermore, these enzymes are also in the midgut, Malpighian tubules, and collateral gland. However, its function in these internal organs is still to be understood (Nakamura and Go, 2005). Laccases in bacteria have various functions such as biosynthesis of pigments (e.g. melanin and brown sore pigment), copper homeostasis, morphogenesis process, and protection of spores against ultraviolet light and hydrogen peroxide. Laccases in fungi are involved in sporulation, production of pigments and formation of fruit body, and pathogenesis of plants (Riviera-Hoyos et al., 2013).

Table 1.2. 2: A table summarising the function of laccases in insects, bacteria, and fungi (Riviera-Hoyos et al., 2013).

ORGANISM	FUNCTION
Insects	Sclerotization of epidermal cuticle
Bacteria	Biosynthesis of pigments, copper homeostasis, morphogenesis process, protection of spores against ultraviolet light and hydrogen peroxide
Fungi	Sporulation, production of pigments, formation of fruit body, pathogenesis in plants

There are three types of wood decay by fungi, namely, brown rot, white rot, and soft rot. Brown rot fungi can decay wood via both non-enzymatic and enzymatic systems. They employ a series of cellulolytic enzymes in the degradation process but lignin degrading enzymes are not involved. They decay wood that is typically brown and crumbly. White rot fungi are involved in the decay of hardwood and their wood decay patterns can take on different forms. White rotted wood normally has a bleached appearance. This may occur uniformly by leaving the wood as a spongy or stringy mass. Alternatively, it may appear as a selective decay or a pocket rot. White rot fungi contain both cellulolytic and lignin degrading enzymes. As a result, they can degrade an entire wood structure under the correct environmental conditions. Soft rot fungi attack wood that has higher moisture and lower lignin content. They can create unique cavities in the cell wall of the wood (Goodell et al., 2008, pp. 9-31). Laccases are particularly abundant in white rot fungi that are involved in lignin metabolism (Brijwani et al., 2010).

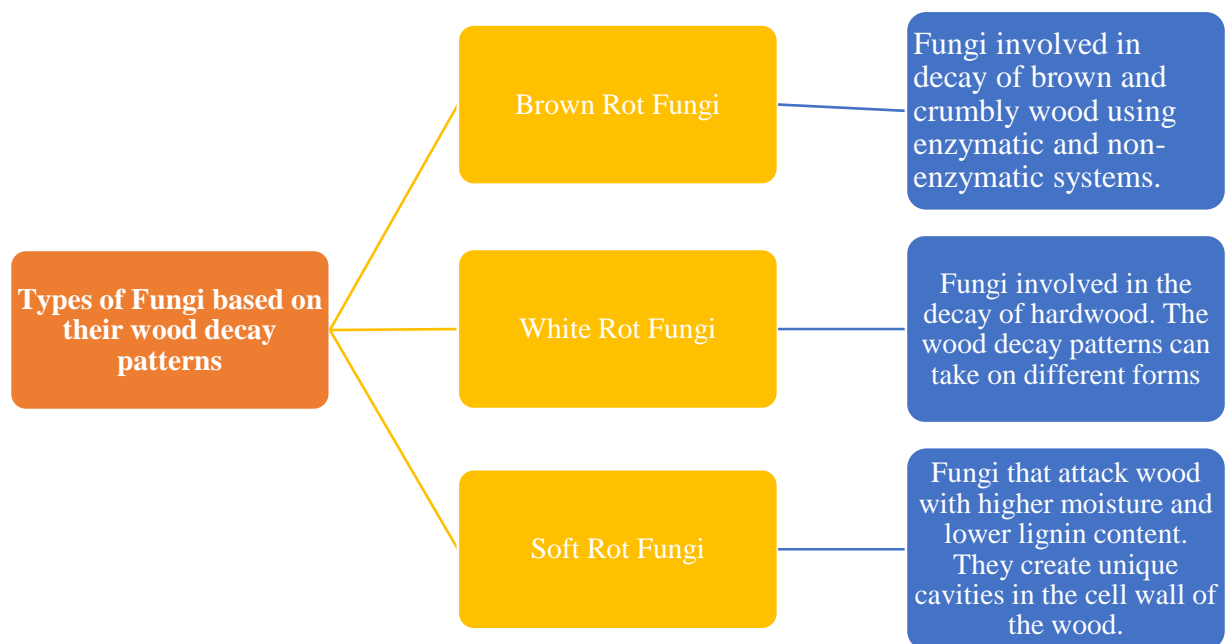


Figure 1.2. 2: A diagram summarising the different types of fungi based on their wood decay patterns (Goodell et al., 2008, pp. 9-31).

Lignin, cellulose, and hemicellulose are known to be efficiently decomposed and transformed to carbon dioxide by white rot *Basidiomycetes* (Riviera-Hoyos et al., 2013). During lignin biodegradation, aryl ether (β -O-4) linkages are broken down. This is followed by the release of phenolic compounds (acids, aldehydes, and ketones) from the oxidative degradation of the side chains from the *p*-hydroxyphenyl, guaiacyl, and syringyl lignin units (Pardo et al., 2013). Although intracellular laccases have been

reported in fungi, they mostly consist of laccases which are monomeric extracellular glycoproteins. The molecular weight of fungal laccases ranges between 50-140 kDa depending on the size and glycosylation patterns (Riviera-Hoyos et al., 2013). Fungal laccases have higher redox potential (+800 mV) than bacterial and plant enzymes. The redox potential of laccase in laccase-producing fungi have been reported as 790 mV in *Trametes villosa*, 450 mV in *Myceliophthora thermophila*, 750 mV in *Pycnoporus cinnabarinus*, and 780 mV in *Botrytis cinerea* (Brijwani et al., 2010).

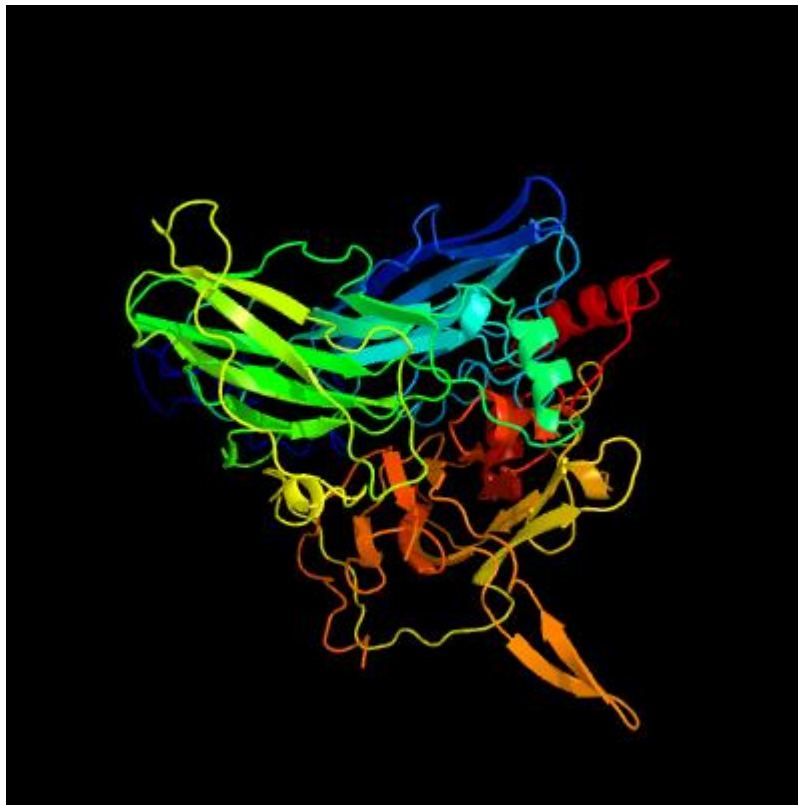


Figure 1.2.3: An image of the predicted structure of laccase in *Thielavia arenaria* (MW: 80 kDa) as generated using Phyre2 protein fold recognition server. Model dimensions (Å): X: 63.859, Y: 61.753, Z: 67.394. Rainbow-colour-code indicates the protein chain from blue at the N-terminus to red at the C-terminus. The sequence for multicopper oxidase was obtained from NCBI pBLAST and entered into the Phyre2 server (GenBank: ORY61466.1).

1.2.1 Enzyme assays for the detection of laccase

Laccases can accept a wide variety of substrates. As a result, the application zone of the enzyme can be widened further with the utilisation of radical-forming mediators such as 2,2'-azino-bis (3-ethylbenzothiazoline-6-sulphonic acid) (ABTS) and N-hydroxy-acetanilide (NHA) (Fu et al., 2013).

ABTS Assay

ABTS is a non-phenolic dye that is widely used as a substrate to study catalytic reactions of enzymes such as laccase and peroxidase. Laccase enzyme oxidises ABTS to its more stable cation radical form. An intense blue-green colour develops as a result of the cation radical in the reaction mixture. The development of the intense blue-green colour is further correlated to laccase enzyme activity (Kameshwar and Qin 2017). In a study by Valle et al., (2014), the enzyme sample was mixed with water, sodium acetate buffer, and ABTS. The mixture was incubated for 10 minutes after which the reaction was interrupted by the addition of 5% trichloroacetic acid (w/v). The absorbance was then measured at 420 nm, as the absorbance increased at this wavelength due to the oxidation of ABTS. In another ABTS assay carried out by Kameshwar and Qin (2017), sodium azide was used to inhibit the reaction between laccase and ABTS. In the assay, sodium azide lowered the concentration of ABTS cation radical by dilution. It inhibits laccase enzyme and thereby prevents the further formation of cation radical.

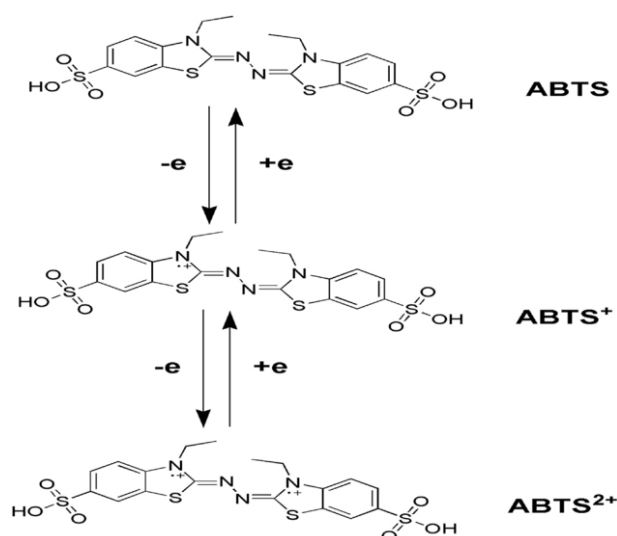


Figure 1.2.1. 1: A schematic representation of the reaction mechanism of the ABTS Assay (Christopher et al., 2014).

DMP Assay

2,6-Dimethoxyphenol (DMP) is a plant phenolic compound. It is a well-known substrate for laccase and is involved in the thermal degradation of hardwood. Laccase converts 2,6-DMP into 3,5,3',5'-tetramethoxydiphenoquinone which is a straw coloured product (Kameshwar and Qin, 2017). In a study by Sahay et al., (2008), the reaction was monitored by measuring the change in absorbance at a wavelength of 468 nm.

Syringaldazine Assay

Syringaldazine is a substrate that allows easy and rapid detection of the laccase enzyme. When laccase enzyme is treated with dilute syringaldazine solution in ethanol, a colour change occurs from yellow to deep purple. The colour change is a result of two-fold phenol dehydrogenation of syringaldazine and intramolecular pairing of free radicals. This in turn produces a highly coloured tetramethoxyazo-bis-methylene quinone complex. The absorbance of the tetramethoxy-azo-bis-methylene quinone complex is measured at 525 nm. It is only when syringaldazine directly reacts with the laccase enzyme that colour formation occurs. Furthermore, the colour development is rapid at all pH conditions but the colour fades rapidly outside the pH range of 3-7 (Kameshwar and Qin 2017).

Amplex Red Assay

A fluorescence-based method for the assay of laccase was developed by Wang et al., (2017a). This method was used to detect laccase activities in soil samples. The assay principle is based on the oxidation of amplex red to resorufin in the presence of oxygen. The reaction is catalysed by laccase. The fluorescence intensity is measured at 583 nm. Amplex Red is a derivative of resorufin that is non-fluorescent and colourless. Resorufin, on the other hand, is a coloured and highly fluorescent substance. This assay has advantages over the current methods in use for the detection of laccase. These advantages include high sensitivity, wide linear range, stability, reproducibility, strong anti-interference ability and good selectivity.

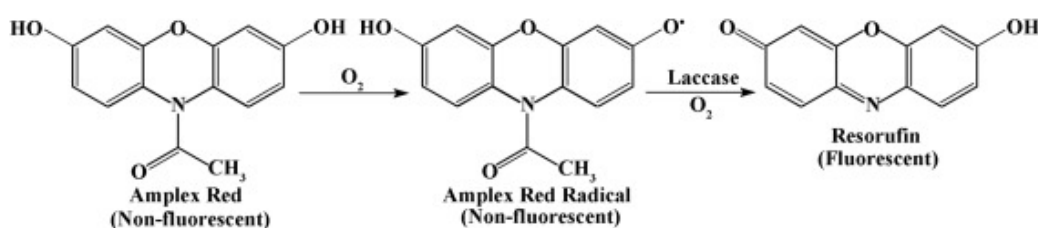


Figure 1.2.1. 2: A schematic representation of the reaction mechanism of the Amplex Red Assay (Wang et al., 2017a).

1.3 Catalase

Catalase (EC 1.11.1.6), also referred to as H₂O₂:H₂O₂ oxidoreductase, is an antioxidant enzyme that is present in all aerobic organisms including archaea, bacteria, fungi, plants, and animals (Vatsyayan and Goswami 2016; Sharma and Ahmad 2014, pp. 131-148; Kirkman and Gaetani 1984). The enzyme is monophyletic in origin and is grouped into three clades. In clade 1 are green algae and plants, in clade 2 are archaea, bacteria, and fungi, and in clade 3 are archaea, bacteria, fungi, and animals. Archaea, bacteria, and fungi are found in two clades, namely clades 2 and 3. The subunits in clades 1 and 3 are between 55 to 69 kDa while the subunits in clade 2 are larger and are between 75 to 86 kDa. Catalase is a homotetramer (Vatsyayan and Goswami 2016). There are four haem groups in each tetrameric molecule. The haem groups contain iron in the ferric state (Kirkman and Gaetani 1984). Catalases are categorised into four main groups, namely, the monofunctional catalases, the catalase-peroxidases, the non-haem catalases, and minor catalases. Monofunctional catalases are the most widely studied group of catalases and their predominant activity is the disintegration of hydrogen peroxide. Catalase-peroxidases exhibit catalatic activity as well as significant peroxidatic activity. Non-haem catalases contain a manganese-rich reaction centre instead of a haem group in the active site. Minor catalases include peroxidases that exhibit a low level of catalatic activity (Nicholls et al., 2000).

Catalase breaks down hydrogen peroxide (H₂O₂) into water and dioxygen in two steps, without the need for additional electron-donor substrates (Liu and Kokare 2017, pp.267-298; Martins and English 2014; Hansberg et al., 2012; Kirkman and Gaetani 1984). Firstly, an H₂O₂ molecule is reduced to water. Consequently, the catalase haem Fe³⁺ is oxidised to oxyferryl species (Fe⁴⁺=O). Next, a second molecule of H₂O₂ is oxidised to water and oxygen with the concomitant reduction of the oxyferryl species that regenerates the haem Fe³⁺ (Vatsyayan and Goswami 2016). H₂O₂ is used as a second messenger for cellular regulation but it can also be toxic to the cell if present in large amounts. Catalases are active at higher H₂O₂ concentrations (Hansberg et al., 2012).



Figure 1.3. 1: The equation of chemical reaction depicting the decomposition of hydrogen peroxide into water and oxygen in the presence of catalase

There are similarities in molecular weight, number of subunits, and types of prosthetic groups in catalases from different sources (Kirkman and Gaetani 1984).

There are at least eight microbial strains that can produce catalases. They include *Penicillium variable*, *Aspergillus niger*, *Saccharomyces cerevisiae*, *Micrococcus lysodeikticus*, *Thermoascus aurantiacus*, *Bacillus subtilis*, and *Rhizobium radiobacter* (Liu and Kokare 2017, pp.267-298). It has been reported that fungi are high producers of catalase. Two different catalases have been obtained from *Cladosporium fulvum* while three different catalases have been obtained from *Aspergillus fumigatus*. Additionally, four catalase genes have been isolated from *Aspergillus nidulans*. An acid stable catalase has been isolated from *A. niger* (Isobe et al., 2006). Catalase from *A. niger* is an intracellular enzyme (Liu and Kokare 2017, pp.267-298). A thermostable catalase has also been obtained from *T. aurantiacus* (Isobe et al., 2006).

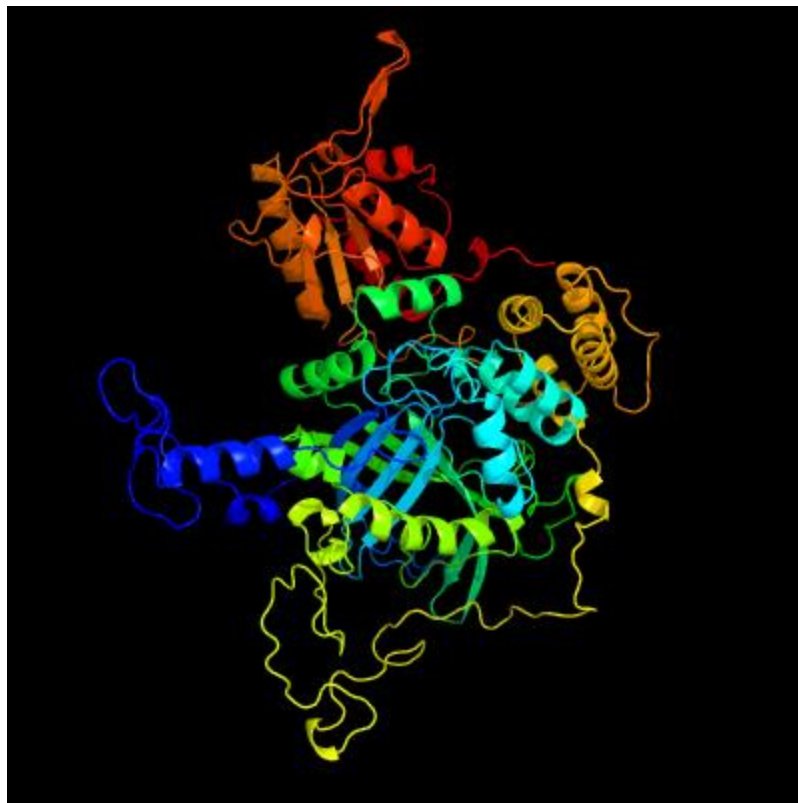


Figure 1.3. 2: An image of the predicted structure of catalase in *Neurospora crassa* (MW: 82 kDa) as generated using Phyre2 protein fold recognition server. Model dimensions (Å): X: 109.210, Y: 73.056, Z: 83.151. Rainbow-colour-code indicates the protein chain from blue at the N-terminus to red at the C-terminus. The sequence for catalase was obtained from NCBI pBLAST and entered into the Phyre2 server (ID: 3872372).

1.3.1 Enzyme assays for the detection of catalase

A spectrophotometric method for assaying catalase activity was developed by Beers and Sizer (1952). The study used the decrease in ultraviolet absorption by hydrogen peroxide as a function of time to follow the catalase-peroxide reaction. The ultraviolet absorption spectrum of hydrogen peroxide was measured from 200 to 400 nm. The optical density could be used at any wavelength in this range to measure the concentration of peroxide. This is because optical density increases linearly with peroxide concentration in accordance with the Beer-Lambert law. Furthermore, under a variety of conditions, the method used for the breakdown of hydrogen peroxide followed first order kinetics. Additionally, the products of the reaction, namely, oxygen and water, as well as the concentration of catalase employed do not absorb light in this spectral region. As a result, the ultraviolet absorption directly measures peroxide concentration in the catalase-peroxide system. It was reported that this method suited catalase kinetics (Beers and Sizer, 1952). A study by Martins and English (2014) assayed for catalase activity using similar methods. In the study, the analyte was mixed with H₂O₂ and potassium phosphate buffer. At 240 nm, H₂O₂ decomposition was monitored. Another study by Trawczyńska and Wójcik (2015) assayed for catalase activity in yeast cells by measuring the increase in dissolved oxygen that resulted from the enzymatic decomposition of H₂O₂. The yeast cells were permeabilised in ethanol and added to H₂O₂ solution with phosphate buffer at pH 7 that was degassed with N₂. Using the slope of the oxygen concentration versus time profile after baseline subtraction, the catalase activity was measured.

1.4 Dehydrogenase

Dehydrogenases are widely distributed enzymes and represent a majority of redox enzymes (Leech et al., 2008). They catalyse the oxidation of a substrate by transferring hydrogen to an acceptor (Lackie, 2013). Dehydrogenases are commonly used to reduce carbonyl groups of aldehydes and ketones as well as carbon-carbon double bonds (Johannes et al., 2006). NAD⁺/NADP⁺ or flavins are the most common acceptors (Lackie, 2013). Pyrroloquinoline quinone (PQQ) is another cofactor for dehydrogenases (Johannes et al., 2006). It is reduced by two electrons at a higher redox potential than NAD⁺ or FAD. There are two structural types of PQQ-containing enzymes, namely, quinoproteins and quino-hemo-proteins. Quinoproteins contain PQQ in the active site only; e.g. glucose, aldose, and glycerol dehydrogenases. Quino-hemo-proteins contain

PQQ and one or more heme groups; e.g. fructose dehydrogenase and alcohol dehydrogenase (Laurinavicius et al., 2004). Dehydrogenases are mostly NAD^+ dependent (Leech et al., 2008). It is understood that more than 300 dehydrogenase enzymes utilise NAD^+ as a cofactor (Zhang et al., 2004). NAD^+ is not directly bound to the enzyme. However, it is essential as it acts as a carrier of two electrons and one proton. Therefore, the biocatalytic function of dehydrogenases is activated by NAD^+ (Leech et al., 2008). This review will focus on FAD/FMN-containing dehydrogenases.

Flavin-containing dehydrogenases contain either FAD or flavin mononucleotide (FMN) as cofactors. FAD and FMN are the redox active prosthetic group. It is reported that FAD mostly binds to a Rossmann fold while FMN binds to a flavodoxin-like fold or TIM-barrel (Huijbers et al., 2017). The Rossmann fold is a widely distributed super-secondary structure that is composed of alternating beta strand and alpha helical segments. The beta strands are hydrogen bonded to form a central beta sheet with helices on either side (Hanukoglu, 2015). It is a known RNA-binding domain in several dehydrogenases; e.g. lactate dehydrogenase (Hanukoglu, 2015; Bollenbach et al. 2004). This is important as dehydrogenases can bind RNA (Evguenieva-Hackenberg et al., 2002). The TIM-barrel fold is made up of an eightfold repeat of beta-alpha units. It is arranged so that eight parallel beta strands on the inside are covered by eight alpha helices on the outside. Enzymes such as triosephosphate isomerase and orotidine 5'-monophosphate decarboxylase are TIM-barrel enzymes. In the protein data bank database of known protein structures the TIM-barrel is the most common enzyme fold. It is seen to catalyse completely unrelated reactions across the different enzyme families (Wierenga, 2001, pp. 193-198).

An example of a flavin dehydrogenase enzyme is choline dehydrogenase (EC 1.1.99.1). It catalyses the four-electron oxidation of choline to glycine betaine via betaine-aldehyde intermediate (Lambou et al., 2013; Gadda and McAllister-Wilkins, 2003; Huang and Lin, 2003). Subsequently, betaine aldehyde is oxidised to glycine betaine which is a small, water-soluble organic molecule that is essential for the protection of plants, animals, and bacteria against abiotic stress (Lambou et al., 2013). The enzyme acts as an iron-sulphur flavoprotein as it contains FAD and an iron-sulphur cluster, as its two redox centres (Huang and Lin, 2003). Cellobiose dehydrogenase is another example. This is a hemoflavoenzyme containing one haem b and one FAD per molecule (Baminger et al.,

1999). The enzyme has a role in the catalysis of cellobiose oxidation to cellobiono- γ -lactone in the presence of a suitable hydrogen or electron acceptor (Dekker, 1980). It is thought to play a part in the degradation of both cellulose and lignin (Baminger et al., 1999). In *Sporotrichum pulverulentum*, it contains FAD as the prosthetic group and is specific for cellobiose as well as other cello-oligosaccharides. It is known that this enzyme is produced extracellularly by the white-rot fungi *Polyporus versicolor* and *Chrysosporium lignorum* when grown on cellulosic substrates. The thermophilic white-rot fungus *Sporotrichum thermophile* has also been reported for cellobiose dehydrogenase activity when grown on cellulose (Dekker, 1980). The enzyme has also been identified in a variety of soft-rot and brown-rot organisms (Baminger et al., 1999).

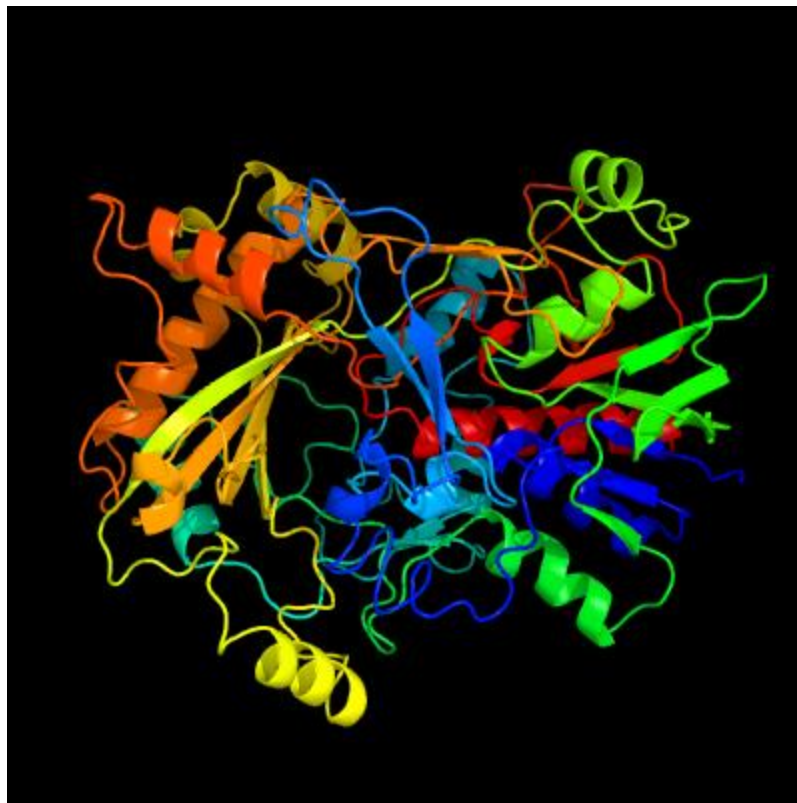


Figure 1.4. 1: An image of the predicted structure of FAD-linked dehydrogenase enzyme in *Phanerochaete chrysosporium* (81 914 Da) as generated using Phyre2 protein fold recognition server. Model dimensions (Å): X: 62.498, Y: 63.241, Z: 68.752. Rainbow-colour-code indicates the protein chain from blue at the N-terminus to red at the C-terminus. The sequence for choline dehydrogenase was obtained from NCBI pBLAST and entered into the Phyre2 server (ID: 41989250). There is no clear biochemical evidence indicating the presence of FAD as a cofactor (Gadda and McAllister-Wilkins 2003).

1.4.1 Enzyme assays for the detection of dehydrogenase

A very common method for the detection of dehydrogenase activity is by measuring the absorbance of the reduced form of nicotinamide adenine dinucleotide phosphate

(NAD(P)H) at 340 nm. As high background noise is created by cell lysates and the 96-well plate, this method is not suitable for high-throughput screening. Although it is possible to use special plates that do not absorb in the UV range, it is expensive for large-scale screening efforts. Therefore, colorimetric assays, involving either a synthetic compound or a secondary enzyme, are quite amenable to high-throughput screening methods (Johannes et al., 2006).

NBT/PMS Assay

Nitroblue tetrazolium (NBT) is a tetrazolium salt that can be reduced to formazan dyes which absorb light in the visible region and have maximal absorption at 555 nm (Johannes et al., 2006). NAD(P)H, a dehydrogenase coenzyme, reacts with NBT in the presence of the transferring agent phenazine methosulphate (PMS). The reaction produces an insoluble blue-purple formazan which links the production of NAD(P)H to the catalytic activity of a dehydrogenase enzyme (Johannes et al., 2006; Mayer and Arnold, 2002). The reaction is irreversible under biological conditions. However, the increase in colour can be monitored easily by vision on a standard 96-well plate reader or on filter discs. The assay can successfully monitor dehydrogenase activity on electrophoretic gels, nitrocellulose membranes, and in liquid phase. Furthermore, transferring agents other than PMS such as the enzyme diaphorase or 8-di-methylamino-2-benzophenoxazine (Meldola's Blue) can be used. An alternative to NBT is the compound *p*-rosaniline. Although transferring agents are not necessary when using *p*-rosaniline, bisulphite must be added to aid the conversion of the dye into its rose-coloured form (Johannes et al., 2006). Furthermore, *p*-rosaniline is a carcinogen and mutagen (IHC World, 2018).

The assay has been used to identify *E. coli* 6-phosphogluconate dehydrogenase variants with higher activity and thermostability by measuring the increase in absorbance at 580 nm (Johannes et al., 2006; Mayer and Arnold, 2002). It has also been used to detect alcohol dehydrogenase activity in liquid phase and lactate dehydrogenase activity on nitrocellulose membranes (Mayer and Arnold, 2002).

DCPIP Assay

2,6-dichlorophenol-indophenol (2,6-DCPIP) is a redox dye that acts as an electron acceptor (Brugger et al., 2014). It is intense blue in colour (Vemuluri et al., 2017; VanderJagt et al., 1986). The assay is based on the direct enzymatic reduction of 2,6-DCPIP (Brugger et al., 2014). When it is reduced, DCPIP becomes colourless (Vemuluri et al., 2017). Baminger et al., (1999) assayed for cellobiose dehydrogenase activity by following the decrease in absorbance of 2,6-DCPIP spectrophotometrically at 520 nm for the first five minutes of reaction. DCPIP is widely used in assaying for cellobiose dehydrogenase activity. Other efficient electron acceptors include azino-di-(3-ethyl-benzthiazolin-6-sulphonic acid) cation radical, 1,4-benzoquinone dyes such as methylene blue, phenoxazine dyes such as Meldola's Blue and ferricyanide, phenothiazine, and cytochrome c (equine) (Kameshwar and Qin, 2017). A disadvantage of some of the alternative electron acceptors is the cost. For example, 5 grams of equine cytochrome c costs € 4 380.00 (Sigma-Aldrich, 2018).

1.5 Lytic Polysaccharide Monooxygenase

Lytic polysaccharide monooxygenases (LPMOs) are copper-dependent oxidoreductases that have been discovered and characterised in the past 5-10 years (Martínez et al., 2017; Frandsen and Lo Leggio, 2016; Nekiunaite et al., 2016). While laccase is a multi-copper oxidase made up of a cluster of four copper atoms in its active site, LPMOs have a type 2 copper site with only two histidines (Frandsen and Lo Leggio 2016; Rodríguez-Delgado et al., 2015). They are active only in the presence of molecular oxygen and an electron donor (Brenelli et al., 2018). They have a copper binding site. One copper atom is coordinated by three nitrogen ligands provided by two histidine imidazoles and the N-terminal amino group in a T-shaped histidine brace arrangement. The reaction mechanism of LPMOs involves reduction of the copper in the active site by an electron donor. This is followed by the activation of dioxygen (Loose et al., 2014). The oxidative cleavage of glycosidic linkages of polysaccharides is catalysed by LPMOs in the presence of molecular oxygen and an electron donor. The cleavage occurs by hydroxylation of either the C1 or C4 of the glycosidic bond. This makes LPMOs instrumental in the degradation of recalcitrant crystalline polysaccharides such as cellulose and chitin (Nekiunaite et al., 2016). The action of LPMOs can be triggered by a variety of electron donors ranging from complex systems such as plant-derived and fungal phenols, glucose-methanol-choline oxidoreductases, cellobiose dehydrogenases, or photosynthetic

pigments such as chlorophylls to small-molecule reductants such as sulphur-containing species, ascorbate, pyrogallol or gallic acid (Villares et al., 2017).

Some LPMOs can also oxidise non-crystalline hemicelluloses and soluble cello-oligosaccharides. Furthermore, starch-active LPMOs have also been discovered (Nekiunaite et al., 2016). LPMOs are widely distributed across the bacterial and fungal kingdoms. Saprotrophic fungi are the most abundant source of LPMOs, with some species containing over 30 genes that encode LPMOs. These enzymes are secreted at an early stage of degradation when fungi are grown in the presence of lignocellulosic material or cellulose (Villares et al., 2017). Currently, there are four auxiliary activity (AA) enzyme families of LPMOs in the Carbohydrate Active Enzyme database. They are AA9, AA10, AA11 and AA13. The AA9-type LPMOs are exclusive to fungi and have a preference for cellulose (Villares et al., 2017). The AA11-type LPMOs are also exclusive to fungi while the AA10-type LPMOs are dominated by bacterial enzymes and also contain members from viruses and eukaryotic organisms (Loose et al., 2014). AA9-type LPMOs have a β -sandwich fold structure with a planar surface of approximately 1,200 Å². Cellulose and cello-oligosaccharides can bind to this surface (Villares et al., 2017). LPMOs open up the inaccessible polysaccharide material for hydrolysis by the classical glycosyl hydrolase enzymes (Hemsworth et al., 2015; Vaaje-Kolstad et al., 2010). As a result, LPMOs reduce the enzyme load for the deconstruction of polysaccharides (Hemsworth et al., 2015).

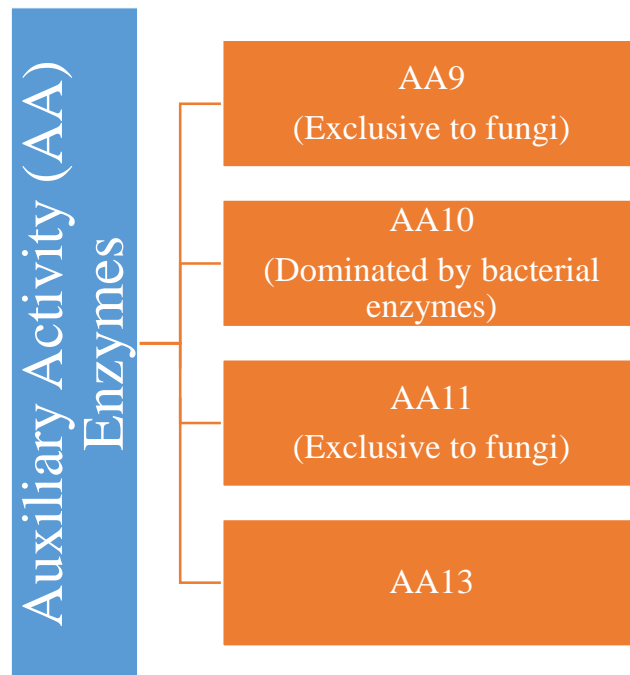


Figure 1.5. 1: An image summarising the three main families of LPMOs in the auxiliary activity enzyme class (Villares et al., 2017).

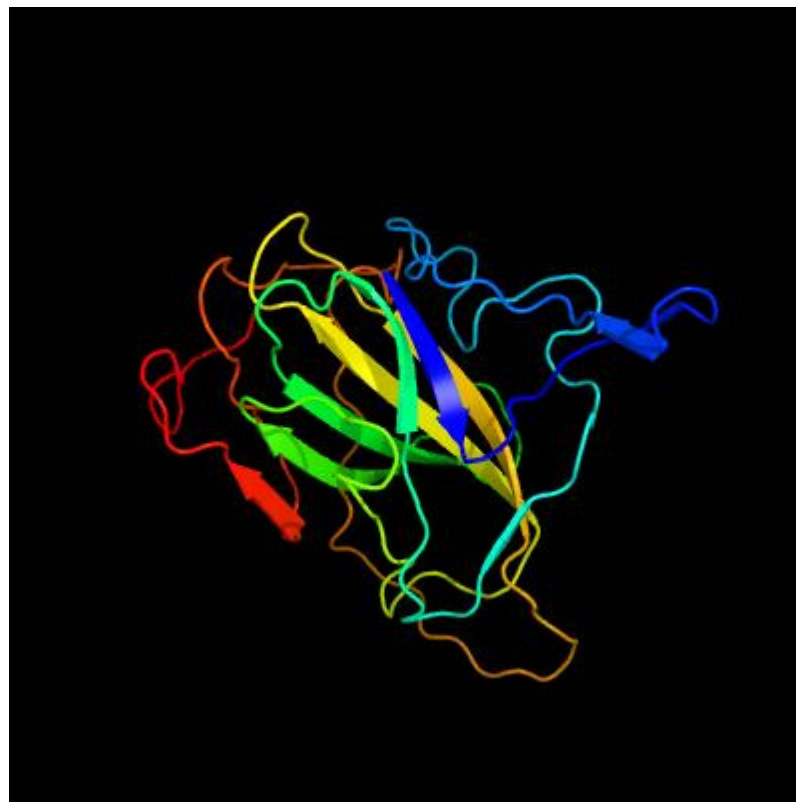


Figure 1.5.2: An image of the predicted structure of a copper-dependent polysaccharide monooxygenase enzyme in *Aspergillus oryzae* (~23 kDa) as generated using Phyre2 protein fold recognition server. Model dimensions (Å): X: 42.279, Y: 46.686, Z:54.700. Rainbow-colour-code indicates the protein chain from blue at the N-terminus to red at the C-terminus (ID: 30972848).

1.5.1 Enzyme assays for the detection of LPMO

Currently, it is challenging to analyse LPMO activity even at the qualitative level. There are a number of reasons for this such as the complexity of the products, the insolubility of the substrate, autoxidation of reactants, lack of commercially available standards, and complicated analytical methods (Loose et al., 2014). Moreover, the assays that are currently in use for assay of LPMO activity require long incubation times. The LPMO, together with cellobiose dehydrogenase or a reductant, needs to be incubated at elevated temperatures (37 °C-50 °C) for several hours or up to three days. As a result, these assays are both time-consuming and labour-intensive and are not ideal for the monitoring of fermentation processes or the progress of a purification procedure. However, they are advantageous for investigating the substrate specificity and reaction mechanism (Kittl et al., 2012).

Kittl et al., (2012) developed a fluorimetric assay to measure the oxygen reducing side reactivity of LPMOs by quantifying the formation of H₂O₂. It is based on a proposed reaction mechanism that assumes the production of H₂O₂ as a by-product of an easily accessible side-reaction of LPMOs. There have been no reports of the reduction of oxygen to H₂O₂ by LPMOs and this is not the proposed in-vivo function. Instead, it is thought that the side-reaction occurs in the absence of the natural substrate cellulose. The reaction mechanism of the assay involves reduction of the type-2 copper in the LPMO by ascorbate or cellobiose dehydrogenase, the proposed natural interaction partner of LPMOs. Consequently, molecular oxygen is activated by a one electron reduction. The H₂O₂ that is produced in the reaction is selectively and sensitively detected by horseradish peroxidase (HRP) coupled conversion of Amplex Red to resorufin. The assay time is 10 minutes and resorufin fluorescence was noted to be stable for 40 minutes. Kittl et al. (2012) showed that the formation of H₂O₂ is directly proportional to the concentration of LPMO by adding different amounts of LPMO to the assay mixture. The H₂O₂ produced is dependent on the availability of a suitable reductant for the LPMO type-2 copper centre. The reductant/electron donor used in the study was either ascorbate or cellobiose, together with cellobiose dehydrogenase. Production of H₂O₂ occurred in proportion to the concentration of added LPMO for both the ascorbate and the cellobiose dehydrogenase-driven assay (Kittl et al., 2012). This method, however, cannot be used to determine the substrate cleaving rates of LPMOs (Loose et al., 2014).

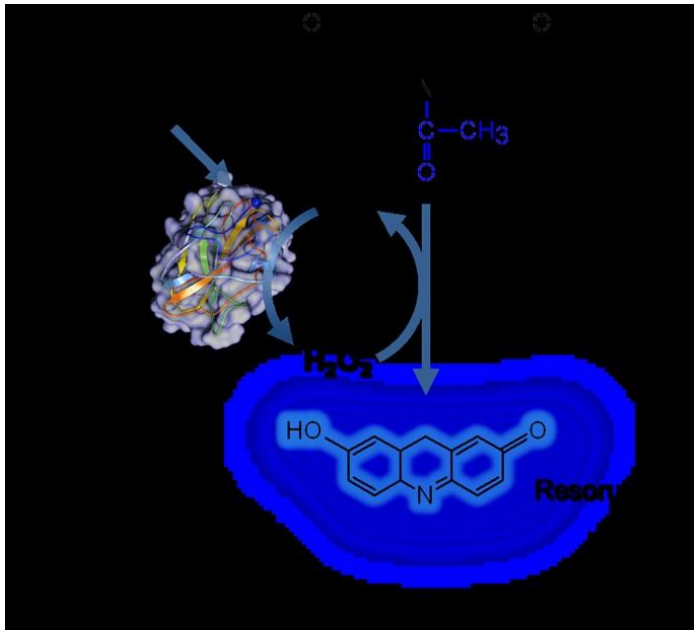


Figure 1.5.1. 1: Schematic representation of the PMO Activity Assay (Kittl et al., 2012)

Loose et al. (2014) developed a method for rapid and reproducible quantitative analysis of LPMO activity towards chitin. The method is based on careful copper saturation of the enzyme combined with a fast chromatographic method. Through this method, Loose et al., (2014) demonstrated that there is evidence of LPMO activity in a virulence factor that is not directly involved in the conversion of chitin or other biomass polysaccharides. An example of this is the colonisation factor GbpA in *Vibrio cholerae* which allows the organism to attach to both aquatic transfer vectors and the epithelial cell surfaces of the host. GbpA is a four-domain protein that has an N-terminal LPMO10 domain. Additionally, a study by Vaaje-Kolstad et al. (2010) used a multi-step assay involving several enzymes to determine an initial substrate oxidation rate on the order of $\sim 1 \text{ min}^{-1}$ of oxidized product for CBP21 which is a chitin-active LPMO10.

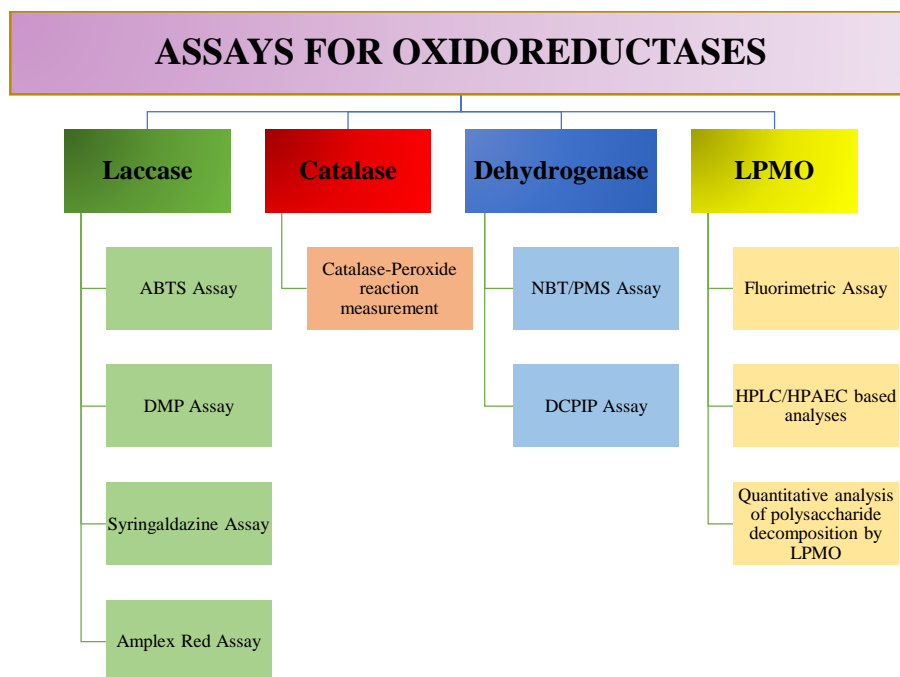


Figure 1.5.1. 2: A diagram summarising the different assay methods currently available for the four different oxidoreductases discussed in this review.

Table 1.5.1. 1: A table summarising some of the assays that are currently in place for the enzymes discussed in this review. The advantages and disadvantages of each of the assay methods are also listed.

Enzymes	Assays	Advantages	Disadvantages
Laccase	1) ABTS	<ul style="list-style-type: none"> • ABTS is soluble in water and organic solvents • Detection limit of 0.06 mU/mL • Cost efficient • No interference issues • Convenient • Reproducible 	<ul style="list-style-type: none"> • Can be time-consuming
	2) DMP	<ul style="list-style-type: none"> • Quantitative • Method efficiency 	<ul style="list-style-type: none"> • Spontaneous auto-oxidation of DMP • Not cost efficient • Lower catalytic efficiency than ABTS • Time consuming
	3) Syringaldazine	<ul style="list-style-type: none"> • Method efficiency • Time efficiency 	<ul style="list-style-type: none"> • Limited solubility of quinone produced from syringaldazine in aqueous media • Lower catalytic efficiency than ABTS • Not cost efficient
	4) Amplex Red	<ul style="list-style-type: none"> • Sensitivity • Detection limit of 1.76 U/L • Reproducible 	<ul style="list-style-type: none"> • Requires equipment that measures fluorescence intensity • Time-consuming with regards to assay set-up • Interference issues
Catalase	Catalase-Peroxide reaction measurement	<ul style="list-style-type: none"> • Various kits available commercially that are variations of the Catalase-Peroxide reaction principle 	<ul style="list-style-type: none"> • Some commercially available kits may take approximately 1-2 hours to obtain results

		<ul style="list-style-type: none"> Detection limit of 0.5 U/mL and quantification limit of 1.8 U/mL 	<ul style="list-style-type: none"> Some assay kits are expensive Reproducibility issues
Dehydrogenase	1) NBT/PMS	<ul style="list-style-type: none"> Assay can be utilised for any oxidoreductase that utilises either NADH or NADPH as a cofactor Reproducible Sensitive (can detect activity in 3 μL of cell lysate) 	<ul style="list-style-type: none"> PMS is light-sensitive and expensive when compared to other reagents The reaction is irreversible Lacks specificity
	2) DCPIP	<ul style="list-style-type: none"> Quick Reproducible 	<ul style="list-style-type: none"> Lacks specificity Only applicable for use in the absence of thiol protecting agent or other strong reducing substrate in the enzyme
LPMO	1) HPLC or HPAEC based analyses 2) Fluorimetric assay	<ul style="list-style-type: none"> Can easily reveal LPMO activity on hemicellulosic substrates 	<ul style="list-style-type: none"> Need for additional enzymes Semi-quantitative nature of the action of LPMOs Lacks specificity as methods are based on indirect measure of LPMO
	3) quantitative analysis of polysaccharide decomposition by LPMO enzymes alone		Monitors LPMO activity toward polysaccharide substrates without any additional enzyme

1.6 Applications of Oxidoreductases

The classical fungal oxidoreductases include ligninolytic peroxidases in basidiomycetes and multicopper oxidases (mainly laccases). They have differences in their redox potentials and abilities to act on lignin-derived products. Some of the new heme- and copper-containing oxidoreductases of biotechnological interest include unspecific peroxygenases (UPOs), dye-decolourising peroxidases, and LPMOs. UPOs are involved in the catalysis of a wide variety of regio- and stereo-selective oxyfunctionalizations using H₂O₂ as the oxygen source and terminal electron acceptor. These oxidoreductases are biocatalysts of interest to establish a bio-based economy. Their greatest potential is in the production of polymer building blocks, sustainable chemicals and materials from plant biomass within lignocellulose biorefineries. However, at present, oxidoreductases are mostly employed in the form of whole-cell catalysts in specific segments of the chemical industry, such as P450 monooxygenases for selective hydroxylations. They are not utilised as isolated protein biocatalysts in medium and large scale biotransformations. However, fungal oxidoreductases have been engineered to obtain several industrial target reactions such as i) intermediates for dyestuff production, including amine and phenolic derivatives, indole and indole derivatives, and aniline polymers; ii) intermediates for flavours and fragrances, agrochemicals and active pharmaceutical ingredients, epoxidation products and drug metabolites; and iii) precursors for specialty polymers (Martínez et al., 2017).

Most biotechnologically useful laccases are of fungal origin. Fungal laccases can oxidise compounds that are structurally similar to lignin. Due to their ability to oxidise organic and inorganic substrates such as mono, di, polyphenols, aminophenols, and methoxyphenols as well as metal complexes, laccases are attractive candidates for diverse biotechnological applications. The enzyme has gained attention due to its ability to degrade a range of recalcitrant pollutants (Upadhyay et al., 2016). Therefore, one of the many biotechnological applications of laccase includes the mitigation of environmental pollution (Dias et al., 2017). Fungal laccases can be employed in the bioremediation of phenolic compounds and in the detoxification of pollutants. They can convert materials such as plastic, wood, paint, and jet fuel into nutrients. Laccases are also being utilised in pulp and paper processing industry as they can depolymerise lignin and delignify wood pulps (Upadhyay et al., 2016).

Catalases are employed in the textile industry for the removal of H_2O_2 from fabric (Amorim et al., 2002). Since chlorine bleaching is more toxic, peroxide bleaching is used (Doshi and Shelke, 2001). Cotton fabric is bleached with H_2O_2 prior to the dyeing process in order to degrade reactive dyes. However, the residues from the bleaching bath must be removed from the fabric and machinery prior to the application of the desired fabric dye. Although successive washes of the fabric with water or chemical reducers can reduce the residual bleaching agent concentration and improve dyeing, it requires a large volume of water, a longer processing time, and the use of products that are harmful for the environment. Therefore, catalases are utilised as an alternative to decrease water consumption, and the energy and time required (Amorim et al., 2002). Approximately 30-40 litres of water per kilogram of fabric are required for the removal of excess reducing agent. Catalase can act in cold water and also saves on the use of large quantities of water, as rinsing is not required after catalase treatment (Doshi and Shelke, 2001). Another industrial application of catalases is in the food industry for the removal of H_2O_2 that is used for sterilisation (Liu and Kokare 2017). Milk can be treated with H_2O_2 in farms where heat pasteurisation is not technically feasible. H_2O_2 treatment is also advantageous for cheese making. Pasteurisation removes pathogens as well as acid-forming microorganisms present in milk. However, the addition of 1 ml of 33% of H_2O_2 at the farm presents a means of milk preservation. This is followed by the addition of another 1 ml of H_2O_2 at the dairy, heating to 50 °C for 30 minutes, cooling to 35 °C, and the addition of catalase. Furthermore, approximately half of the Swiss cheese manufactured in the United States is produced using this treatment as it improves the body characteristics of the cheese and also reduces the number of undesirable microorganisms (Richardson, 1975).

Dehydrogenases, oxidases, peroxidases, and monooxygenases can be used for biocatalytic oxidation reactions. This is especially significant for flavin-dependent oxidoreductases which can react directly with molecular oxygen and avoid other cofactors, cosubstrates (also known as coenzymes), or metal catalysts for oxidation reactions. Flavin-oxidoreductases have also demonstrated enormous catalytic versatilities. A particular area of interest for flavoenzymes is electrochemistry in the application of suitable enzymes in biosensors or biofuel cell applications. Dehydrogenases that lack oxygen reactivity are also highly favoured. The reason for this is because the stability of the biocatalyst is affected when the electrode-bound enzymes

react with oxygen to produce H₂O₂ (Brugger et al., 2014). There are also potential uses of cellobiose dehydrogenases in the pulp and paper industry (Duarte et al., 1999). Fungal cellobiose dehydrogenases can produce H₂O₂ *in-situ* making them useful for biotechnological applications such as cotton bleaching, laundry detergents or antimicrobial functionalization of medical devices. Unlike glucose oxidases, these cellobiose dehydrogenases can directly use polysaccharide derived mono- and oligosaccharides as substrates. The versatile properties of cellobiose dehydrogenase have made it possible for its application in biosensors for the detection of lactose, glucose, and catecholamines. It is also useful in biodegradation (Sygmund et al., 2013). Their biodegradation capacity is a result of highly non-specific, free-radical-mediated processes resulting from the activities of enzymes such as laccases, manganese peroxidase, and lignin peroxidase (Ciullini et al. 2008). However, cellobiose dehydrogenases have low activity with oxygen as the electron acceptor and this limits their industrial use for H₂O₂ production. Therefore, there is a need for recombinant cellobiose dehydrogenase enzymes with increased oxygen reactivity for biotechnological applications (Sygmund et al., 2013).

LPMOs are viewed as a breakthrough in the enzymatic degradation of cellulose. They oxidatively cleave glycosidic linkages and leave the substrate more susceptible to hydrolysis by conventional cellulases (Villares et al., 2017). LPMOs are a key component of latest generation enzyme cocktails for the industrial production of lignocellulosic ethanol (Villares et al., 2017; Lo Leggio et al., 2015). They have also become a central factor in industrial biomass conversion as they provide access to the full calorific and chemical value of recalcitrant polysaccharides including cellulose, hemicellulose, and chitin (Lo Leggio et al., 2015). Furthermore, a potential role of LPMOs in the pathology of infectious diseases such as cholera has been proposed. Thus, LPMOs may be relevant in the field of medicine (Johansen, 2016).

1.7 Conclusion

This review has focused on fungal oxidoreductases, with particular emphasis on four different enzymes, namely, laccases, catalases, dehydrogenases, and LPMOs as well as the various assays in use for their detection.

As laccases have broad substrate specificity, there are a wide range of assays in use for their detection. These include the ABTS assay, DMP assay, syringaldazine assay and the Amplex Red assay. The challenge lies in developing assays that are sensitive and specific. However, laccases have a huge potential for industrial applications as they can catalyse reactions using inexpensive oxygen from the air without the need of expensive cofactors. Catalases, are widely studied enzymes and have a wide range of commercially available kits to assay for catalase activity; e.g. Merck, Abcam, Cayman Chemical, Sigma-Aldrich, and Megazyme. Dehydrogenases are widely distributed enzymes that catalyse the oxidation of a substrate by transferring hydrogen to an acceptor. They require cofactors such as NAD⁺/NADP⁺, flavins (FAD/FMN) or pyrroloquinoline quinone. The assays in use for detecting dehydrogenase activity include NBT/PMS assay and DCPIP assay. They lack specificity and fail to focus on the complete catalytic cycle of the enzyme. Additionally, oxygen can interfere with the results. LPMOs have only been discovered in the past ten years. They make recalcitrant polysaccharides more susceptible for cleavage by traditional hydrolases. There are currently no ‘convenient’ assays for the detection of LPMOs. However, Kittl et al. (2012) developed an indirect fluorimetric method to detect LPMO activity that is based on a proposed reaction mechanism that assumes the production of H₂O₂ as a by-product of an easily accessible side-reaction of LPMOs. So, there is a need for further research on assay development for oxidoreductases that enables their successful detection. Oxidoreductases have a wide range of applications including in the food industry, textile industry, medicine, pulp and paper industry, and biofuel industry. With advancements in knowledge and scientific discoveries, oxidoreductases will continue to enhance all areas of our lives and the planet we live on.

1.8 Project Aims and Plans

The aim of this research project was to discover industrially relevant oxidoreductases in fungi. The organism used for the discovery of these enzymes is *Talaromyces emersonii*, a thermophilic, soft-rot ascomycete fungus.

Reports in the scientific literature of discoveries and developments in the field of oxidoreductases during the past decade were reviewed, with particular emphasis on laccases, catalases, dehydrogenases, and lytic polysaccharide monooxygenases. This review also focused on commonly-used assay methods for their detection and some of their biotechnological applications.

Mass spectrometric analysis had previously been carried out on the in-house *T. emersonii* cocktail, as well as on fractions pooled from hydrophobic interaction chromatography of the in-house *T. emersonii* cocktail. The mass spectrometry analysis generated a large list of amino acid sequences. While the mass spectrometric analysis identified the names of the vast majority of proteins present in the in-house enzyme cocktail, there still remained a few unknown proteins. Bioinformatics analyses was used to identify the unknown proteins and select four oxidoreductases for further studies.

After finalising the four oxidoreductases for further studies, an SOP was drafted for their detection and quantification. Shake flask culturing were carried out to avail of fresh enzyme cocktails for analysis. The effect of components to induce enzyme activity were also investigated when enzyme yields were low and not as expected. Following optimisation of the culture conditions, the fermentation process was scaled-up from shake flasks to benchtop bioreactors. Partial purification of the enzyme cocktail was carried out using hydrophobic interaction chromatography prior characterisation of the enzymes of interest. The pH and temperature optima of each of the enzymes was investigated. A mass spectrometry analysis of the fractions was also carried out to identify the effect of inducers on enzyme activity. These studies enabled a preliminary evaluation of the enzymes' potential usefulness in industrial applications.

CHAPTER 2: MATERIALS & METHODS

2.1 Equipment

Class	Model	Source/Supplier
Autoclave	Tomy SX-700E	Mason Technology, 228 South Circular Road, Dublin 8, Ireland
Benchtop Bioreactor	Biostat [®] B	Sartorius Stedim Biotech GmbH, August-Spindler Straße 11, 37079 Goettingen, Germany
Bioreactor	Biostat C	School of Biotechnology, DCU
Centrifuge	Eppendorf 5810 Centrifuge	Eppendorf UK Limited, Eppendorf House, Gateway 1000 Whittle Way, Arlington Business Park, Stevenage, SG1 2FP
Centrifuge	Heraeus [™] Labofuge [™] 400 Centrifuges	School of Biotechnology, DCU
Chromatography System	ÄKTA Pure 25 System	GE Healthcare Life Sciences, VWR International Ltd., Orion Business Campus, Northwest Business Park, Ballycoolin, Blanchardstown, Dublin 15, Ireland
Digital Precise Water Bath	WB-22	Daihan Scientific, 326, Sinpyoungsukhwaro Jijeong-myeon, Wonju, South Korea
Ice Machine	Scotsman AF 80	Hubbard Systems, 106 Claydon Business Park, Gt. Blakenham, Ipswich, Suffolk, IP6 0NL
Incubator	Incubator IN55	Memmert GmbH + Co. KG, Äußere Rittersbacher Straße 38, D-91126, Schwabach

Laminar Flow Cabinet	Mars 1200 Biohazard Safety Cabinet (Safety Class 2)	LaboGene A/S, Bjarkesvej 5, DK-3450 Allerød
Microcentrifuge	Hettich Mikro 22	Andreas Hettich GmbH & Co.KG, Föhrenstr. 12, D-78532 Tuttlingen
Microplate Spectrophotometer	Multiskan™ GO	Fisher Scientific, Bishop Meadow Road, Loughborough, Leicestershire, LE11 5RG
Microtitre Plate Shaker	SSM5	Cole-Parmer Scientific Experts, Beacon Road, Stone, Staffordshire, ST15 0SA, UK
Portable pH Meter	Seven2Go pH meter S2-Food-Kit	Mason Technology, 228, South Circular Road, Dublin 8, Ireland
Precise Shaking Incubator	WIS-30R	Daihan Scientific, 326, Sinpyoungsukhwaro Jijeong-myeon, Wonju, South Korea
Protein Electrophoresis Equipment	Mini PROTEAN® Tetra Cell and System	Bio-Rad Laboratories Ltd., The Junction, Station Road, Watford, Hertfordshire, WD17 1ET
UV Gel Imager	ChemiDoc™ MP Imaging System	Bio-Rad Laboratories Ltd., The Junction, Station Road, Watford, Hertfordshire, WD17 1ET
Waterbath	WNB 29	Memmert GmbH + Co. KG, Äußere Rittersbacher Straße 38, D-91126, Schwabach

2.2 Consumables

Consumables	Supplier
Black Assay Plates (96-well microtiter plates)	Medical Supply Company Ltd., Damastown, Mulhuddart, Dublin 15, Ireland
Bottle-Top Vacuum Filtration Systems, PES	VWR International Ltd., Orion Business Campus, Northwest Business Park, Ballycoolin, Blanchardstown, Dublin 15, Ireland
Catalase Assay Kit	Megazyme, Industrial Development Agency Business Park, Southern Cross Road, Irishtown, Bray, Co. Wicklow, Ireland
Centrifugal Concentrators	Sigma Aldrich Ireland Ltd., Vale Road, Arklow, Co. Wicklow, Ireland
Vivacon 500 (30 kDa MWCO)	Sigma Aldrich Ireland Ltd., Vale Road, Arklow, Co. Wicklow, Ireland
General Plastic Consumables e.g. microcentrifuge tubes, pipette tips, 96-well PCR plates, 96-well microtiter plates, 2 mL and 1.5 mL centrifuge tubes, 0.2 mL PCR Tube Strips etc.	Sarstedt Ltd., Drinagh Sinnottstown, Wexford, Co. Wexford
Mini-PROTEAN Precast Gels	Bio-Rad Laboratories Ltd., The Junction, Station Road, Watford, Hertfordshire, WD17 1ET
Nalgene™ Rapid-Flow™ Sterile Disposable Filter Units with PES Membrane (0.2 µm)	Fisher Scientific Ireland, Suite 3, Plaza 212, Blanchardstown Corporate Park 2, Ballycoolin, Dublin 15
PD-10 Desalting Columns	Sigma Aldrich Ireland Ltd., Vale Road, Arklow, Co. Wicklow, Ireland
Single Use Sterile Disposable Syringe Filter (0.45 µm)	Sparks Lab Supplies Ltd., Unit J-7, Greenogue Business Park, Rathcoole, Co. Dublin, Ireland
Single Use Sterile Disposable Syringe Filter (0.45 µm)	Fisher Scientific Ltd., Suite 3, Plaza 212, Blanchardstown Corporate Park 2, Ballycoolin, Dublin 15

2.3 Reagents

All reagents were of analytical grade unless stated otherwise.

Acros Organics (Part of Thermo Fisher Scientific) (Geel, Belgium):

Dimethyl sulphoxide (DMSO) ($\geq 99\%$ Ultrapure Grade, $(\text{CH}_3)_2\text{SO}$, 78.14 g/mol, #IC19018691)

37% v/v Hydrochloric acid (HCl, 36.45 g/mol, #124630026)

Sulphuric Acid, 96% extra pure, solution in water (H_2SO_4 , 98.07 g/mol, #133610026)

Bio-Rad Laboratories (Perth, United Kingdom)

10 X Tris/Glycine/SDS (TGS) Buffer (25 mM Tris, 192 mM Glycine, 0.1% (w/v) SDS, pH 8.3, #161-0732)

Quick Start™ Bradford Protein Assay Kit consisting of 1 X Bradford Dye Reagent and Bovine Serum Albumin (BSA) protein standards at seven pre-diluted concentrations (0.125, 0.25, 0.5, 0.75, 1.0, 1.5, and 2.0 mg/ml). (#5000207)

Fisher Scientific (Leicestershire, United Kingdom)

Amplex Red ($\text{C}_{14}\text{H}_{11}\text{NO}_4$, 257.25 g/mol, #A12222)

Citric Acid Monohydrate ($\text{C}_6\text{H}_8\text{O}_7$, 192.123 g/mol, #10338903)

Copper (II) Sulphate Pentahydrate ($\text{CuSO}_4 \cdot 5\text{H}_2\text{O}$, 249.68 g/mol, #10695482)

D-Glucose anhydrous ($\text{C}_6\text{H}_{12}\text{O}_6$, 180.156 g/mol, #10570364)

Glycerol ($\text{C}_3\text{H}_8\text{O}_3$, 92.094 g/mol, #10021083)

NuPAGE® LDS Sample Buffer (4 X) (10 mL, #11549166)

NuPAGE® Reducing Agent (10 X) (250 μL , #10424012)

PageRuler™ Unstained Protein Ladder (250 μL , #11802124)

Sodium Acetate Trihydrate ($\text{C}_2\text{H}_9\text{NaO}_5$, 136.079 g/mol, #10142350)

Megazyme (Bray, Co. Wicklow, Ireland)

Catalase (*Aspergillus niger*, ~ 4,960 U/mg) in 3.2 M ammonium sulphate)

Neogen® (Michigan, USA)

Potato Dextrose Agar (PDA) (500 g, #NCM0018A)

Sigma Aldrich Ireland Ltd., Vale Road, Arklow, Co. Wicklow, Ireland

ABTS Tablets (10 mg)

Acetic Acid ($\geq 99.8\%$, anhydrous, $\text{CH}_3\text{CO}_2\text{H}$, 60.05 g/mol, #109088)

25% (v/v) Ammonium Hydroxide solution (NH_4OH , 35.05 g/mol, #09860)

Ammonium Sulphate ($\geq 99.0\%$, $(\text{NH}_4)_2\text{SO}_4$, 132.14 g/mol, #A4915)

Antifoam SE-15 (#A8582)

Laccase from *Trametes versicolor* (0.87 U/mg, #101661795)

Potassium Hydroxide (KOH, 56.11 g/mol, #1.05021)

Potassium Phosphate Dibasic (K_2HPO_4 , 174.18 g/mol, #1551128)

Potassium Phosphate Monobasic (KH_2PO_4 , 136.084 g/mol, #1551139)

Sodium Azide (NaN_3 , 65.01 g/mol, #769320)

Sodium Citrate Dihydrate ($\geq 99\%$, Food Grade, $\text{CHO}(\text{COONa})(\text{CH}_2\text{COONa})_2 \cdot 2\text{H}_2\text{O}$, 294.10 g/mol, #W302600)

Sodium Hydroxide ($\geq 98\%$, NaOH, 40.00 g/mol, #30620)

Sodium Phosphate Dibasic (anhydrous) (Na_2HPO_4 , 141.96 g/mol, #RES20908-A7)

Sodium Phosphate Monobasic (anhydrous) (NaH_2PO_4 , 119.98 g/mol, #S8282)

Titanium Silicon Oxide (nanopowder, < 50 nm particle size) (TiSiO_4 , 139.94 g/mol, #1001606976)

2.4 Buffer Preparations

2.4.1 Preparation of 0.1 M Acetate Buffer (pH 3.6, pH 4.0, and pH 5.0)

In order to prepare 0.1 M acetate buffer, 25 mL of 0.1 M acetic acid solution and 25 mL of 0.1 M sodium acetate solutions were first prepared. Acetic acid (0.1 M) was made up by adding 144 μ L of glacial acetic acid to 24.856 mL of ultrapure water. Sodium acetate (0.1 M) was prepared by dissolving 0.34 g of sodium acetate trihydrate to a final volume of 25 mL of ultrapure water. The acetic acid and sodium acetate solutions were mixed in the proportions indicated in the table below. The final volume was adjusted to 15 mL with ultrapure water and the final pH adjusted using 1 M HCl. The buffer solutions were stored at 4 °C.

Table 2.4.1. 1: A table displaying the volumes (mL) of 0.1 M Acetic Acid and 0.1M Sodium Acetate required for the preparation of 0.1 M Acetate Buffer at pH 3.6, 4.0, and 5.0.

mL of 0.1 M Acetic Acid	6.95	6.15	2.22
mL of 0.1 M Sodium Acetate	0.56	1.35	5.28
pH	3.6	4.0	5.0

2.4.2 Preparation of 0.1 M Sodium Phosphate Buffer (pH 6.2, pH 7.0, and pH 8.0)

In order to prepare 0.1 M sodium phosphate buffer, 0.1 M sodium phosphate monobasic and sodium phosphate dibasic solutions were prepared. Sodium phosphate monobasic (0.1 M) was prepared by dissolving 2.07 g of sodium phosphate monohydrate in 150 mL of ultrapure water. Sodium phosphate dibasic (0.1 M) was prepared by dissolving 5.36 g of sodium phosphate dibasic in 200 mL of ultrapure water. The sodium phosphate monobasic and dibasic solutions were mixed in the proportions indicated in the table below. The final volume was adjusted to 10 mL with ultrapure water and the final pH adjusted using a pH meter. The buffer solutions were stored at 4 °C.

Table 2.4.2. 1: A Table displaying the volumes (mL) of 0.1 M Sodium Phosphate Monobasic and 0.1 M Sodium Phosphate Dibasic required for the preparation of 0.1 M Sodium Phosphate buffer at pH 6.2, 7.0, and 8.0.

mL of 0.1 M Sodium Phosphate Monobasic	6.95	6.15	2.22
mL of 0.1 M Sodium Phosphate Dibasic	0.56	1.35	5.28
pH	6.2	7.0	8.0

2.4.3 Preparation of 0.1 M Citrate Buffer (pH 3.0, pH 4.0, and pH 5.0)

In order to prepare 0.1M citrate buffer, 0.1 M citric acid and 0.1 M sodium citrate dihydrate solutions were first prepared. Citric acid (0.1 M) was prepared by dissolving 0.5254 g of citric acid monohydrate in 25 mL of ultrapure water. Sodium citrate (0.1 M) was prepared by dissolving 2.94 g of sodium citrate dihydrate in 100 mL of ultrapure water. The citric acid and sodium citrate solutions were mixed in the proportions indicated in the table below. The final volume was adjusted to 10 mL with ultrapure water and the final pH adjusted measured using a pH meter. The buffer solutions were stored at 4 °C.

Table 2.4.3. 1: A Table displaying the volume (mL) of 0.1 M Citric Acid and 0.1 M Sodium Citrate required for the preparation of 0.1 M Citrate Buffer at pH 3.0, 4.0, and 5.0.

mL of 0.1 M Citric Acid	4.65	3.3	2.05
mL of 0.1 M Sodium Citrate	0.35	1.7	2.95
pH	3.0	4.0	5.0

2.4.4 Preparation of 0.1 M Potassium Phosphate Buffer (pH 6.0, pH 7.0, and pH 8.0)

In order to prepare 0.1 M potassium phosphate buffer, 1 M potassium phosphate mono- and dibasic stock solutions were first prepared. Potassium phosphate monobasic solution (1 M) was prepared by dissolving 3.40 g in 25 mL of ultrapure water. Potassium phosphate dibasic solution (1 M) was prepared by dissolving 8.71 g in 50 mL of ultrapure water. The potassium phosphate monobasic and dibasic solutions were mixed in the proportions indicated in the table below. The final volume was adjusted to 10 mL with

ultrapure water and the final pH adjusted using 1 M HCl. The buffer solutions were stored at 4 °C.

Table 2.4.4. 1: A Table listing the volume (mL) of 1 M Potassium Phosphate Dibasic and 1 M Potassium Phosphate Monobasic for the preparation of 0.1 M Potassium Phosphate Buffer at pH 6.0, 7.0, and 8.0.

mL of 1 M Potassium Phosphate Dibasic	0.13	0.62	0.94
mL of 1 M Potassium Phosphate Monobasic	0.87	0.39	0.06
pH	6.0	7.0	8.0

2.4.5 Preparation of 0.1 M and 20 mM Potassium Phosphate Buffer (pH 6.4)

In order to prepare 0.1 M potassium phosphate buffer at pH 6.4, 13.61 g of potassium phosphate monobasic was dissolved in 1L of ultrapure water. The solution was filtered using 0.2 µm polyethersulphone filter. This was the stock solution and was stored at room temperature.

Potassium phosphate buffer (20 mM) was prepared by dissolving 20 mL of the 0.1 M potassium phosphate stock solution in 80 mL of ultrapure water. Using a pH meter, the pH was adjusted to 6.4 using 1 M Hydrochloric acid (HCl) and 1 M Potassium Hydroxide (KOH). The solution was stored at room temperature.

2.4.6 Preparation of 150 mM Potassium Phosphate Buffer, pH 7.0

Potassium phosphate dibasic (1.31 g) was dissolved in 25 mL of ultrapure water. Using a pH meter, the pH of the solution was adjusted to 7.0 using 1 M HCl. The final volume of the solution was made to 50 mL with ultrapure water. The solution was filtered using 0.2 µm sterile filter and was stored at 4 °C.

2.5 Preparation of Reagents and Solutions

2.5.1 Preparation of 1 M HCl

16.52 mL of 37% (v/v) HCl was dissolved in 183.48 mL of ultrapure water using safety precautions. The solution was mixed and stored at room temperature.

2.5.2 Preparation of 5 M and 1 M Potassium Hydroxide

In order to prepare 5 M potassium hydroxide (KOH) solution, 56.11 g of KOH was dissolved in a total of 250 mL of ultrapure water using safety precautions. The solution was stirred using a magnetic stirrer to completely dissolve the KOH. The solution was filtered using a sterile 0.2 µm filter. This solution was the stock solution and was tightly capped to prevent carbon dioxide absorption from the air.

In order to prepare 1 M KOH, 20 mL of 5 M KOH solution was added to 80 mL of ultrapure water. The solution was mixed well and served as the working solution of KOH. Both the stock and working solutions of KOH were stored at room temperature.

2.5.3 Preparation of 0.5 M Copper Sulphate solution

In a 100 mL glass beaker, 6.24 g of copper (II) sulphate pentahydrate was dissolved in 50 mL of ultrapure water using a magnetic stirrer. Once the copper (II) sulphate pentahydrate was fully dissolved, it was filtered using a 0.2 µm sterile filter and transferred to a 50 mL sterilin tube. The solution was stored at room temperature.

2.5.4 Preparation of 0.5 M Sulphuric Acid solution

Sulphuric acid (14.06 mL) was added to 485.94 mL of ultrapure water to a final volume of 500 mL using safety precautions. The solution was mixed together in a 1 L Duran bottle and was autoclaved at 121 °C for 30 minutes. After autoclaving, the solution was stored at room temperature for use in the culture of *T. emersonii* in 5 L fermenters.

2.5.5 Preparation of 4% (v/v) Antifoam SE-15

Antifoam SE-15 (20 mL) was added to 480 mL of ultrapure water in a 1 L Duran bottle. The final volume was 500 mL. The solution was autoclaved at 121 °C for 30 minutes. After autoclaving, the solution was stored at room temperature for use in the culture of *T. emersonii* in 5 L fermenters.

2.5.6 Preparation of 25% (v/v) Ammonium Hydroxide base

In a fumehood, 500 mL of 25% ammonium hydroxide base from Sigma-Aldrich was measured and poured into a 500 mL graduated cylinder. The solution was transferred to a 1 L Duran bottle and stored at room temperature for use in the culture of *T. emersonii* in 5 L fermenters.

2.6 Culture Preparation

2.6.1 Preparation of PDA

PDA (19.5 g) was dissolved in 500 mL of ultrapure water by constant swirling in a 1L Duran glass bottle (no heating was required). The mixture was sterilised by autoclaving at 121 °C and 15 psi for 15 minutes. It was then cooled to 45 °C. Approximately 25 mL each, of the sterilised PDA, was poured into sterile petri dishes in a laminar flow cabinet and the agar was allowed to cool and set. The PDA plates were stored at 5 °C.

2.6.2 Preparation of Glycerol stocks

In order to prepare glycerol stocks of *Talaromyces emersonii*, 20% (v/v) glycerol solution was first prepared. Glycerol (20 mL) and ultrapure water (80 mL) were mixed thoroughly in a 100 mL Duran glass bottle. The 20% (v/v) glycerol solution was sterilised by autoclaving at 121 °C and 15 psi for 15 minutes.

In the laminar flow cabinet, 15 mL sterilin tubes were aliquoted with approximately 10 mL of the sterilised 20% (v/v) glycerol solution. A PDA plate containing actively growing culture of *Talaromyces emersonii* was removed from a 45 °C incubator. Two 1 cm² plugs from the outer regions of the actively growing fungal mycelial mat on the PDA plates were aseptically transferred to each of the 15 mL sterilin tubes. The tubes were clearly labelled and dated and stored at – 80 °C until required. The glycerol stocks could be stored at – 80 °C for up to five years. The stocks were thawed at room temperature prior to use.

2.6.3 Fermentation of *Talaromyces emersonii* in Shake Flasks or Fermenters

The culture of *T. emersonii* in shake flasks and fermenters involved the following steps:

- a) Sub-culture of *T. emersonii* from glycerol stocks onto fresh PDA plates. The glycerol stock was streak-plated on to fresh PDA plates using sterile 10 µL loops. The inoculated PDA plates were incubated at 45 °C for five days to allow for growth.
- b) Transfer of spores from PDA plates to glucose medium. Spores from the actively growing mycelial mat of *T. emersonii* from the previously inoculated PDA plates were transferred to a primary starter culture flask (250 mL flat-bottomed conical flask). The primary starter culture flask contained a 2% (w/v) glucose medium.

The inoculated primary starter culture flask was incubated at 45 °C for 48 hours in a shaker incubator at 250 rpm. After 48 hours, the contents of the primary starter culture flask were transferred to a secondary starter culture flask (1000 mL flat-bottomed conical flask). The secondary starter culture flask contained a 0.5% (w/v) glucose medium. The inoculated secondary starter culture flask was incubated for 24 hours at 45 °C in a shaker incubator at 250 rpm.

- c) Transfer of culture from the secondary starter culture flask to the high-solids production medium. The high-solids production medium contained components to enhance protein yield by *T. emersonii*. The medium was optimised in-house. The high solids production media could be set up in 1 L baffled flasks or in fermenters. The inoculated production medium began the fermentation process. The shake flasks and fermenters were run for 120-144 hours depending on the protein yield. Fractions were harvested at 0, 24, and 120 or 144 hours. After 24 hours, 1 mM CuSO₄ (final concentration in medium) was added to some of the shake flasks to induce the production of laccase.

2.7 Enzyme Cocktail Clean-up

2.7.1 Concentration and Buffer Exchange

The enzyme cocktails were concentrated using either the 500 µL or 20 mL Vivaspin® centrifugal concentrators. The 500 µL centrifugal filter units enabled small-scale concentration and buffer exchange for samples between 100-500 µL. The 20 mL concentrators allowed concentration and buffer exchange for samples up to 20 mL. They had a polyethersulphone membrane with a molecular weight cut-off of 10 kDa.

The concentrators were filled to the maximum volume (500 µL or 20 mL). The samples were then centrifuged for the recommended amount of time (17700 RCF for 30 minutes on fixed angle rotor for 500 µL concentrator and 3220 RCF for 45 minutes on swing bucket rotor type for 20 mL concentrator. 3220 RCF was the maximum allowed RCF for swing bucket rotor type). The filtrate container was emptied and the concentrator was refilled to the maximum volume with the buffer of choice (20 mM Potassium phosphate buffer, pH 6.4). The samples were centrifuged again as previously. The filtrate container was emptied and this process was repeated two more times. The concentrated, buffer

exchanged sample was recovered from the bottom of the concentrator pocket with a pipette.

2.8 Assays

2.8.1 Bradford Assay Method for Protein Concentration

The Bradford assay method was used to monitor and quantify protein in the fermentation fractions that were harvested at different time points (Bradford, 1976). The crude harvested fractions as well as concentrated and buffer exchanged harvested fractions were analysed. The samples were diluted appropriately (typically two- to ten- fold) to achieve a concentration suitably determinable by the assay. The samples were assayed in quadruplicates. Bovine serum albumin (BSA) standards (0.125-1.0 mg/ml) were prepared and assayed in quadruplicates along with the samples. Samples (5 μ L) were mixed with 250 μ L of 1X Bio-Rad Bradford Dye Reagent. The reaction mixture in the 96-well microplate was shaken for 10 minutes at 25 °C in the microplate reader. After 10 minutes, absorbances were determined at 595 nm using a Multiskan GO Microplate Reader.

2.8.2 Laccase Assay using ABTS as the substrate

Preparation of 5 mg/mL ABTS

Three ABTS tablets (10 mg/mL each) were dissolved in 6 mL of ultrapure water in a 15 mL sterilin tube. The solution was mixed vigorously until the tablets were fully dissolved in the buffer. The solution was prepared fresh and stored in ice and protected from light.

Preparation of enzyme control

The enzyme control used for the assay was laccase from *Trametes versicolor* with specific activity of 0.87 U/mg. A 10 mg/mL stock solution of the enzyme control was prepared by dissolving 20 mg of laccase powder in 2 mL of ultrapure water. The stock solution was diluted as detailed in the table below:

Table 2.8.2. 1: A Table displaying the volumes (μL) of laccase standard solution and ultrapure water required for the preparation of specific Units/mL of laccase for the laccase standard curve.

Tubes	8.7 U/mL Laccase Standard Dilution (μL)	Ultrapure Water (μL)	Laccase Concentration (Units/mL)
1	10 mg	1000	8.7
2	1.84 of Tube 1	1998.16	0.008
3	2.3 of Tube 1	1997.7	0.01
4	2.3 of Tube 1	997.7	0.02
5	4.6 of Tube 1	995.4	0.04
6	6.9 of Tube 1	993.1	0.06
7	9.2 of Tube 1	990.8	0.08
8	11.5 of Tube 1	988.5	0.1
9	0	250	0

Assay Procedure

Sample: Enzyme sample (50 μL) and ultrapure water (50 μL) in a 96-well PCR plate were incubated in 80 μL of 0.1 M citrate buffer (pH 3.0) for 30 minutes at 50 °C for enzyme test, enzyme blank, and substrate blank reaction mixtures respectively. After incubation, 50 μL each, of the reaction mixture was transferred to a 96-well microtitre plate, at room temperature. ABTS (50 μL) was added to the enzyme test and substrate blank wells of 96-well microtitre plates. The enzyme test samples were assayed in triplicate. The enzyme blank and substrate blank were included in duplicate. The enzyme blank consisted of 50 μL of the reaction mixture (containing enzyme sample and 0.1 M citrate buffer) from the 96-well PCR plate mixed with 50 μL of ultrapure water. The substrate blank consisted of 50 μL of the reaction mixture from the 96-well PCR plate (containing ultrapure water and 0.1 M citrate buffer) mixed with 50 μL of ABTS.

Enzyme Control: In a 96-well microtitre plate, 50 μL of the control enzyme was mixed with 50 μL of ABTS. The enzyme control was added as triplicates.

Absorbances were measured at 405 nm using the Multiskan GO Microplate Reader.

2.8.3 Laccase assay using Amplex Red as the substrate

Preparation of 80 μM of Amplex Red

DMSO (1.9 mL) was added to the vial containing 5 mg Amplex Red. The solution was mixed well. Stock solutions of Amplex Red were prepared by aliquoting 100 μL each of the Amplex Red-DMSO solution prepared above into 0.2 mL PCR Tube Strips. The stock solutions were stored at – 18 °C protected from light until required for use. Working solution of Amplex Red (80 μM) was prepared by dissolving 100 μL of the stock solution in 62.5 μL of DMSO and 12.5 mL of ultrapure water in a 15 mL sterilin tube.

Preparation of enzyme control

The enzyme control used for the assay was laccase from *Trametes versicolor* with specific activity of 0.87 U/mg. A 10 mg/mL stock solution of the enzyme control was prepared by dissolving 20 mg of laccase powder in 2 mL of ultrapure water. The stock solution was diluted as detailed in the table in section 2.8.2 above.

Assay Procedure

Sample: For the enzyme test samples, 120 μL of 0.1 M citrate buffer (pH 3.0) was mixed with 15 μL of enzyme sample and 15 μL of the Amplex Red solution in a 96-well PCR plate. The enzyme test samples were assayed in triplicate. An enzyme blank and substrate blank was also included in duplicate. The enzyme blank consisted of 15 μL of the enzyme sample mixed with 135 μL of 0.1 M citrate buffer (pH 3.0). The substrate blank consisted of 135 μL of 0.1 M citrate buffer (pH 3.0) and 15 μL of Amplex Red solution. The reaction mixture was incubated at 50 °C for 20 minutes. From the 96-well PCR plate, 100 μL each of the reaction mixture was transferred to a Black Assay Plate (96-well) after 10 minutes.

Enzyme Control: Eighty μL of 0.1 M citrate buffer (pH 3.0) was mixed with 10 μL of enzyme control and 10 μL of the Amplex Red solution in a Black Assay Plate (96-well). The reaction mixture was incubated at room temperature for 20 minutes. The enzyme control was assayed in triplicate.

The fluorescence spectra of laccase-Amplex Red reactions were measured at 583 nm using a high-throughput system (excitation 530 nm, emission 583 nm).

2.8.4 Catalase Assay using the Megazyme Assay Kit

The catalase assay kit by Megazyme contained the following reagents: 30 mL of 1.5 M potassium phosphate buffer at pH 7.0, lyophilised powder of peroxidase plus 4-aminoantipyrine, 20 mL of 3,5-Dichloro-2-hydroxybenzenesulphonate (DHBS) solution, 10 mL of ~ 1.3 M H_2O_2 standard solution and 4 g of catalase standard. The assay principle was based on measuring the decrease in H_2O_2 concentration following incubation of the analyte sample with an H_2O_2 standard solution. The reagents were prepared as per the manufacturer's instructions. The recommended assay procedure by the manufacturer was optimised for use at a microtitre scale.

Preparation of 15 mM Sodium Azide

In the Fume Hood, 97.5 mg of sodium azide was dissolved in 100 mL of ultrapure water in 250 mL glass beaker. The solution was mixed well until the azide was completely dissolved. The solution was transferred to a sterile 100 mL container. It was stored at 4 °C.

Preparation of Chromogenic Reagent

Potassium phosphate buffer (1.5 M, pH 7.0, and 30 mL) was added to ultrapure water (250 mL) in a 500 mL glass beaker. The beaker was covered in tin foil to protect the contents from light. Ten millilitres of the solution was added to the vial containing lyophilised powder of peroxidase plus 4-aminoantipyrine to resuspend the contents in the vial. The resuspended solution in the vial was transferred back to the beaker. The vial containing the DHBS solution was also emptied in to the 500 mL beaker. The pH was adjusted to 7.0 using 1 M HCl. The solution was constantly stirred using a magnetic stirrer. The reagent was aliquoted to 15 mL sterilin tubes covered in tin-foil to protect the contents from light. The sterilin tubes were stored at – 20 °C. According to the manufacturer, the reagent was stable for more than one year.

Preparation of 130 mM Hydrogen Peroxide working solution

0.2 mL of ~ 1.3 M H₂O₂ standard solution was added to 2 mL of 150 mM potassium phosphate buffer, pH 7.0 in a 2 mL microtube. The working solution of H₂O₂ was prepared fresh for each assay. It was stored in ice and was protected from light.

Preparation of Catalase Standards

The catalase standard provided in the assay kit was catalase powder from *Aspergillus niger* with specific activity of ~ 1.6 U/mg. However, the catalase standard used in the assays was catalase from *Aspergillus niger* in 3.2 M ammonium sulphate suspension. This was purchased separately from Megazyme and was preferred due to ease of use. The catalase solution had 400 000 U/mL of catalase activity. The control enzyme stock was first diluted to 2000 U/mL by diluting (dilution factor of 200). Five microlitres of catalase standard stock was added to 995 µL of 150 mM potassium phosphate buffer, pH 7.0. The 2000 U/mL catalase solution was diluted further as detailed in the table below.

Table 2.8.4. 1: A Table displaying the volumes (μL) of catalase standard solution and ultrapure water required for the preparation of specific Units/mL of catalase for the catalase standard curve.

Tubes	2,000 Units/mL Catalase Standard Dilution (μL)	Assay Buffer (μL)	Catalase Concentration (Units/mL)
1	5	995	2000
2	250 of Tube 1	750	500
3	140 of Tube 2	360	140
4	120 of Tube 2	380	120
5	100 of Tube 2	400	100
6	400 of Tube 5	100	80
7	375 of Tube 6	125	60
8	400 of Tube 7	200	40
9	250 of Tube 8	250	20
10	0	500	0

The diluted catalase standards were prepared fresh for each assay.

Assay Procedure

Ten microlitres of the diluted catalase standards and enzyme samples were added in triplicates to separate wells in a 96-well PCR plate. Ten microlitres of H_2O_2 working solution was added to each of the enzyme test, substrate blank, as well as the diluted catalase standard wells and the reaction mixtures were mixed. An enzyme blank and substrate blank were also included in duplicates for the test enzyme samples. The enzyme blank included 10 μL of enzyme sample and 10 μL of 20 mM potassium phosphate buffer, pH 6.4. The substrate blank contained 10 μL of 20 mM potassium phosphate buffer, pH 6.4 and 10 μL of H_2O_2 (130 mM). The PCR plate containing the reaction mixture was incubated at 35 °C for 2.5 minutes. The reaction was quenched by the addition of 180 μL of sodium azide after 10 minutes. Five microlitres of the reaction mix was transferred from the PCR plate to a 96-well microtitre plate and 145 μL of the chromogenic reagent was added to each of the wells. The microtitre plate was shaken on a microplate shaker for 30 minutes at 400 rpm. The absorbance was measured at 520 nm after 30 minutes using a Multiskan GO Microplate Reader.

2.8.5 Sodium Dodecyl Sulphate Gel Electrophoresis (SDS-PAGE)

1X Running Buffer: 1X running buffer was prepared by the addition of 100 mL of 10X pre-mixed TGS buffer to 900 mL of ultrapure water in a 1L graduated cylinder. The mouth of the cylinder was covered firmly in parafilm and the graduated cylinder was inverted gently to mix the solution.

Sample Preparation: Enzyme sample (19.5 μL) was mixed with 7.5 μL of 4 X lithium dodecyl sulphate (LDS) sample buffer and 3 μL of 10 X NuPAGE[®] reducing agent in a 1.5 mL Eppendorf centrifuge tube. The samples were mixed using a Vortex for 5 seconds and centrifuged for 1 minute at 3220 RCF. The samples were heated at 70 °C in a heat block for 10 minutes. The samples were then chilled on ice and centrifuged for 1 minute at 3220 RCF.

Electrophoresis: The comb and a green tape were removed from the gel prior to positioning the gel firmly on the gel holder cassette. The module was placed in the electrophoresis tank. The 1 X running buffer was filled in the inner chamber to check for leaks. After confirming that there were no leaks, the inner and outer chambers of the tank were filled with 1 X running buffer up to the appropriate guideline on the tank.

The protein ladder was loaded on the first lane. The protein samples were loaded into the remaining lanes. The volume of sample loaded into lanes depended on the number of wells on the gel. Fifteen μL of sample was loaded in a 12-well gel and 10 μL of sample was loaded in a 15-well gel. The inner chamber was topped up with 1 X running buffer and the tank was closed using the lid. The tank was connected to the power supply unit. The red lead (+) was inserted into the red output jack and the black lead (-) was inserted into the black output jack. Voltage was set to 200 V and the Run button was pressed to begin electrophoresis. Current flow was ensured by checking for bubbles rising from the electrode at the bottom of the tank. The gel run was completed in ~ 30-40 minutes.

The gel was imaged immediately after electrophoresis using the Bio-Rad ChemiDoc[™] MP Imaging System.

2.9 Protein Purification

Protein purification of the enzyme cocktail was carried out using the AKTA pure 25 system (at MBio) and a fraction collector (at DCU) to separate and characterise individual enzymes. HIC was the method of choice for initial purification of the *T. emersonii* cocktail. The hydrophobic properties of proteins were exploited by HIC. Protein-medium interactions were promoted by the addition of salt to the mobile phase. The proteins were adsorbed to the medium in a mobile phase containing a high concentration of salt. Most of the bound proteins were effectively desorbed by simply washing with elution buffer. Ammonium sulphate (1.2 M) had the best potential to reduce the complexity of the enzyme cocktail. Increasing the ammonium sulphate concentration resulted in an increase in the binding capacity of the column.

2.9.1 Preparation of 2 M Sodium Hydroxide

Using safety precautions, sodium hydroxide (80.0 g) was weighed out and added to a 1 L beaker. Ultrapure water (800 mL) was added to the beaker along with a magnetic stirrer. The solution was mixed vigorously until the sodium hydroxide was completely dissolved. The volume was adjusted with ultrapure water to 1 L in a volumetric flask. The solution was filtered through a 0.2 micron polyethersulphone filter, transferred to a borosilicate glass bottle, and stored at room temperature for up to three months. The borosilicate glass bottle holding the hydroxide solution was tightly capped to prevent carbon dioxide absorption from the air.

2.9.2 Preparation of 50 mM Sodium Phosphate/1.2 M Ammonium Sulphate, pH 7.0

Ammonium sulphate (158.57 g) and sodium phosphate (6.00 g) were weighed out and added to a 1 L beaker. The buffer solution was made up on a balance with an error of 0.01g. Ultrapure water (800 mL) was added to the beaker along with a magnetic stirrer. The solution was mixed vigorously until the mixture was completely dissolved. The pH was adjusted to pH 7.0 using 2 M sodium hydroxide. The volume was adjusted using ultrapure water to 1 L in a volumetric flask. The buffer was filtered through a 0.2 micron polyethersulphone filter, transferred to a borosilicate glass bottle and stored at room temperature.

2.9.3 Preparation of 50 mM Sodium Phosphate, pH 7.0

Sodium phosphate monobasic (5.999 g) was weighed out and added to a 1 L beaker. Ultrapure water (800 mL) was added to the beaker along with a magnetic stirrer. The solution was mixed vigorously until the sodium phosphate monobasic was completely dissolved. The pH was adjusted to pH 7.0 using 2 M sodium hydroxide. The volume was adjusted using ultrapure water to 1 L in a volumetric flask. The buffer was filtered through a 0.2 micron polyethersulphone filter, transferred to a borosilicate glass bottle and stored at room temperature.

2.9.4 Sample Preparation

Twenty-five mL of a 1/10 dilution in start buffer was prepared. The sample was filtered using 0.2 micron polyethersulphone filter. The start buffer was 50 mM sodium phosphate/1.2 M ammonium sulphate, pH 7.0.

2.9.5 Sample Application

The column (5 mL Hitrap Butyl HP column) was equilibrated with 5-10 column volumes (CV) of start buffer (50 mM sodium phosphate/1.2 M ammonium sulphate, pH 7.0; Mobile phase A).

Sample was applied to the column using the air sensor. Typically, the sample applied to the HIC column was dependent on protein concentration. A typical protein loading was between 20 and 40 mg total protein.

The column was washed with 5-10 CV of start buffer. Elution was carried out using a linear gradient of 50 % Mobile phase B (50 mM sodium phosphate, pH 7.0) over 50 X CV. The proportion of elution buffer was increased until the salt concentration reached a minimum, that is, salt-free buffer (100% elution buffer). The column was washed with 5 CV of salt-free elution buffer to elute any remaining hydrophobically bound material. The column was re-equilibrated with 5-10 CV of start buffer. Fractions were collected at all stages for further analysis.

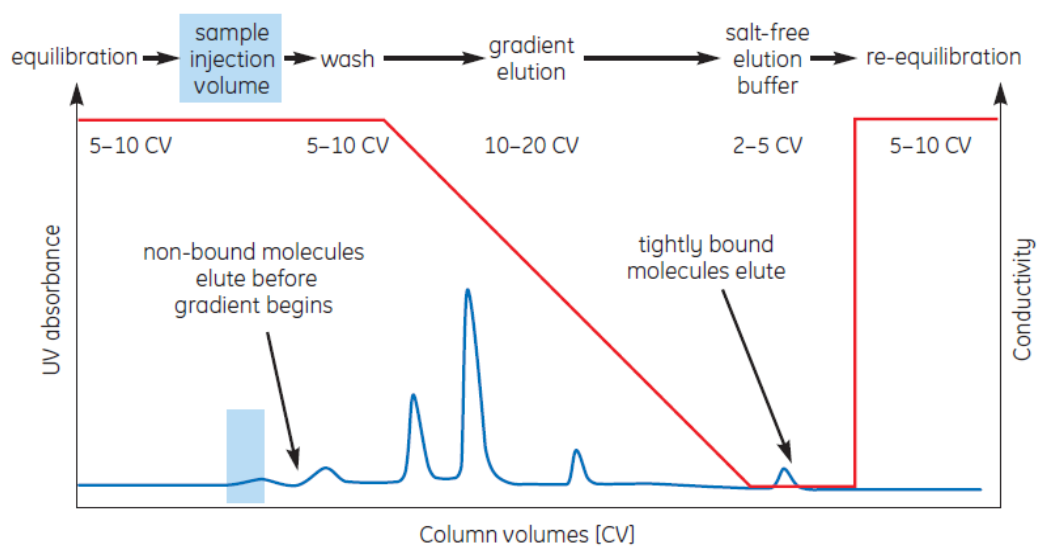


Figure 2.9.5. 1: Hydrophobic Interaction Chromatography separation showing a linear gradient

2.10 Proteomics Analysis

2.10.1 Sample Preparation

Protein extract (30 μ L) was mixed with 200 μ L of urea (8 M urea in 0.1 M Tris/HCl, pH 8.5) in a filter unit and centrifuged at 14000 \times g for 15 minutes. 200 μ L of urea was added

to the filter unit again and centrifuged at 14000 x g for 15 minutes. The flow-through from the collection tube was discarded. Iodoacetamide in urea solution (0.05 M; 200 μ L) was added to the filter unit. The mixture was mixed at 600 rpm in a thermo-mixer for 1 minute and then, incubated without mixing for 20 minutes. The filter units were centrifuged again for 10 minutes at 14000 x g. Urea (100 μ L) was added to the filter unit and centrifuged at 14000 x g for 15 minutes. This step was carried out twice. Ammonium bicarbonate solution (0.05 M; 100 μ L) was added to the filter unit and centrifuged at 14000 x g for 10 minutes. This step was carried out twice. Ammonium bicarbonate (40 μ L) with trypsin (enzyme to protein ration 1:100) was added to the filter unit and mixed at 600 rpm in thermo-mixer for 1 minute. The filter units were incubated in a wet chamber for 37 °C for 4-18 hours. After incubation, the filter units were transferred to new collection tubes. The filter units were then centrifuged at 14000 x g for 10 minutes. Ammonium bicarbonate (40 μ L) was added to the filter units after which they were centrifuged at 14000 x g for 10 minutes. The mixture in the filter unit was acidified using trifluoroacetic acid and the filtrate was desalted. The mixture was then stored at - 20 °C and analysed by mass spectrometry.

2.10.2 Label-free Liquid Chromatography Spectrometry

Mass spectrometric analysis of supernatant peptides was performed using an Ultimate 3000 NanoLC system coupled to a Q-Exactive mass spectrometer. 500 ng of each digested sample was loaded by an auto-sampler onto a C18 trap column. The trap column was switched on-line with an analytical Biobasic C18 Picofrit column. Peptides were eluted over a 65-minute binary gradient of Solvent A (2% (v/v) acetonitrile and 0.1% (v/v) formic acid in LC-MS grade water) and Solvent B (80% (v/v) acetonitrile and 0.1% (v/v) formic acid in LC-MS grade water). The 65-minute binary gradient was as follows: 3% solvent B for 5 minutes, 3-10% solvent B for 5 minutes, 10-40% solvent B for 30 minutes, 40-90% solvent B for 5 minutes, and 90% solvent B for 5 minutes and 3% solvent B for 10 minutes. The column flow rate was set to 0.3 μ L/min. Data were acquired with Xcalibur software. The mass spectrometer was externally calibrated and operated in positive, data-dependent mode. A full survey mass spectrometry scan was performed in the 300-1700 m/z range with a resolution of 140000 (m/z 200) and a lock mass of 445.12003. Collision-induced dissociation fragmentation was carried out with the fifteen most intense ions per scan and at 17500 resolution. Within 30 seconds, a dynamic

exclusion window was applied. An isolation window of 2 m/z and one microscan were used to collect suitable tandem mass spectra.

2.10.3 Protein Identification and Quantification

Proteins present in the Control vs. Copper Sulphate vs. Titanium Silicate proteomes were initially identified using Proteome Discoverer 1.4 against Sequence HT using the UniProtKB database (*Talaromyces emersonii*). The following search parameters were used for protein identification: (i) peptide mass tolerance set to 10 ppm, (ii) MS/MS mass tolerance set to 0.02 Da, (iii) an allowance of up to two missed cleavages, (iv) carbamidomethylation set as a fixed modification, and (v) methionine oxidation set as a variable modification. Peptides were filtered using a minimum XCorr score of 1.5 for 1, 2.0 for 2, 2.25 for 3, and 2.5 for 4 charge states, with peptide probability set to high confidence. XCorr was a search-dependent score employed by the SEQUEST HT search engine in Proteome Discoverer. It reflected the number of fragment ions that were common to two different peptides with the same precursor mass. Since the XCorr value was dependent upon the number of identified fragment ions, its value was usually higher for larger peptides. XCorr scores were filtered based on charge state, whereby, larger XCorr thresholds were used for higher charge states. For quantitative analysis, samples were evaluated with MaxQuant software (version 1.6.1.0) and the Andromeda search engine was used to explore the detected features against the UniProtKB database for *Talaromyces emersonii*. The following search parameters were used: (i) first search peptide tolerance of 20 ppm (ii) main search peptide tolerance of 4.5 ppm (iii) cysteine carbamidomethylation set as a fixed modification (iv) methionine oxidation set as a variable modification (v) a maximum of two missed cleavage sites, and (vi) a minimum peptide length of seven amino acids. The false discovery rate was set to 1% for both peptides and proteins using a target-decoy approach. Relative quantification was performed using the MaxLFQ algorithm. The “proteinGroups.txt” file produced by MaxQuant was further analysed in Perseus (version 1.5.1.6). Proteins that matched to the reverse database or a contaminants database or that were only identified by site were removed. The LFQ intensities were log₂ transformed, and only proteins found in all eight replicates in at least one group were used for further analysis. Data imputation was performed to replace missing values with values that simulate signals from peptides with low abundance chose from a normal distribution specified by a downshift of 1.8 times the mean standard deviation of all measured values and a width of 0.3 times this standard

deviation. A two-sample t-test was performed using $p < 0.05$ on the post imputed data to identify statistically significant differentially abundant proteins.

**CHAPTER 3: RESULTS & DISCUSSION – BIOINFORMATICS
ANALYSES**

3.1 Organism of Choice

The aim of this project is to discover industrially relevant oxidoreductases in fungi. The organism used for this purpose is *Talaromyces emersonii*.

T. emersonii is a thermophilic aerobic fungus. It is found naturally in compost heaps and other eco-systems degrading biomass-rich materials. *T. emersonii* is a ‘soft-rot’ species and can degrade all parts of plant material. It is a member of the Ascomycota phylum and produces comprehensive carbohydrate enzyme systems, including cellulolytic, hemicellulolytic, pectinolytic, and amylolytic enzymes, as well as an array of oxidoreductase and proteolytic activities. The advantage of using *T. emersonii* as a source of enzyme is that the microorganism has a long history of use in the food, beverage, agri-feed and pharmaceutical sectors. It is a ‘generally regarded as safe’ (GRAS) organism. A characteristic feature of many of the *T. emersonii* enzymes isolated to date is their thermotolerance or thermostability (Enzyme Consultancy Company, 2010).

T. emersonii is a filamentous fungus. Its taxonomic classification is as follows:

Kingdom: Fungi

Phylum: Ascomycota

Order: Eurotiales

Family: Trichocomaceae

Genus: *Talaromyces*

Species: *Talaromyces emersonii*

T. emersonii colonies on PDA grow very well, reaching whole plate in 5 days at 45 °C, forming abundant ascocarps and mixed with conidial structures. The colour is first white and then showing yellow shades which turn reddish-brown in age (Enzyme Consultancy Company, 2010).

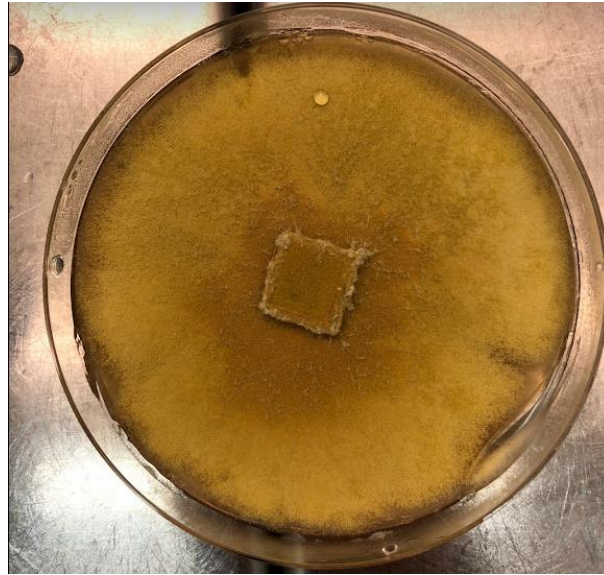


Figure 3.1. 1: An image of *T. emersonii* grown on PDA plate

3.2 Bioinformatics Analysis Procedure

The first step in the identification of oxidoreductases involved bioinformatics analysis of the results obtained from mass spectrometry. Bioinformatics analyses were carried out using Geneious and National Center for Biotechnology Information (NCBI) protein Basic Local Alignment Search (pBLAST).

Previously, mass spectrometry analysis had been carried out on two samples; namely, the in-house *T. emersonii* cocktail and pools of fractions from hydrophobic interaction chromatography of this cocktail. The mass spectrometry analysis generated a large list of proteins. While the mass spectrometric analysis identified the names of the vast majority of proteins present in the in-house cocktail, there still remained a few unknown proteins. Each identified protein (both known and unknown proteins) from the mass spectrometry data had a corresponding Talem code. Talem code refers to the in-house code for each gene present in *Talaromyces emersonii*. The Talem code enables easier identification of the protein sequences of the genes of interest in the bioinformatics tool Geneious

Oxidoreductases, as well as unknown proteins identified by mass spectrometry, were selected for bioinformatics analysis. The corresponding Talem code of each of the protein of interest was entered on the bioinformatics tool Geneious (<https://www.geneious.com/>). This generated the amino acid sequence of the proteins of interest. The amino acid

sequences obtained from Geneious for each of the proteins of interest were then entered on pBLAST as a BLAST search

(<https://blast.ncbi.nlm.nih.gov/Blast.cgi?PAGE=Proteins>). The search compared the query sequence with a library of sequences and identified sequences that resembled the query sequence (see Fig 3.2.1). Thus, it was possible to identify the unknown proteins from the mass spectrometry results. It also enabled confirmation that the oxidoreductases listed in the mass spectrometry data were correctly identified.

On completing the bioinformatics analysis, four main types of oxidoreductases present in the *T. emersonii* cocktail were selected for further identification by experimental analyses. The four main oxidoreductases selected were laccase, catalase, dehydrogenase, and copper-dependent lytic polysaccharide monooxygenase. These were the four oxidoreductases selected as bioinformatics analysis of the mass spectrometry data indicated that oxidoreductases were not as abundant in *T. emersonii* when compared to the glycosyl hydrolase family of enzymes. Furthermore, laccase, catalase, dehydrogenase, and copper-dependent lytic polysaccharide monooxygenase were the most common of the oxidoreductases in *T. emersonii* that were identified by mass spectrometry.

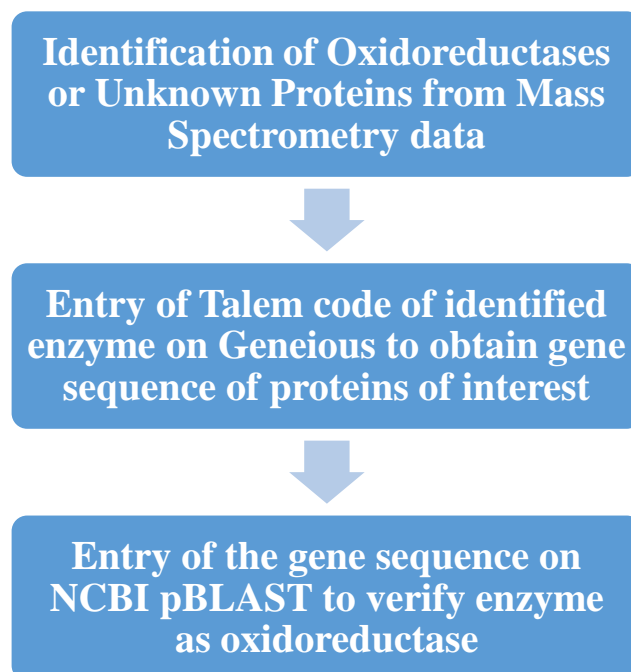


Figure 3.2. 1: The workflow for the identification of oxidoreductases of interest using data obtained from Mass Spectrometry, Geneious, and pBLAST

The bioinformatics workflow that enabled the identification of two oxidoreductase enzymes from the mass spectrometry data is outlined in detail below.

	A	B	C	D	E	F	G
1		Pool 1	Pool 2	Pool 3	Pool 4	Pool 5	Pool
2	Talem1p7_000240					Talem1p7_000240	
3	Talem1p7_00072	Talem1p7_00072	Talem1p7_000729		Talem1p7_00072	Talem1p7_000729	
4	Talem1p7_00073	Talem1p7_00073	Talem1p7_000739				
5	Talem1p7_00076	Talem1p7_00076	Talem1p7_00076	Talem1p7_00076	Talem1p7_00076	Talem1p7_000760	
6	Talem1p7_00081	Talem1p7_00081	Talem1p7_000811				
7	Talem1p7_00081	Talem1p7_000818					
8	Talem1p7_001201					Talem1p7_001201	
9	Talem1p7_001260			Talem1p7_00126	Talem1p7_00126	Talem1p7_001260	
10	Talem1p7_001448			Talem1p7_00144	Talem1p7_00144	Talem1p7_001448	
11	Talem1p7_001722		Talem1p7_00172	Talem1p7_00172	Talem1p7_00172	Talem1p7_001722	
12	Talem1p7_001871		Talem1p7_00187	Talem1p7_00187	Talem1p7_00187	Talem1p7_001871	
13	Talem1p7_00221	Talem1p7_00221	Talem1p7_002217				
14	Talem1p7_00276	Talem1p7_00276	Talem1p7_00276	Talem1p7_00276	Talem1p7_00276	Talem1p7_002789	
15	Talem1p7_003165		Talem1p7_003165				
16	Talem1p7_003349			Talem1p7_00334	Talem1p7_00334	Talem1p7_003349	
17	Talem1p7_003356			Talem1p7_00335	Talem1p7_00335	Talem1p7_003356	
18	Talem1p7_003788			Talem1p7_00378	Talem1p7_003788		
19	Talem1p7_00410	Talem1p7_00410	Talem1p7_00410	Talem1p7_00410	Talem1p7_00410	Talem1p7_004109	
20	Talem1p7_00442	Talem1p7_00442	Talem1p7_00442	Talem1p7_00442	Talem1p7_00442	Talem1p7_004424	
21	Talem1p7_004873		Talem1p7_00487	Talem1p7_004873			
22	Talem1p7_00494	Talem1p7_00494	Talem1p7_00494	Talem1p7_00494	Talem1p7_00494	Talem1p7_004943	
23	Talem1p7_00570	Talem1p7_00570	Talem1p7_005704				
24	Talem1p7_00580	Talem1p7_00580	Talem1p7_005803				
25	Talem1p7_00633	Talem1p7_00633	Talem1p7_00633	Talem1p7_00633	Talem1p7_00633	Talem1p7_006393	
26	Talem1p7_006470		Talem1p7_006470				
27	Talem1p7_00656	Talem1p7_006561					
28	Talem1p7_00657	Talem1p7_00657	Talem1p7_00657	Talem1p7_006572			
29	Talem1p7_00674	Talem1p7_00674	Talem1p7_006743				
30	Talem1p7_007190				Talem1p7_007190		
31	Talem1p7_00719	Talem1p7_00719	Talem1p7_00719	Talem1p7_00719	Talem1p7_007192		
32	Talem1p7_007483			Talem1p7_007483			
33	Talem1p7_00805		Talem1p7_00805	Talem1p7_00805	Talem1p7_00805		

Figure 3.2. 2: A snapshot of the Talem codes generated for the various proteins identified from mass spectrometry.

As can be seen in figure 3.2.2, the peptide sequences identified through mass spectrometry had a corresponding Talem code. While some proteins were identified, others remained unidentified. The Talem codes of unidentified proteins as well as oxidoreductase enzymes were entered on Geneious. Geneious is a DNA, RNA, and protein sequence alignment, assembly, and analysis software platform (Center for Cancer Research, no date). This was pivotal in obtaining the complete amino acid sequence of the proteins of interest.

```

>Talem1p7_011732 CATALASE
MRAVQLPSLAGLIGAASAVGCPYLTGQLDGREVHNPHEFQRRQDSGDAAAST
EQFLSQFYLNNDNSYMTTVDVGGPISDQNSLRAGERGPTLLEDIFRQKIQHFDH
ERVPERAVHARGAGAHGTFTSYGNWSNITAASFLSAEGKETPVFVRFSTVAGS
RGSSDTARDVHGFATRFYTDEGNFDIVGNNIPVFFIQDAILFPDLIHAVKPSPENE
IPQAATAHDSA WDFFSQQPSALHTVFWAMSGHGIPRSFRHMDGFGVHTFRFVT
DDGSSKL VKFHWTSLQGRAGLVWEEAQA AAGKNLDYMRQDLYDNEAGRYP
EWELGVQIVDEEDQLKFGFDLLDPTKILPVEYVPITPLGKLQLNRNPLNYFAETE
QIMFQPGHIVRGIDFTEDPLLQGR LFSYLDTQLNRNGGPNFEQLPINRPRVPFHN
NNRDGASQAFIPLNKAAYSPNTLNNGNPKQANQTVGDGFFTPGRTASGRLLR
AVSSTFSDVWSQPRLFYNLVP AEQQFLINAIRFENS NVKSEVVRKNVITQLNR
VDNDLARRVARAIGVEEPEPDPTYHNNKTANVGTFTGTP LKRIDGLKVGVLAT
VGDPSISQGGQSLSDT LSDSNVVTVVAESFTDGVDALYTNSDATNFDAVIVA
DGAEGLFAPSSFTAQPTNSSSTASLYPAGRPLQILVDAFRFGKPVGALGSGSKAL
DAAGISKSRPGVYVANSISEAFTDAIEDGLRTFKFLDRFALDE

```

```

> Talem1p7_007190 LACCASE
MGVFTFVATVFFQVFPFVGNDNGQIPLDLNVPVPGVQFRPYIPPEIAEQISYKQP
DKNFVCHYPSLIGWELCNGPDSRNCWLRDTQTKQIFSQFDIETDYEALWPPGI
TRYEWLEVSEHTISPDGFPKAGQVFNETYPGLIEACWGDELVIHVTNKLDPNG
TTIHWHGVRQLHSNDADGVNAITQCPIAQNTFTYRFTATQYGHWSYHSHYSL
QYPNGVAGPLLIHGPN SANWDLAWDP IFMEDWVHQS AFTEFVHELFPKLPES
DSVLLGGQGQFNSGGSIFTRIVPSGKRILLRLINTSADMHFIFSIDNHALKVVETD
FVPIEPYVTNSLSIAIGQRYSVIETNQTVDNYWIRTVPVQACSSNKTTLTGLTGI
LRYEGAPTALPTTTTQQGISYVCEDEPLASLKPIVRWEVGSSPANNVTDSTYEV
GQQIGRDGVL RWTIGEKPMFLNFS DPTLLSLDNKTFDPEYDVYKYDYDNKWW
YIVVTGNGELLPPVPGLDNSTRKFFNVSHPIHMHGHDFAILGRGDEPYNEDTDP
LTFNYHNPPRRDVALLPSNGWLA VAFRSDNPGVWLLHCHIAWHASSGLALQL
LERQGEILDVLGRQRVGAVEQTCIGWDQWLKIDGEKIDQEDSGI

```

Figure 3.2. 3: An image of the complete amino acid sequences of proteins obtained by entering the Talem codes on Geneious. The sequences highlighted in yellow refer to the peptide sequences obtained from mass spectrometry analysis. Alternatively, entering the peptide sequences obtained through mass spectrometry in Geneious could also be used to generate complete amino acid sequences of the proteins of interest.

Geneious was pivotal in obtaining the complete amino acid sequences of the proteins. However, the names of the proteins could not be identified using Geneious. The complete amino acid sequences of the proteins were entered on pBLAST to confirm and identify the results obtained from mass spectrometry.

catalase [Rasamsonia emersonii CBS 393.64]

Sequence ID: [XP_013328798.1](#) Length: 741 Number of Matches: 1

[See 1 more title\(s\) ▾](#)

Range 1: 1 to 741 [GenPept](#) [Graphics](#) [▾ Next Match](#) [▲ Previous Match](#)

Score	Expect	Method	Identities	Positives	Gaps
1518 bits(3929)	0.0	Compositional matrix adjust.	741/741(100%)	741/741(100%)	0/741(0%)
Query 1		MRAVQLLPSLAGLIGAASAVGCPYL TGQLDGREVHNPHEFQRRQDSGDAAASTEQFLSQF			60
Sbjct 1		MRAVQLLPSLAGLIGAASAVGCPYL TGQLDGREVHNPHEFQRRQDSGDAAASTEQFLSQF			60
Query 61		YLNDNNSYMTTDVGGPISDQNSLRAGERGPTLLEDIFRQKIQHFDHERVPERAVHARGA			120
Sbjct 61		YLNDNNSYMTTDVGGPISDQNSLRAGERGPTLLEDIFRQKIQHFDHERVPERAVHARGA			120
Query 121		GAHGTFSTSYGNWSNITAASFLSAEGKETPVFVRFSTVAGSRGSSDARDVHGFATRFYTD			180
Sbjct 121		GAHGTFSTSYGNWSNITAASFLSAEGKETPVFVRFSTVAGSRGSSDARDVHGFATRFYTD			180
Query 181		EGNFDIVGNNIPVFFIQDAILFPDLIHAVKPSPENEIPQAATAHDSAWDFFSQQPSALHT			240
Sbjct 181		EGNFDIVGNNIPVFFIQDAILFPDLIHAVKPSPENEIPQAATAHDSAWDFFSQQPSALHT			240
Query 241		VFWAMSGHGIPRSFRHMDGFGVHTFRFVTDDGSSKLVKFWHTSLQGRAGLVWEEAQAAG			300
Sbjct 241		VFWAMSGHGIPRSFRHMDGFGVHTFRFVTDDGSSKLVKFWHTSLQGRAGLVWEEAQAAG			300
Query 301		KNLDYMRQDLYDNI EAGRYPEWELGVQIVDEEDQLKFGFDLLDPTKILPVEYVPIITPLGK			360
Sbjct 301		KNLDYMRQDLYDNI EAGRYPEWELGVQIVDEEDQLKFGFDLLDPTKILPVEYVPIITPLGK			360
Query 361		LQLNRNPLNYFAETE QIMFQPGHIVRGIDF TEDPLLQGR LFSYLDTQLNRNGGPNFEQLP			420
Sbjct 361		LQLNRNPLNYFAETE QIMFQPGHIVRGIDF TEDPLLQGR LFSYLDTQLNRNGGPNFEQLP			420
Query 421		INRPRVPFHNNNRD GASQAF IPLNKAAYS PNTLNNGNPKQANQTVGDGFF TTPGRTASGR			480
Sbjct 421		INRPRVPFHNNNRD GASQAF IPLNKAAYS PNTLNNGNPKQANQTVGDGFF TTPGRTASGR			480
Query 481		LLRAVSS TFSDVWSQPRLFYNSLVAEQQFLINAI RFENSNVKS EVVRKNVITQLNRVDN			540
Sbjct 481		LLRAVSS TFSDVWSQPRLFYNSLVAEQQFLINAI RFENSNVKS EVVRKNVITQLNRVDN			540
Query 541		DLARRVARAIGVEEPEPDPTYHNNKTANVGTFGT PLKRIDGLKVGVLATVGD PDSISQG			600
Sbjct 541		DLARRVARAIGVEEPEPDPTYHNNKTANVGTFGT PLKRIDGLKVGVLATVGD PDSISQG			600
Query 601		QSLSDTLSDSNVVVTVAESF TDGVDALYTN SDATNFDAVIVADGA EGLFAPS SFTAQPT			660
Sbjct 601		QSLSDTLSDSNVVVTVAESF TDGVDALYTN SDATNFDAVIVADGA EGLFAPS SFTAQPT			660
Query 661		NSSSTASLYPAGRPLQILVDAFRFGK PVGALGSGSKALDAAGISKSRPGVYVANSISEAF			720
Sbjct 661		NSSSTASLYPAGRPLQILVDAFRFGK PVGALGSGSKALDAAGISKSRPGVYVANSISEAF			720
Query 721		TDAIEDGLRTRFKFLDRFALDE 741			
Sbjct 721		TDAIEDGLRTRFKFLDRFALDE 741			

Figure 3.2. 4: A snapshot of the results obtained in pBLAST that confirmed the identity of the protein as a catalase as was indicated in the mass spectrometry results. After entering the Talem code of the unknown proteins in Geneious, complete amino acid sequence of the protein was obtained. The amino acid sequence was entered on pBLAST as a query sequence in order to identify the protein.

Download GenPept Graphics

Multicopper oxidase [Rasamsonia emersonii CBS 393.64]
 Sequence ID: [XP_013325101.1](#) Length: 661 Number of Matches: 1
[See 1 more title\(s\)](#)

Range 1: 1 to 661 [GenPept](#) [Graphics](#) [Next Match](#) [Previous Match](#)

Score	Expect	Method	Identities	Positives	Gaps
1175 bits(3039)	0.0	Compositional matrix adjust.	586/668(88%)	594/668(88%)	39/668(5%)
Query 1	MGVFTFVATVFFQVFPFVGNQIPLDLNVVPVGVQFRPYIPPEIAEQISYKQPKNFV				60
Sbjct 1	MGVFTFVATVFFQVFPFVGNQIPLDLNVVPVGVQFRPYIPPEIAEQISYKQPKNFV				60
Query 61	CHYPSLIGWELCNGPDSRNCWLRDTQTKQPIFSQFDIETDYEALWPPGITREYWLEVSEH				120
Sbjct 61	CHYPSLIGWELCNGPDSRNCWLRDTQTKQPIFSQFDIETDYEALWPPGITREYWLEVSEH				120
Query 121	TISPDGFPKAGQVFNETYPGLIEACWGDELVIHVTKLPDNGTTIHWHGVRQLHSNDAD				180
Sbjct 121	TISPDGFPKAGQVFNETYPGLIEACWGDELVIHVTKLPDNGTTIHWHG+ +H + A				180
Query 181	G-VNAITQCPAQNTFTYRFTATQ-----YGH				208
Sbjct 181	AFANYTRTTPMGLMQLPNVQLRKTKPLTVSRLRSMACCNPSLESVDIANPAFSSSGHS				240
Query 209	WYHSHYSLQYPNGVAGPLLHIGPNSANWDLAWDPIFMEDWVHQSAFTFVHELFPKPLPE				268
Sbjct 241	WYHSHYSLQYPNGVAGPLLHIGPNSANWDLAWDPIFMEDWVHQSAFTFVHELFPKPLPE				300
Query 269	SDSVLLGGQGGFNSGGGIFTRIVPSGKRILLRLINTSADMHFIFSIDNHALKVVETDFVP				328
Sbjct 301	SDSVLLGGQGS-----SRYPFIDFDTNH--LRCLVTSADMHFIFSIDNHALKVVETDFVP				353
Query 329	IEPYVTNSLSIAIGQRYSVIIETNQTVDNWIRTVPVQACSSNKTTLTGLTGILRYEGAP				388
Sbjct 354	IEPYVTNSLSIAIGQRYSVIIETNQTVDNWIRTVPVQACSSNKTTLTGLTGILRYEGAP				413
Query 389	TALPTTTTQGGISYVCEDEPLASLKPIVRWEVGSPPANNVTDSTYEVGQQIGRDGVLRT				448
Sbjct 414	TALPTTTTQGGISYVCEDEPLASLKPIVRWEVGSPPANNVTDSTYEVGQQIGRDGVLRT				473
Query 449	IGEKPMFLNFSIPTLLSLDNKTFDPEYDVYKYDYDNKVVYIVVTGNGELLPPVPGLDNST				508
Sbjct 474	IGEKPMFLNFSIPTLLSLDNKTFDPEYDVYKYDYDNKVVYIVVTGNGELLPPVPGLDNST				533
Query 509	RKFFNVSHPIHMHGHDFAILGRGDEPYNEDTDPLTFNYHNPPRRDVALPSNGWLAVAFR				568
Sbjct 534	RKFFNVSHPIHMHGHDFAILGRGDEPYNEDTDPLTFNYHNPPRRDVALPSNGWLAVAFR				593
Query 569	SDNPGVWLLHCHIAMHASSGLALQLLERQGEILDVLRQVRGAVEQTCIGWDQWLKDGEK				628
Sbjct 594	SDNPGVWLLHCHIAMHASSGLALQLLERQGEILDVLRQVRGAVEQTCIGWDQWLKDGEK				653
Query 629	IDQEDSGI 636				
Sbjct 654	IDQEDSGI 661				

Figure 3.2. 5: A snapshot of the results obtained in pBLAST that confirmed the identity of the protein as laccase as was indicated in the mass spectrometry results. After entering the Talem code of the unknown proteins in Geneious, complete amino acid sequence of the protein was obtained. The amino acid sequence was entered on pBLAST as a query sequence in order to identify the protein.

The pBLAST search confirmed that the proteins of interest were catalase and laccase respectively.

As can be seen in Figure 3.2.4, one of the catalases present in *T. emersonii* was identified in pBLAST with 100% sequence homology between the query sequence obtained from Geneious and the subject sequence in pBLAST. The sequence was 741 amino acids in length. As can be seen in Figure 3.2.5, an 88% sequence match was also found in

pBLAST between the amino acid sequence for laccase obtained from Geneious and the sequence for a multicopper oxidase for *T. emersonii*.

3.3 Discussion

The procedure outlined in section 3.2 was carried out for each of the unknown proteins from the mass spectrometry data. It was also repeated for proteins identified as oxidoreductases by mass spectrometry. This was to ensure that the oxidoreductases were correctly identified. Bioinformatics analysis of the mass spectrometry data provided an understanding of the different types of proteins present in *T. emersonii*. It was also key in deducing that catalase isoforms were present in the in-house *T. emersonii* cocktail. Furthermore, the bioinformatics work enabled progression to the experimental stage of the project.

Of the proteins identified as oxidoreductases, only four were selected for further experimental analyses and characterisation due to time constraints. The oxidoreductases selected for further work were laccase, catalase, dehydrogenase, and lytic polysaccharide monooxygenase.

CHAPTER 4: RESULTS & DISCUSSION - LACCASE

4.1 Introduction

After the selection of candidate enzymes from the mass spectrometry data and bioinformatics, standard operating procedures (SOPs) were drafted for the detection and quantification of laccase activity in the in-house enzyme cocktail.

Two SOPs were drafted for the assay of laccase activity. They involved the use of ABTS and Amplex red as substrates respectively. The assay using ABTS was a spectrophotometric method with a lowest detection limit of 0.6 mU/mL of laccase (Pardo et al., 2013). The assay using Amplex red as the substrate was a fluorimetric assay with a lowest detection limit of 1.76 mU/mL (Wang et al., 2017a). The assays were carried out in quadruplicates unless otherwise stated.

Using the newly-drafted SOPs, laccase assay was initially carried out using the ABTS method for the in-house *T. emersonii* enzyme cocktail which had been obtained through biomass fermentation runs using 5 L benchtop bioreactors. The initial fermentation runs were carried out by the MBio Fermentation Department. However, after the assays were optimised, the *T. emersonii* cocktails were obtained by culturing the organism independently using shake flasks and bench-top bioreactors. This enabled the use of fresh enzyme cocktails for the assays.

4.2 Preliminary Results from the in-house *T. emersonii* cocktail

Table 4.2. 1: A table displaying the mg/mL (\pm SD), U/mL of laccase (\pm SD), and specific activity (U/mg) in the buffer exchanged in-house *T. emersonii* cocktail. SD = Standard Deviation.

Fraction	Protein Conc. (\pm SD) (mg/mL)	U/mL Laccase (\pm SD)	Specific Activity (U/mg)
Buffer Exchanged in-house <i>T.</i> <i>emersonii</i> cocktail	0.913 \pm 0.01	0.01 \pm 0.05	0.013

Laccase activity could not be detected in the crude enzyme cocktail. Therefore, as per the method outlined in section 2.7.1, buffer exchange was carried out to remove nonspecific medium components of low molecular weight from the in-house enzyme cocktail. Laccase activity was then successfully detected in the enzyme cocktail after buffer exchange as can be seen from Table 4.2.1. A positive colour change from light to dark

green was observed indicating the reaction of laccase with ABTS. The laccase activity in the buffer-exchanged enzyme cocktail was 0.01 ± 0.05 U/mL.

Sodium Azide (0.01% final concentration in production medium) was added to the production medium to prevent contamination during culture. Sodium azide was an inhibitor of laccase activity. The reason for this is that laccases contain copper ions that act to accept and transfer electrons to reduce molecular oxygen. Consequently, laccase is susceptible to agents that chelate or reduce copper. Sodium azide is a chelating agent and therefore, acts as an inhibitor of laccase activity (Couto and Toca, 2006).

It was hypothesised that the sodium azide was removed during buffer exchange. Consequently, laccase was detectable in the enzyme cocktail after buffer exchange.

4.3 Preliminary Results from HIC of the in-house *T. emersonii* cocktail

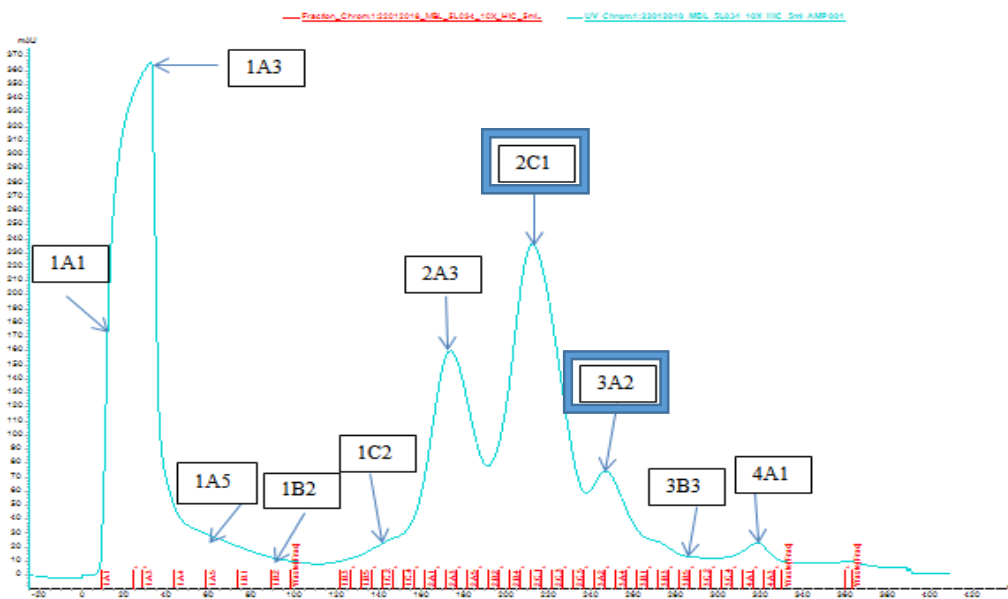


Figure 4.3. 1: An image of the HIC UV profile with linear gradient [1.2 M ammonium sulphate in 50 mM sodium phosphate, pH 7.0] in for the in-house *T. emersonii* cocktail. The UV chromatogram is depicted in blue, the eluted fractions are depicted in red. The image is a screenshot from the ÄKTA Pure 25 Chromatography System software. The fractions that were selected for buffer-exchange are indicated in the figure. The fractions in which laccase activity was detected after buffer-exchange are outlined with a blue frame.

As carried out for the in-house enzyme cocktail, all of the crude fractions obtained from HIC of the *T. emersonii* cocktail were also screened for laccase activity using ABTS as the substrate. The assay was carried out on single samples due to the low sample volumes available for analysis. A spectrophotometric signal was obtained for some of the eluted

HIC fractions. However, despite this, a positive colour change was not observed in the reaction wells as laccase present in the samples were below the LOQ of 0.6 mU/mL. The reaction mixture in the wells was turbid due to the formation of precipitate. Precipitate formation was observed in the reaction wells due to the high salt concentration present in the eluted HIC fractions.

Therefore, it was decided to select specific HIC fractions from the UV chromatogram that formed the peaks and/or were close to those peaks. The selected HIC fractions were 1A1, 1A3, 1A5, 1B2, 1C2, 2A3, 2C1, 3A2, 3B3, and 4A1. The corresponding mL eluted were 14.2 mL (1A1), 33.9 mL (1A3), 63.9 mL (1A5), 93.9 mL (1B2), 146.9 mL (1C2), 176.8 mL (2A3), 216.8 mL (2C1), 246.8 mL (3A2), 276.8 mL (3B3), 316.8 (4A1). These fractions were buffer exchanged as per section 2.7.1 and then were assayed for laccase activity using ABTS. Again, the assay was performed on single samples due to the low sample volumes available. A positive colour change (due to laccase activity on ABTS) was observed in two of the ten fractions that were assayed, namely- 2C1 and 3A2 (shown in Figure 4.3.1).

Although laccase activity was detected in the buffer exchanged HIC fractions, it was below the limit of quantitation. It was hypothesised that the poor yield of the enzyme may have been due to the age of the cocktail, which had been processed and stored at 5 °C for approximately 4 months before a HIC run was carried out (on the ÄKTA Pure 25 Chromatography System by the Senior Scientist at MBio (protein purification method, section 2.9)). Therefore, it was assumed that proteases present in enzyme cocktail had probably broken down the laccase during storage. Consequently, it was decided to set up shake flask fermentations independently of the Fermentation Department in order to provide fresh *T. emersonii* cocktails for assays.

4.4 Shake Flask Analyses

Table 4.4. 1: A table listing the protein concentration (mg/mL) of the shake flask cultures that were set up to obtain fresh enzyme cocktail for assays. nd = not determined.

Time (Hours)	Protein Concentration (mg/mL) (\pm SD)			
	Shake Flask 1A	Shake Flask 1B	Shake Flask 1C	Shake Flask 1D
0	0.45 \pm 0.02	0.46 \pm 0.02	0.44 \pm 0.01	0.50 \pm 0.02
24	0.31 \pm 0.01	0.44 \pm 0.03	0.37 \pm 0.01	0.34 \pm 0.01
96	0.33 \pm 0.01	0.28 \pm 0.01	0.35 \pm 0.01	0.27 \pm 0.01
120	0.36 \pm 0.01	0.39 \pm 0.02	Flask broke: nd	0.39 \pm 0.05

Table 4.4. 2: A table listing the protein concentration (mg/mL) of the shake flask cultures that were set up to obtain fresh enzyme cocktail for assays.

Time (Hours)	Protein Concentration (mg/mL) (\pm SD)			
	Shake Flask 2A	Shake Flask 2B	Shake Flask 2C	Shake Flask 2D
0	0.40 \pm 0.05	0.33 \pm 0.01	0.30 \pm 0.02	0.31 \pm 0.01
96	0.26 \pm 0.01	0.16 \pm 0.01	0.26 \pm 0.03	0.33 \pm 0.01
120	0.26 \pm 0.02	0.12 \pm 0.00	0.33 \pm 0.02	0.35 \pm 0.01
144	0.23 \pm 0.02	0.08 \pm 0.01	0.32 \pm 0.02	0.35 \pm 0.00

Table 4.4. 3: A table listing the protein concentration (mg/mL) of the shake flask cultures that were set up to obtain fresh enzyme cocktail for assays. There are two values for protein concentration for Shake Flask 3C. The values in italics refer to the protein concentration estimated following buffer exchange.

Time (Hours)	Protein Concentration (mg/mL) (\pm SD)					
	Shake Flask 3A	Shake Flask 3B	Shake Flask 3C		Shake Flask 3D	Shake Flask 3E
0	0.29 \pm 0.01	0.29 \pm 0.01	0.31 \pm 0.01	0.85 <i>\pm0.08</i>	0.30 \pm 0.00	0.28 \pm 0.00
96	0.25 \pm 0.00	0.23 \pm 0.01	0.24 \pm 0.01	0.77 \pm <i>0.10</i>	0.22 \pm 0.01	0.24 \pm 0.01
120	0.38 \pm 0.03	0.35 \pm 0.02	0.39 \pm 0.01	0.63 \pm <i>0.04</i>	0.38 \pm 0.02	0.36 \pm 0.01
144	0.23 \pm 0.00	0.22 \pm 0.00	0.24 \pm 0.01	0.63 \pm <i>0.06</i>	0.23 \pm 0.01	0.18 \pm 0.01

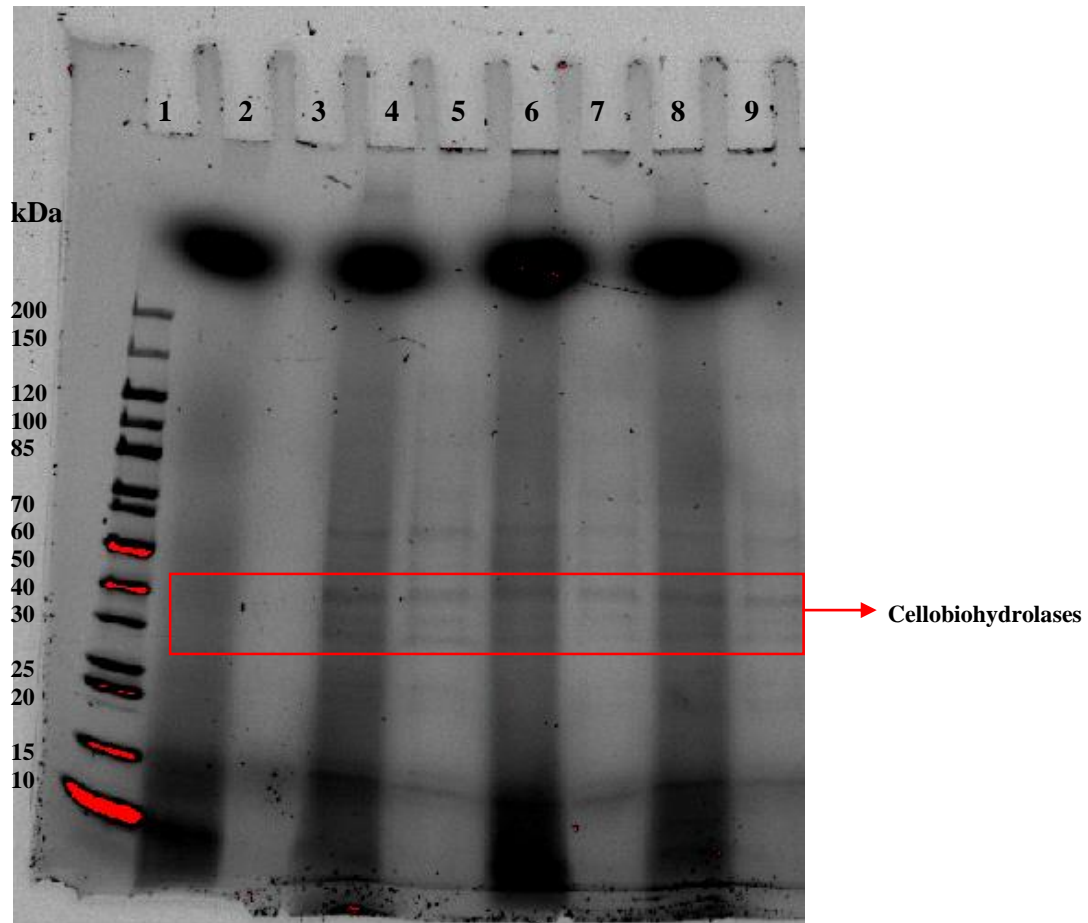


Figure 4.4. 1: SDS-PAGE analysis displaying the typical profile of *T. emersonii* proteins from Shake Flask 3C fractions before and after buffer exchange. The arrow corresponds to the protein bands formed by Cellobiohydrolase isoforms (~30-42 kDa).

(Lane 1: PageRuler™ Unstained Protein Ladder; Lane 2: 0 Hours Non-Buffer Exchanged; Lane 3: 0 Hours Buffer Exchanged; Lane 4: 96 Hours Non-Buffer Exchanged; Lane 5: 96 Hours Buffer Exchanged; Lane 6: 120 Hours Non-Buffer Exchanged, Lane 7: 120 Hours Buffer Exchanged, Lane 8: 144 Hours Non-Buffer Exchanged, Lane 9: 144 Hours Buffer Exchanged).

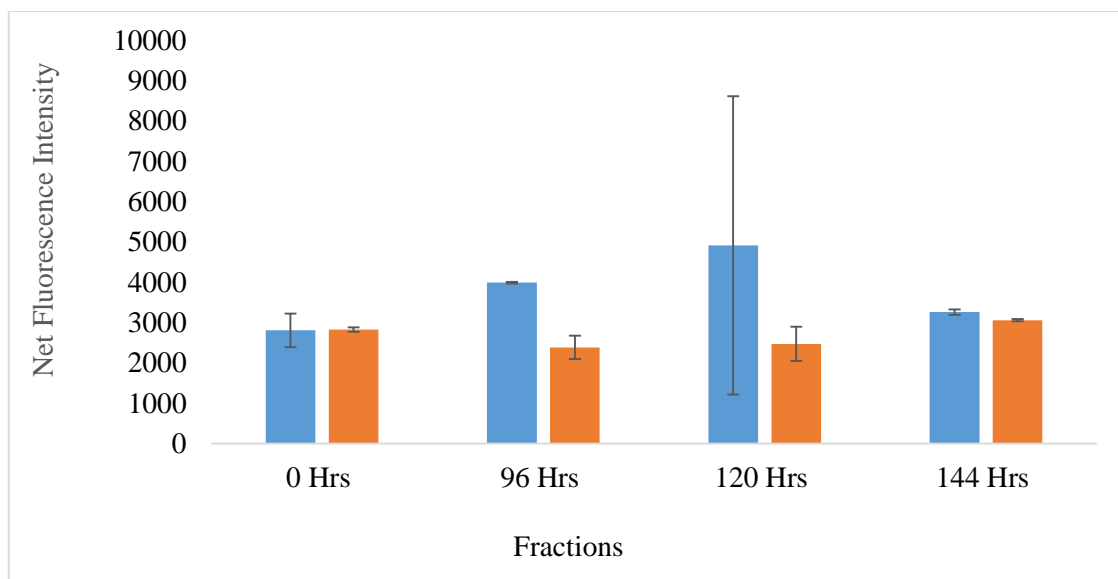


Figure 4.4. 2: Net fluorescence intensity of Shake Flask 3C Fractions (Pre- and Post- Buffer Exchange). A graph showing the difference in the net fluorescence intensity of the Shake Flask 3C fractions before and after buffer exchange at 0, 96, 120, and 144 hours. The blue and orange represent net fluorescence intensity before and after buffer exchange respectively. The net fluorescence intensity refers to the blank adjusted fluorescence intensity values.

As mentioned previously, training was received at MBio for the culture of *T. emersonii* in shake flasks and benchtop bioreactors to provide fresh cocktails for the enzyme assays. It was decided to begin the culture at a smaller scale using shake flasks. To do so, several initial trials were carried out in shake flasks to optimise the enzyme production conditions. The method used for the culture of *T. emersonii* is described in section 2.6. The outcome of three optimised shake flask experiments is indicated in Tables 4.4.1, 4.4.2, and 4.4.3 and Figure 4.4.1.

The protein concentration was quantified using the Bradford Assay (section 2.8.1). Protein concentration was analysed at specific time points to gain an understanding of the protein production at different times in the culture process. This also served as a means of comparison between previous batches that were cultured both (i) independently and (ii) by the MBio Fermentation Department. Furthermore, shake flask cultures were usually undertaken in quadruplicates or quintuplicates. Due to time constraints, it was not feasible to assay enzyme cocktails from each of the shake flask fractions. Therefore, knowledge of the protein concentration in each of the enzyme cocktails from the different shake flasks enabled selection of the flask with the highest protein concentration for further analyses.

The protein concentration results of three different shake flask batches (Tables 4.4.1, 4.4.2, and 4.4.3), indicated that there was an initial decrease in the protein concentration at 24 hours. This was expected, as the decrease was a result of the breakdown of the medium components by the fungus to be utilised for growth. Additionally, time was also required by the fungus to adjust to the new growth environment. There was a slight increase in protein concentration at 96 hours as the fungus adjusted to the growth environment in the medium and began protein production. Allowing for batch to batch variations between the shake flasks, it was clear that the maximum protein production was at 120 hours before a decrease in the protein concentration occurred at 144 hours. This too was as expected due to the exhaustion of nutrients in the medium by the fungus.

An SDS-PAGE analysis was also undertaken to ensure that the protein profile was similar to that obtained in previous batches at MBio (see figure 4.4.1). Black aggregates were visible at the top of the gel for the non-buffer exchanged fractions. This is thought to be due to the inadequate denaturation of proteins by the sample buffer. From the gel, a difference was observed between the non-buffer-exchanged and buffer-exchanged fractions. It was evident that nonspecific production medium components such as salts were removed from the enzyme cocktail following buffer exchange. The protein bands were more clearly visible in the buffer-exchanged fractions for all time points except for 0 hours. No protein bands were observed at 0 hours. This was as expected as protein production did not begin until 96 hours. The protein bands observed for 96, 120, and 144 hours were indicative of the typical glycosyl hydrolase enzymes.

From previous shake flask trials, it was clear that laccase could not be detected in the enzyme cocktails by the ABTS assay method. Therefore, it was decided to carry out buffer exchange of Shake Flask 3C fractions from 0, 96, 120, and 144 hours prior to assay by the more sensitive Amplex Red assay method. Shake Flask 3C was selected to be used for buffer-exchange and for further assays it had the highest protein concentration of the five flasks that were set up. The protein concentration was estimated to be greater in the buffer-exchanged fractions than in the crude enzyme cocktail fractions, as can be seen in Table 4.4.3 for Shake Flask 3C. Removal of nonspecific low molecular weight components such as salts present in the production medium probably accounts for the differences in the protein concentration. Furthermore, through buffer-exchange, the ultrapure water used to store the enzyme cocktail fractions was replaced with buffer (20

mM Potassium phosphate buffer, pH 6.4) that was more optimum for laccase storage and activity. This was also thought to have influenced the detection of laccase after buffer-exchange.

As shown in Figure 4.4.2, an Amplex Red fluorescence signal was detected for Shake Flask 3C fractions before and after buffer exchange. Although laccase could be detected, the very low U/mL levels of laccase could not be quantified. Furthermore, the fluorescence intensity signal was higher in the crude shake flask fractions instead of the buffer exchanged shake flask fractions. This may be due to interference of nonspecific production media components such as salts present in the crude fractions. However, the difference in fluorescence intensity values was not statistically significant ($p > 0.01$).

Because of the low yields encountered, it was decided to use inducers to enhance laccase expression by *T. emersonii*.

4.5 Induction of Laccase Activity in Shake Flasks

Table 4.5. 1: A table listing the protein concentration (mg/mL) of the shake flask cultures that were set up to obtain fresh enzyme cocktail for assays. Four shake flasks were set up: two were controls and two contained 1 mM copper sulphate added after 24 hours of culture. The values in italics beside Shake Flasks 4A and 4D refer to the protein concentration after 2 X concentration and buffer-exchange.

Time (Hours)	Protein Concentration (mg/mL) (\pm SD)					
	Shake Flask 4A (Control)		Shake Flask 4B (Control)	Shake Flask 4C (+ CuSO ₄)	Shake Flask 4D (+ CuSO ₄)	
0	0.35 \pm 0.03		0.45 \pm 0.02	0.46 \pm 0.01	0.36 \pm 0.01	
24	0.19 \pm 0.01		0.20 \pm 0.02	0.20 \pm 0.02	0.18 \pm 0.02	
96	0.23 \pm 0.02		0.23 \pm 0.04	0.60 \pm 0.03	0.61 \pm 0.02	
120	0.34 \pm 0.03	<i>0.37 \pm 0.03</i>	0.24 \pm 0.02	0.59 \pm 0.03	0.65 \pm 0.02	<i>1.56 \pm 0.06</i>

Table 4.5. 2: A table listing the protein concentration (mg/mL) of the shake flask cultures set up to obtain fresh enzyme cocktail for assays. Four shake flasks were set up: two were controls and two contained 1 mM copper sulphate after 24 hours of culture. The values in italics beside Shake Flasks 5A and 5B refer to the protein concentration after 2 X concentration and buffer-exchange. The protein concentration for one of the two of the control Shake Flasks could not be quantified as a result of breakage of the flask during culture due to technical difficulties.

Time (Hours)	Protein Concentration v(mg/mL) (\pm SD)					
	Shake Flask 5A (Control)		Shake Flask 5B (+ CuSO ₄)		Shake Flask 5C (+ CuSO ₄)	
0	0.24 \pm 0.02		0.34 \pm 0.05		0.41 \pm 0.01	
24	0.15 \pm 0.01		0.15 \pm 0.03		0.20 \pm 0.02	
120	0.19 \pm 0.00	<i>0.24 \pm 0.02</i>	0.42 \pm 0.01	<i>0.49 \pm 0.02</i>	0.43 \pm 0.02	

Table 4.5. 3: A table listing the protein concentration (mg/mL), U/mL of laccase, U/mg of laccase specific activity, IU/mL of β -Glucosidase, Glucanase, and Cellobiohydrolase in Shake Flasks 4A, 4D, 5A, and 5B at 120 hours with copper added at 24 hours. The values in italics refer to the IU/mL of each of the enzymes after 2X concentration and buffer exchange. <LoQ = Below limit of quantitation.

Flask	4A		4D		5A		5B	
1 mM CuSO ₄ [-/+]	-		+		-		+	
Protein (mg/mL)	0.34 \pm 0.03	<i>0.37 \pm 0.03</i>	0.65 \pm 0.02	<i>1.56 \pm 0.06</i>	0.19 \pm 0.00	<i>0.24 \pm 0.02</i>	0.42 \pm 0.01	<i>0.49 \pm 0.02</i>
Laccase (U/mL)	< LoQ		< LoQ	<i>0.14 \pm 0.05</i>	0.017 \pm 0.02	<i>0.020 \pm 0.01</i>	0.019 \pm 0.01	<i>0.045 \pm 0.05</i>
Laccase specific activity (U/mg)	< LoQ		< LoQ	<i>0.009</i>	0.089	<i>0.083</i>	0.045	<i>0.918</i>
β -Glucosidase (U/mL)	0.41 \pm 0.01	<i>1.06 \pm 0.02</i>	1.20 \pm 0.01	<i>4.46 \pm 0.19</i>	0.66 \pm 0.01	<i>1.03 \pm 0.01</i>	1.61 \pm 0.04	<i>4.90 \pm 0.11</i>
Endoglucanase (U/mL)	7.76 \pm 0.17	<i>20.79 \pm 0.65</i>	42.06 \pm 1.36	<i>139.92 \pm 28.88</i>	26.79 \pm 0.36	<i>33.13 \pm 0.53</i>	52.92 \pm 2.57	<i>196.98 \pm 6.63</i>
Cellobiohydrolase (U/mL)	0.10 \pm 0.00	<i>0.21 \pm 0.01</i>	0.31 \pm 0.01	<i>1.26 \pm 0.02</i>	0.23 \pm 0.01	<i>0.41 \pm 0.01</i>	0.43 \pm 0.02	<i>1.48 \pm 0.02</i>

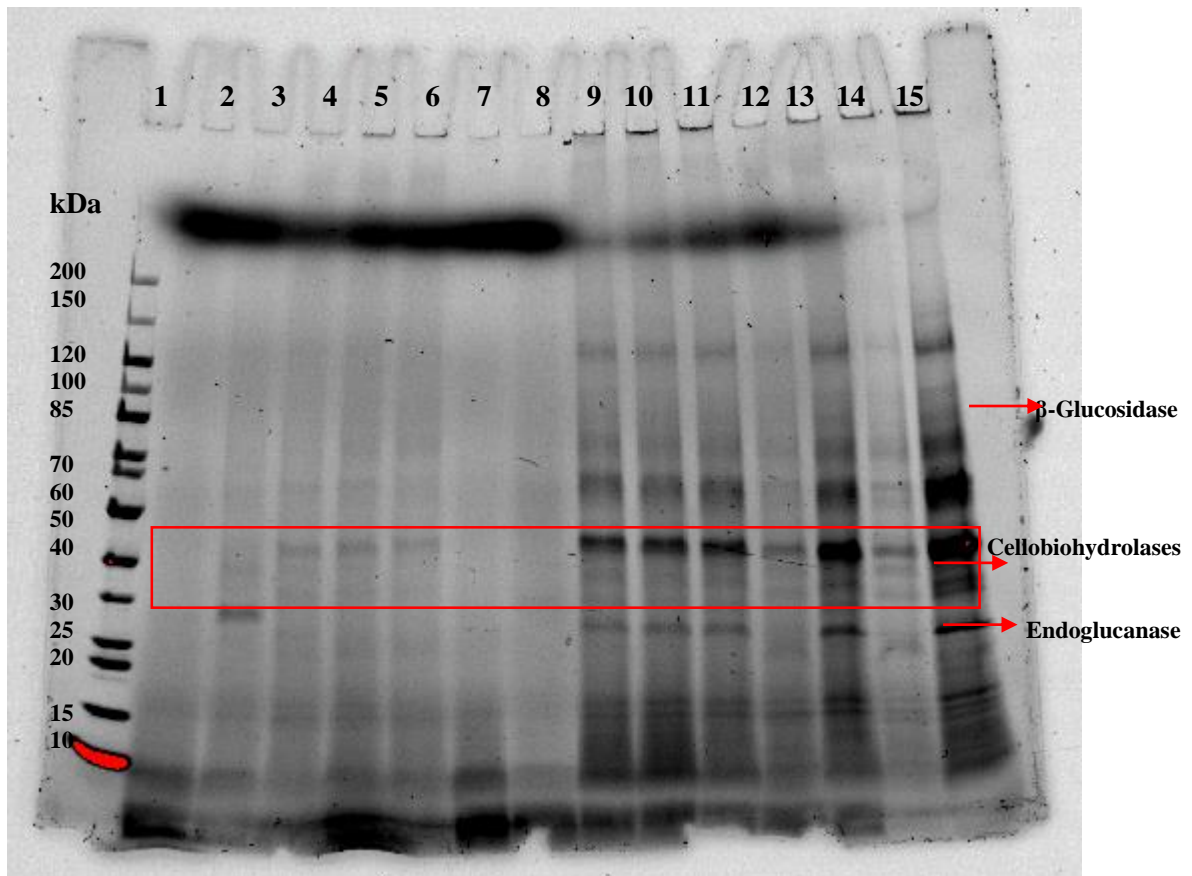


Figure 4.5. 1: SDS-PAGE analysis displaying the typical profile of *T. emersonii* proteins from of Shake Flask 4A and 4D fractions. The arrows correspond to the protein bands formed by β -Glucosidase (~90 kDa), Cellobiohydrolase isoforms (~30-42 kDa), and Endoglucanase (~27 kDa).

Shake Flask 4 A samples were not induced with 1 mM CuSO_4 . Shake Flask 4D fractions were induced with 1 mM CuSO_4 at 24 hours of culture. Lanes 2-6 display protein profile of Shake Flask 4A fractions from 0, 24, 96, 120, and 144 hours Lanes 7-11 display protein profile Shake Flask 4D fractions from 0, 24, 96, 120, and 144 hours.

(Lane 1: PageRuler™ Unstained Protein Ladder; Lanes 2-6: Shake Flask 4A fractions from 0 Hrs, 24 Hrs, 96 Hrs, 120 Hrs, and 144 Hrs; Lanes 7-11: Shake Flask 4D fractions from 0 Hrs, 24 Hrs, 96 Hrs, 120 Hrs, and 144 Hrs; Lane 12: Shake Flask 4A 120 Hrs 2 X Concentrated; Lane 13: Shake Flask 4D 120 Hrs 2 X Concentrated; Lane 14: Shake Flask 4A 120 Hrs 2 X Concentrated and Buffer-Exchanged; Lane 15: Shake Flask 4D 120 Hrs 2 X Concentrated and Buffer-Exchanged).

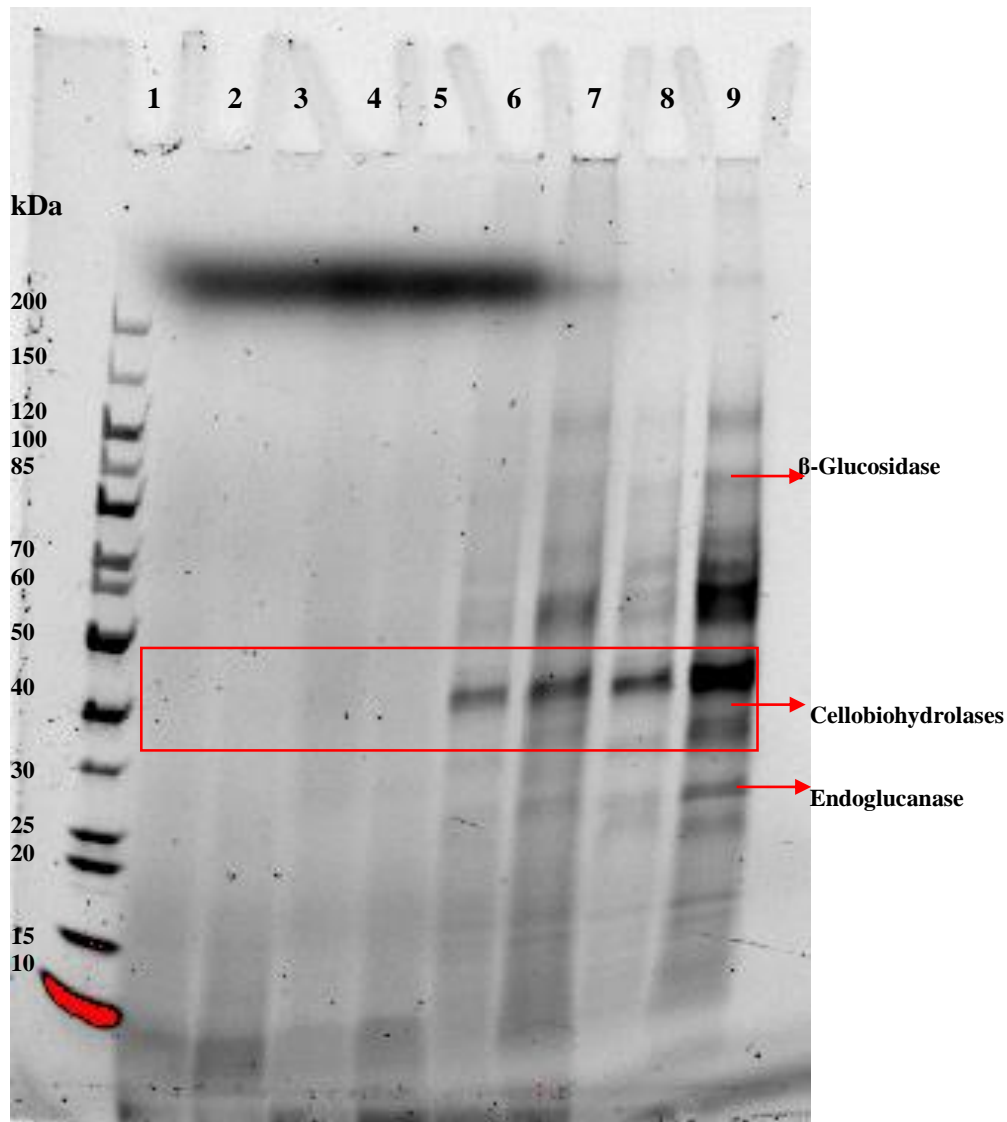


Figure 4.5. 2: SDS-PAGE analysis displaying the typical profile of *T. emersonii* proteins from Shake Flask 5A and 5B fractions. Shake Flask 5 A samples were not induced with 1 mM CuSO₄. Shake Flask 5B fractions were induced with 1 mM CuSO₄ at 24 hours of culture. The arrows correspond to the protein bands formed by β-Glucosidase (~90 kDa), Cellobiohydrolase isoforms (~30-42 kDa), and Endoglucanase (~27 kDa).

(Lane 1: PageRuler™ Unstained Protein Ladder; Lanes 2 and 3: 0 Hrs Sample from Shake Flask 5A and 5B; Lanes 4 and 5: 24 Hrs Sample from Shake Flask 5A and 5B; Lanes 6 and 7: 120 Hrs Sample from Shake Flask 5A and 5B; Lanes 8 and 9: 120 Hrs 2 X Concentrated & Buffer-Exchanged from Shake Flask 5A and 5B).

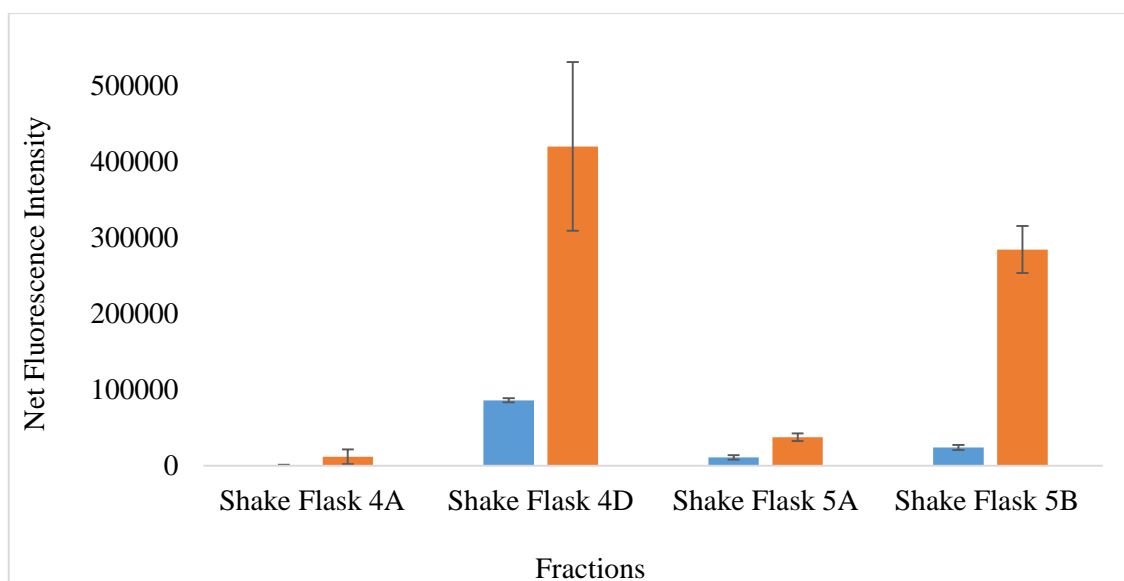


Figure 4.5. 3: Net Fluorescence Intensity of Shake Flask Batches (Pre- and Post- Buffer Exchange). A graph showing the difference in the net fluorescence intensity of the Shake Flasks 4A, 4D, 5A, and 5B fractions, at 120 hours, before and after 2 X Concentration and Buffer Exchange (BE). Shake Flask 4A and 5A are the control fractions while Shake Flask 4D and 5B contains copper sulphate. The blue and orange represent net fluorescence intensity before and after buffer exchange respectively. The net fluorescence intensity refers to the blank adjusted fluorescence intensity values.

Scientific literature was surveyed to identify methods to induce laccase expression in fungi. Copper sulphate was selected for use as the inducer of laccase activity in *T. emersonii*. The reason for the selection of copper sulphate as a potential inducer of laccase activity was due to evidence from scientific studies. Copper was found to be an efficient inducer of laccase when supplemented in the medium in copper sulphate form as it increased the transcription and the activity of the enzyme (Vrsanska et al., 2016). Copper is part of the active centre of laccases and is thus crucial for the synthesis of a catalytically active laccase protein (Kumar et al., 2011). In a study by Gomma and Momtaz (2015), the production medium was spiked with 1 mM copper sulphate to increase laccase activity in *Aspergillus flavus* isolated from soil. It was decided to try this approach in the lab when culturing *T. emersonii* in shake flasks to investigate the effect of copper sulphate on laccase activity.

The method was replicated at small scale (300 mL) in shake flasks. Copper sulphate (final concentration 1 mM in production medium) was added to the flasks after 24 hours and the protein concentration monitored at specific time points. Additionally, by following the in-house SOPs and the assay training provided at MBio, shake flask fractions from 120 hours were also analysed using some of the routine in-house assays, namely, for beta-

glucosidase, endoglucanase, and cellobiohydrolase activities. This was carried out to investigate the effect of copper sulphate on the levels of these enzymes. Control flasks were set up alongside the flasks induced with copper sulphate for comparison.

As can be seen in Tables 4.5.1 and 4.5.2 above, there was an increase in the overall protein concentration after 24 hours in shake flasks induced with copper sulphate. Two shake flasks (1 control and 1 copper sulphate-induced), each with the highest protein concentration at 120 hours, were selected for further analyses. The selected fractions were concentrated two-fold and buffer exchanged. The crude shake flask fractions as well as the 2 X concentrated and buffer exchanged fractions were assayed for the three hydrolase enzymes and analysed by SDS-PAGE. They were also assayed by the Amplex Red method for laccase activity.

As can be seen in figures 4.5.1 and 4.5.2, there was a difference in the intensity of the protein bands formed by SDS-PAGE in the shake flask fractions, with and without copper sulphate. The protein bands were more intense in the copper induced shake flask fractions from 96 hours onwards. The intensity of protein bands formed in the fractions with and without copper sulphate were as expected. It was also interesting to visually observe on the gel, the positive effect of copper sulphate on the glycosyl hydrolases. The positive effect of copper sulphate on the production of the three main glycosyl hydrolases was clearly noticeable on SDS-PAGE analysis as there was an increased band intensity for these enzymes in the copper sulphate induced fractions.

It was observed that the enzymes, beta-glucosidase, endoglucanase, and cellobiohydrolase were upregulated on the addition of copper sulphate in the shake flasks after 24 hours of culture, as shown in Table 4.5.3 above. The most notable induction of activity was observed for the endoglucanase. There was a six-fold increase in endoglucanase activity in copper sulphate induced shake fractions. However, both beta-glucosidase and cellobiohydrolase activities were also upregulated. There was approximately four- and three-fold increase in beta-glucosidase and cellobiohydrolase activity respectively in the copper sulphate induced fractions. The SDS-PAGE analysis served as a visual representation and confirmation of the results obtained from the activity assay of the three enzymes. As shown in Figures 4.5.1 and 4.5.2, the protein bands that were observed were darker throughout the length of the gel in those fractions that had

been induced with copper sulphate. The results obtained indicated that copper sulphate had a significant impact on the expression levels of enzymes from the glycosyl hydrolase families. This was an unexpected outcome, as it had been hypothesised that copper sulphate would upregulate the expression of oxidoreductases only, and laccase in particular.

Laccase activity was detected using Amplex Red in both the shake flask batches (see Figure 4.5.3). In the first batch, laccase activity could only be quantified in Shake Flask 4D (0.14 ± 0.05 U/mL laccase); i.e. the fraction induced with copper sulphate after 24 hours. Although laccase was detected in Shake Flask 4A, it could not be quantified as the activity was below the limit of quantitation. In the second batch, laccase activity was both detected and quantified in Shake Flasks 5A (0.020 ± 0.01 U/mL laccase) and 5B (0.045 ± 0.05 U/mL laccase). The U/mL of laccase present was greater in Shake Flask 5B which had been induced with 1 mM copper sulphate after 24 hours. Overall, the difference in the fluorescence intensity values for the flasks induced with copper sulphate was statistically significant ($p < 0.01$)

It was also found that the Amplex Red method was considerably more sensitive than the ABTS assay. It was difficult to detect and quantify laccase activity in the shake flask fractions using ABTS. The ABTS assay was, however, quicker and easier to set up.

As laccase activity was detected in the shake flasks when induced with copper sulphate, it was decided to scale up and assess the reproducibility of the results. Additionally, it was also hypothesised that scale-up of the culture process would provide higher yields of laccase for further analyses.

4.6 Scale-up of *T. emersonii* Production

Table 4.6. 1: A table listing the protein concentration (mg/mL), U/mL of Laccase, U/mg of Laccase Specific Activity, IU/mL of β -Glucosidase, Endoglucanase, Cellobiohydrolase and U/mL of Xylanase in the various fermentation batches of *T. emersonii* cultured for 140 hours in 5 L and 1 L benchtop bioreactors. The values in italics refer to the protein concentration in the 10 X concentrated fraction of MBL195L01, 6 X concentrated fraction of MBL195L02, 6 X concentrated and buffer exchanged fraction of MBL191L053, and 20 X concentrated fraction of MBL191L054.

Bioreactor Volume and Run #	5 L MBL195L01	5 L MBL195L02	5 L MBL195L03	1 L MBL191L051	1 L MBL191L052	1 L MBL191L053	1 L MBL191L054
1 mM CuSO ₄ [-/+]	-	-	+	-	+	-	+
Protein Concentration (mg/mL)							
0 hours	0.39 ± 0.01	0.20 ± 0.02	0.18 ± 0.01	0.43 ± 0.01	0.42 ± 0.02	0.41 ± 0.02	0.43 ± 0.02
24 hours	0.10 ± 0.01	0.10 ± 0.02	0.09 ± 0.02	0.11 ± 0.01	0.16 ± 0.02	0.14 ± 0.01	0.13 ± 0.01
96 hours	0.42 ± 0.01	nd	nd	nd	nd	nd	nd
120 hours	0.67 ± 0.01	nd	nd	nd	nd	nd	nd
140 hours	0.92 ± 0.07	0.16 ± 0.01	0.72 ± 0.06	0.13 ± 0.01	0.25 ± 0.00	0.32 ± 0.02	0.32 ± 0.02
<i>140 hours</i>	<i>5.44 ± 0.64</i>	<i>0.64 ± 0.03</i>	<i>2.91 ± 0.18</i>				
Laccase (U/mL)	< LoQ	< LoQ	< LoQ	0.001 ± 0.001	0.004 ± 0.001	0.001 ± 0.002	0.005 ± 0.003
Laccase specific activity (U/mg)	< LoQ	< LoQ	< LoQ	0.008	0.016	0.003	0.016
β -Glucosidase (IU/mL)	3.61 ± 0.07 <i>22.13 ± 0.55</i>	1.51 ± 0.04	3.09 ± 0.14	1.25 ± 0.04	2.71 ± 0.05	2.58 ± 0.09	2.85 ± 0.02 <i>32.60 ± 0.3090</i>
Endoglucanase (IU/mL)	316.46 ± 2.92 <i>1917.65 ± 71.52</i>	44.04 ± 3.19	320.50 ± 6.14	82.86 ± 4.75	148.45 ± 6.08	181.02 ± 6.99	182.75 ± 3.52 <i>2052.76 ± 59.15</i>
Cellobiohydrolase (IU/mL)	1.47 ± 0.04 <i>8.28 ± 0.25</i>	0.48 ± 0.01	1.18 ± 0.05	0.37 ± 0.02	0.54 ± 0.01	0.59 ± 0.03	0.68 ± 0.03 <i>7.67 ± 0.28</i>
Xylanase (U/mL)	38.90 ± 1.32 <i>268.69 ± 5.08</i>	8.91 ± 0.21	42.20 ± 1.61	7.80 ± 0.44	13.31 ± 0.49	18.81 ± 0.53	19.19 ± 0.52 <i>219.24 ± 15.23</i>

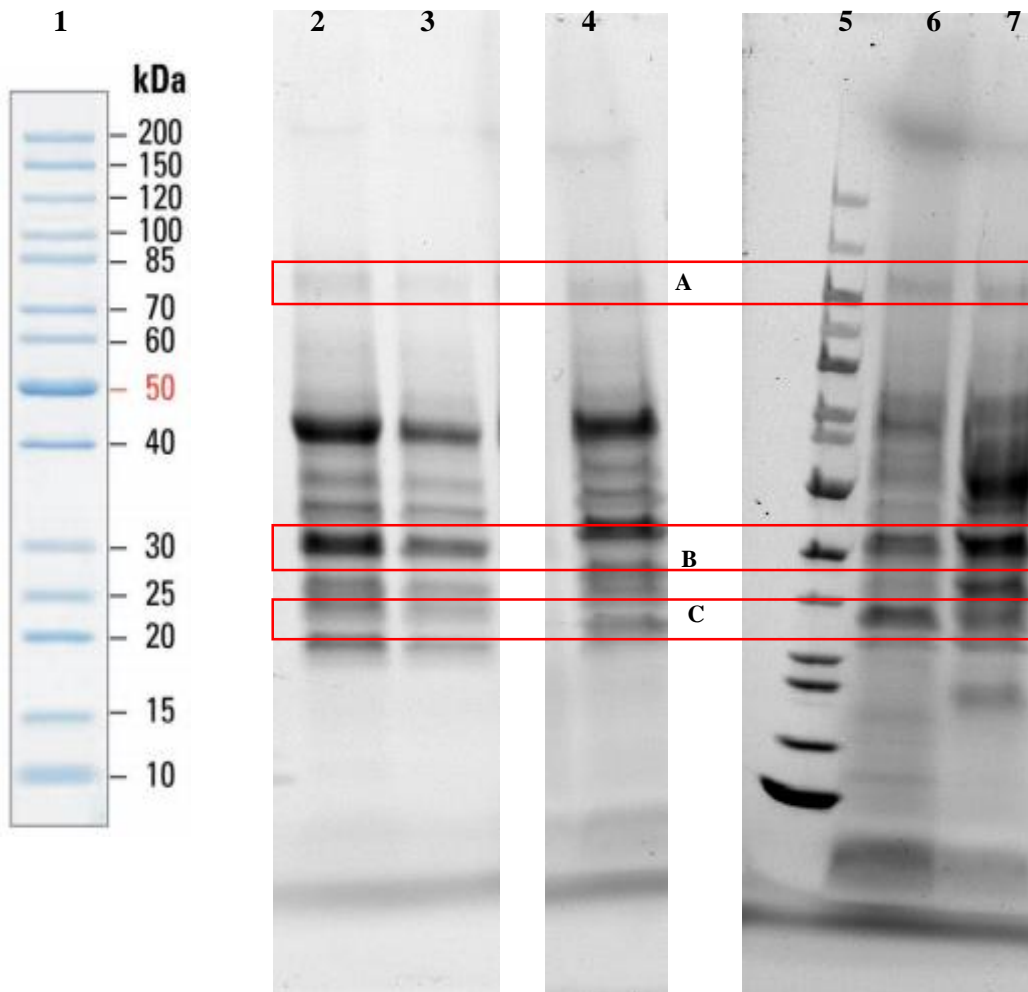


Figure 4.6. 1: SDS-PAGE analyses displaying the typical profile of *T. emersonii* proteins from MBL195L01, MBL195L03 5 L culture fractions. All fractions were control fractions except for MBL195L03 140 Hrs 1 X which was induced with 1 mM CuSO₄ at 24 hours. The approximate location of the three main glycosyl hydrolase enzymes is indicated by letters A, B, and C. A: β -Glucosidase (~90 kDa), B: Cellobiohydrolase isoforms (~30-42 kDa), and C: Endoglucanase (~27 kDa).

(Image 1: PageRuler™ Unstained Protein Ladder; Images 2 and 3: 140 Hrs MBL195L01 10 X 1/10 dilution and 10 X 1/20 dilution; Image 4: MBL195L01 140 Hrs 1 X; Image 5: PageRuler™ Unstained Protein Ladder; Images 6: MBL195L02 140 Hrs 1 X; Image 7: MBL195L03 140 Hrs 1 X + CuSO₄).

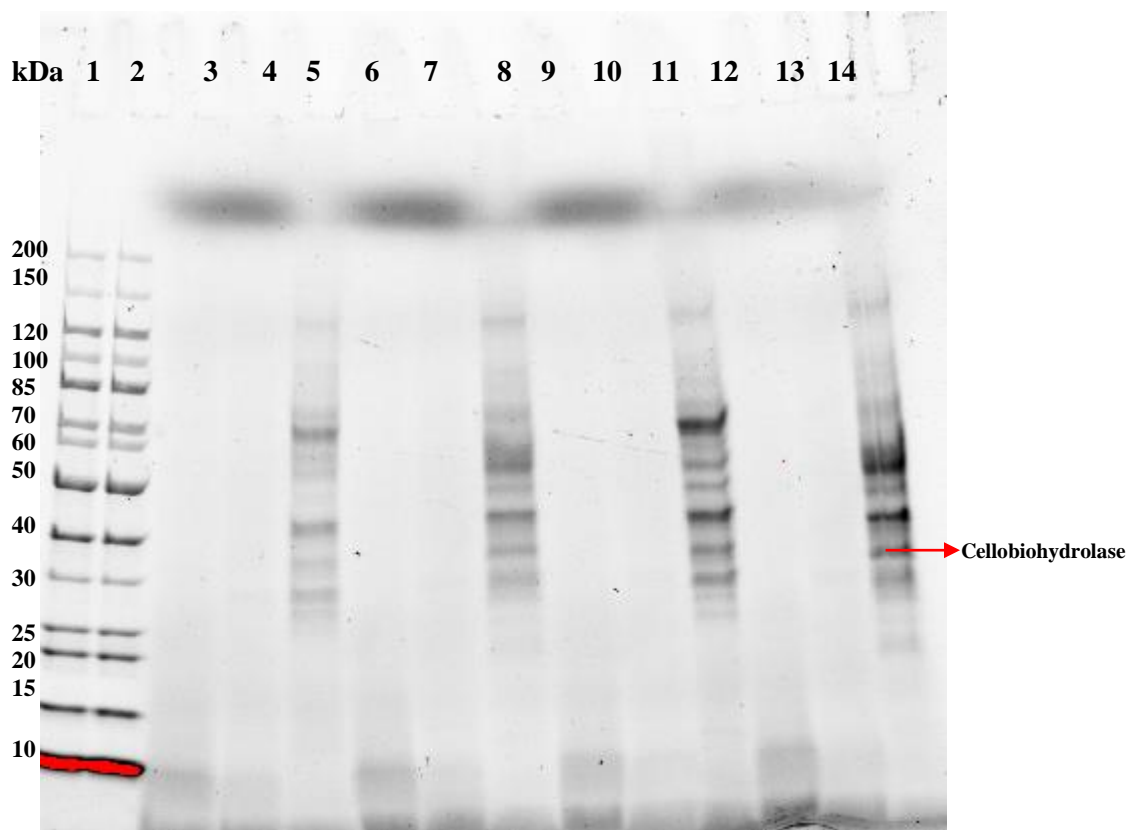


Figure 4.6. 2: SDS-PAGE analysis displaying the typical profile of *T. emersonii* proteins from 1 L fermenter fractions at 0, 24, and 140 hours. Copper sulphate was added at 24 hours to MBL191L052 and MBL191L054 only. The arrow corresponds to the protein bands formed by Cellobiohydrolase isoforms (~30-42 kDa).

(Lane 1: PageRuler™ Unstained Protein Ladder; Lane 2: PageRuler™ Unstained Protein Ladder; Lanes 3-5: MBL191L051 0 Hrs, 24 Hrs, and 140 Hrs; Lanes 6-8: MBL191L052 0 Hrs, 24 Hrs and 140 Hrs; Lanes 9-11: MBL191L053 0 Hrs, 24 Hrs, and 140 Hrs; Lanes 12-14: MBL191L054 0 Hrs, 24 Hrs, and 140 Hrs).

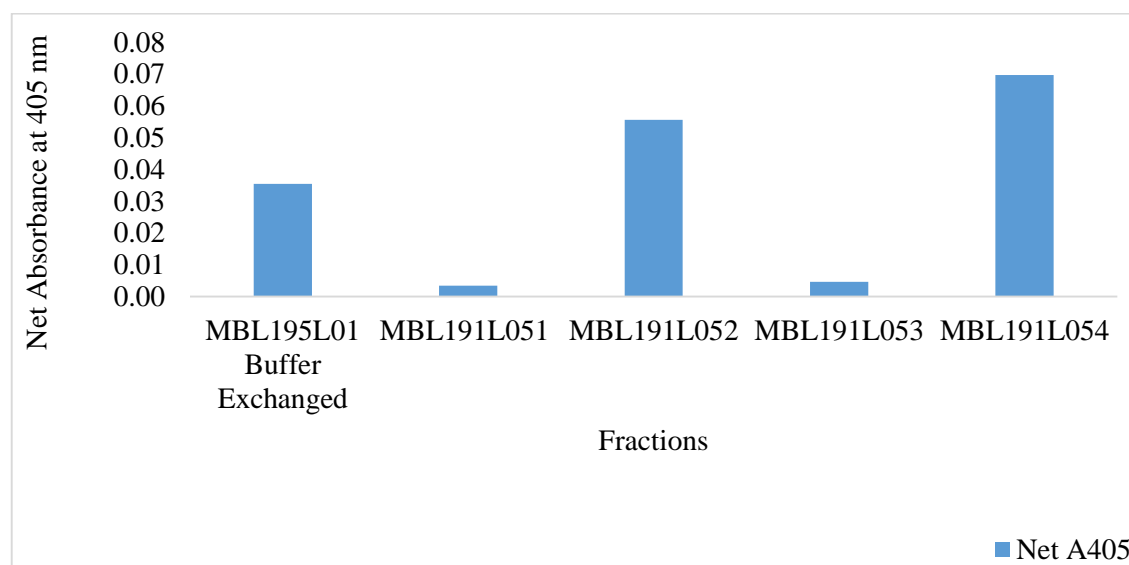


Figure 4.6. 3: Net A_{405} of *T. emersonii* cocktail from 5 L and 1 L fermenter batches using ABTS assay for laccase activity. A bar chart showing the net absorbance of the in-house *T. emersonii* cocktail obtained from 5 L and 1 L fermenter batches. The 1 L fractions were not buffer-exchanged.

T. emersonii culture was scaled-up from shake flasks to benchtop bioreactors to achieve higher yields and sufficient volumes of laccase for further analyses. Several batches of *T. emersonii* were set up on the 5 L and 1 L benchtop bioreactors. Each culture was grown for 140 hours. The protein concentrations for the benchtop bioreactor cultures were analysed at 0, 24, and 140 hours. The protein concentration was analysed only at 96 and 120 hours for the very first batch of culture MBL195L01 (see Table 4.6.1). For the remaining batches, the number of samplings at the various time points were reduced to minimise the risk of contamination. As can be seen in Table 4.6.1, there are differences in protein concentration between MBL195L01 and batches MBL195L02 and MBL195L03. The protein concentration at the different time points was as expected for MBL195L01 and lower than expected for batches MBL195L02 and MBL195L03. The differences in the fold concentrations of the 5 L and 1 L bioreactor fractions (see table 4.6.1) was to accommodate for appropriate dilutions prior to introduction of the enzyme cocktails into the HIC column.

The reason for this was a contamination issue present in the lab that required sterile filtering of the growth medium used in batches MBL195L02 and MBL195L03. It was identified that the cause of the contamination was corn steep liquor, a nutritious and essential constituent of the growth medium. Although the growth medium had been autoclaved at 121°C for 15 minutes, contamination was, nevertheless, still evident. Therefore, it was decided to sterile filter the growth medium prior to autoclaving. Sterile filtration was carried out using 0.2 µm polyethersulphone filter. Although the filtration eliminated contamination, it decreased the protein yield significantly as essential components present in the corn steep liquor could not pass through the filter. The lower protein yield in batches MBL195L02 and MBL195L03 indicated that the additional filtering step had eliminated components essential for growth from the medium. However, as was observed from the shake flask induction experiments in section 4.5., there was an increase in the protein yield in MBL195L03 (with copper sulphate) when compared to MBL195L02. Though the growth medium was filtered for both these batches, copper sulphate was added to MBL195L03 at 24 hours of culture.

Despite the higher protein yield in MBL195L01 when compared to MBL195L02 and MBL195L03, laccase activity was low in all three batches. Although laccase was detected, the level was extremely low and below the limit of quantitation.

T. emersonii culture was also carried out using 1 L benchtop bioreactors after the contamination issue was eliminated. This was achieved by using a fresh stock of corn steep liquor. Although the contamination issue was eliminated, the sampling times were reduced to 0, 24, and 140 hours to minimise the risk. The protein concentration at 140 hours was the same for both MBL191L053 and MBL191L054 as can be seen in Table 4.6.1. This was unexpected as it was hypothesised that the batches induced with 1 mM copper sulphate at 24 hours would have a higher protein concentration than those without. However, this may have been a result of variation with regards to the set-up of the bioreactors and the conditions within them such as changes to dissolved oxygen, pH, and stirring conditions based on the growth of the fungus.

Due to time constraints, the in-house assays for all of the glycosyl hydrolase enzymes were performed by the Associate Scientist in the Analytical Development and Quality Control Department at MBio. As was observed in section 4.5, the enzymes beta-glucosidase, endoglucanase, and cellobiohydrolase were also induced in the batches induced with copper sulphate at 24 hours. Xylanase activity was also positively affected by the addition of copper sulphate. The difference, however, was not as evident for batches MBL191L053 and MBL191L054. This may be due to reasons mentioned above.

As can be seen in Figures 4.6.1 and 4.6.2, the SDS-PAGE analysis showed protein bands that were thicker and more intense at 140 hours for the fractions induced with copper sulphate. MBL195L01 had the thickest protein bands, correlating with the protein concentration values obtained (Table 4.6.1). The protein bands in both the gels were as expected and indicative of the glycosyl hydrolase enzymes present in the enzyme cocktail.

In the 1 L fermenter batches, although laccase activity was detected in all four batches, the activity was higher in the copper sulphate induced batches. The highest laccase activity was detected in MBL191L054 at 140 hours. Therefore, this fraction was concentrated and purified for further characterisation experiments.

4.7 Hydrophobic Interaction Chromatography of MBL191L054

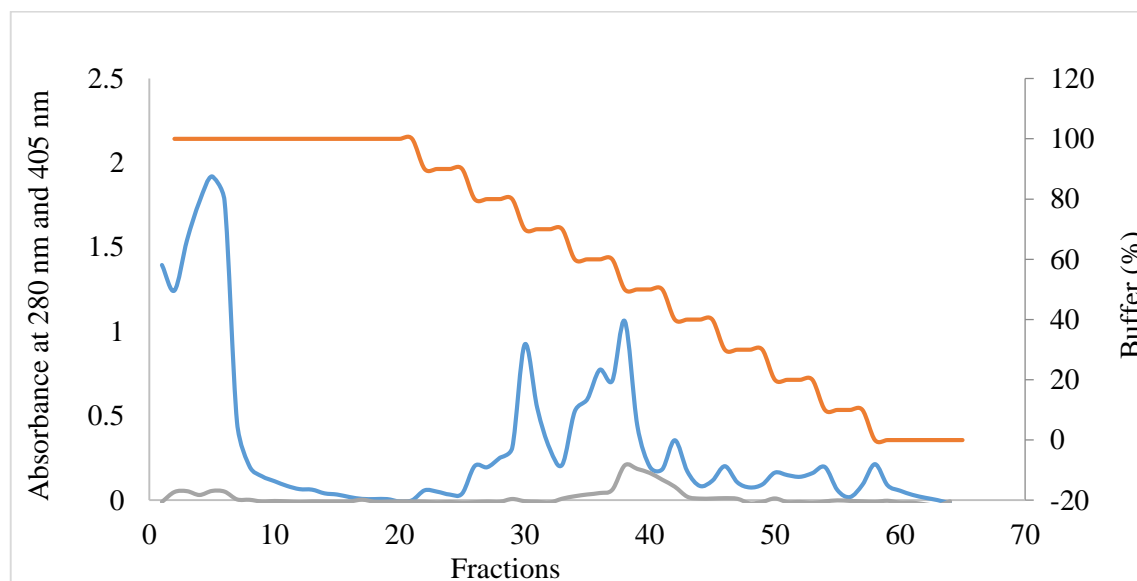


Figure 4.7. 1: An image of the HIC UV profile with linear gradient [1.2 M ammonium sulphate in 50 mM sodium phosphate, pH 7.0] in for MBL191L054. The orange displays the buffer gradient, the blue displays the absorbance of the fractions at 280 nm, and the grey displays the net absorbance of the HIC fractions at 405 nm when screened for laccase activity using ABTS.

Table 4.7. 1: A table listing the protein concentration, laccase activity (U/mL), and laccase specific activity (U/mg) in HIC Fractions that were 2 X concentrated and buffer-exchanged

Fraction	Protein Concentration (\pm SD) (mg/mL)	U/mL Laccase (\pm SD)	Specific Activity (U/mg)
Fraction 37	0.21 ± 0.01	0.25 ± 0.03	1.19
Fraction 38	0.33 ± 0.01	0.37 ± 0.02	1.12
Fraction 39	0.15 ± 0.00	0.33 ± 0.11	2.20

As can be seen in Figure 4.7.1, the 1 L fermenter batch with the highest protein concentration when induced with 1 mM copper sulphate was selected for partial protein purification using HIC. An initial screen for laccase activity using ABTS was carried out for each of the fractions. Laccase activity was detected in fractions 37, 38, and 39 (see Figure 4.7.1). These fractions were, therefore, 2 X concentrated and buffer-exchanged and assayed for laccase activity. The U/mL of laccase activity and U/mL of laccase specific activity is listed in Table 4.7.1. The highest laccase activity was detected in Fraction 38 after it was 2 X concentrated and buffer-exchanged. However, the highest laccase specific activity was in Fraction 39.

Additionally, the results obtained from the screen of the HIC fractions corresponded with the results obtained in the initial HIC screen in section 4.3. The region in the HIC profile where laccase activity was detected was the same.

Fractions 37, 38, and 39 were pooled together, 2 X concentrated, and then buffer-exchanged for further enzyme characterisation experiments.

4.8 Characterisation of Laccase

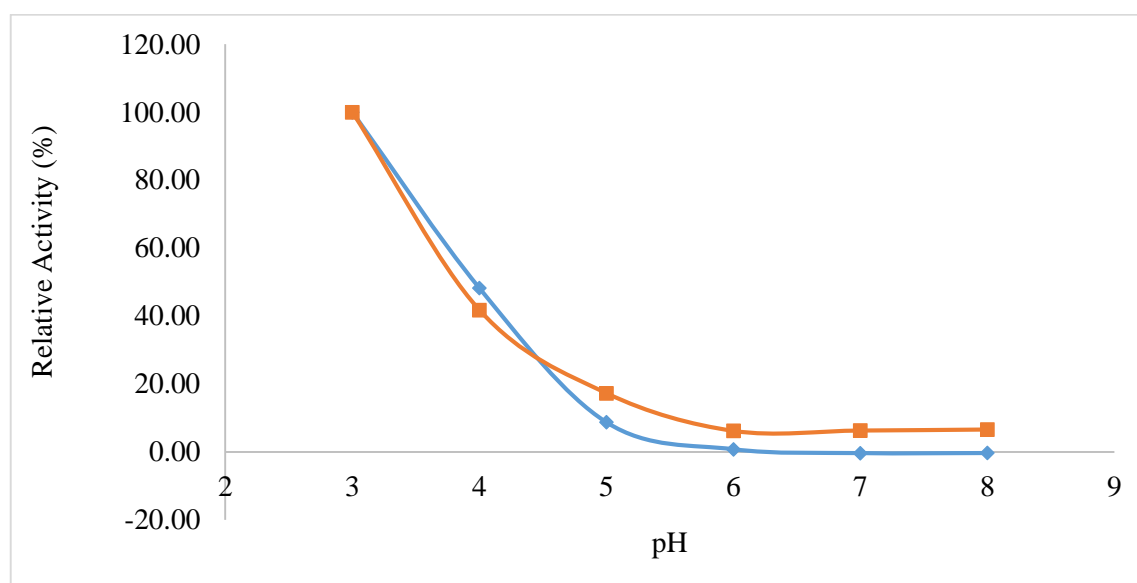


Figure 4.8. 1: A graph of pH vs. Relative Activity (%) of the pooled, 2 X concentrated and buffer-exchanged HIC Fractions (Fractions 37, 38, 39) and 2 X concentrated and buffer-exchanged enzyme cocktail (MBL191L054). The orange refers to the pooled, 2 X concentrated and buffer-exchanged HIC Fractions (Fractions 37, 38, 39) and blue refers to the 2 X concentrated and buffer-exchanged enzyme cocktail MBL191L054.

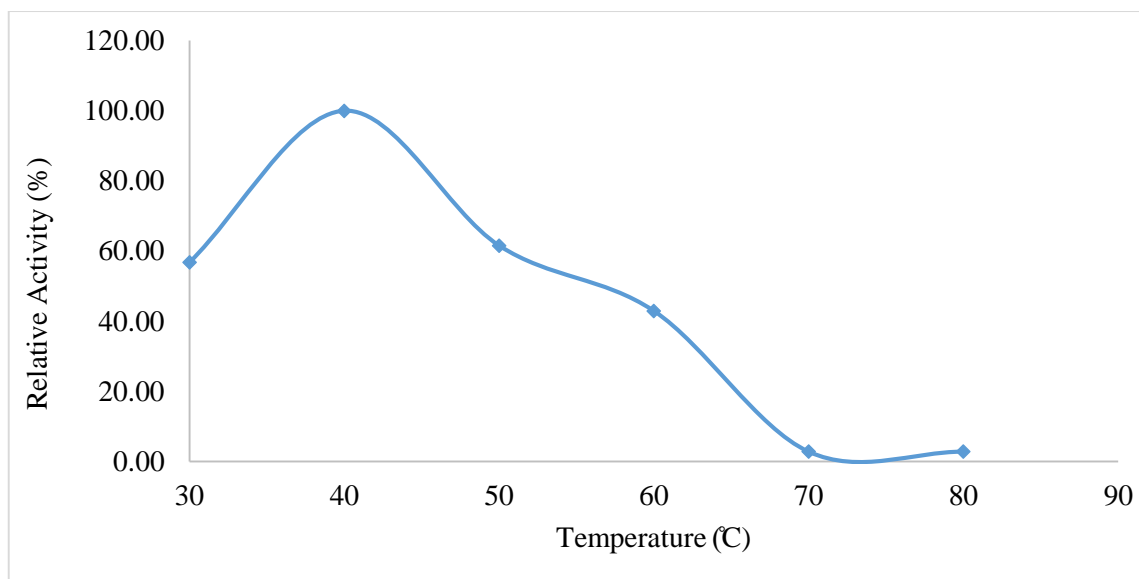


Figure 4.8. 2: A graph of Temperature vs. Relative Activity (%) of the pooled, 2 X concentrated, and buffer-exchanged HIC Fractions (Fractions 37, 38, 39).

Characterisation experiments were carried out on the pooled, 2 X concentrated, and buffer-exchanged HIC fractions to determine the optimum pH and temperature of laccase in *T. emersonii*. The characterisation experiments indicated that the optimum pH for laccase activity was pH 3.0. The buffers used for determination of optimum pH were 0.1 M citrate buffer (pH 3.0 – pH 5.0) and 0.1 M potassium phosphate buffer (pH 6.0 – pH 8.0). The buffers were selected based on a study by Chefetz et al., (1998) on the purification and characterisation of laccase from *Chaetomium thermophilum*. The organism was a cellulolytic fungus exhibiting laccase activity when it was grown at 45 C. *C. thermophilum* was isolated from composting municipal solid waste during the thermophilic stage of the process.

The temperature optima experiments indicated that the optimum temperature for laccase activity was 40°C. The characterisation assays were performed in triplicates and could not be repeated due to insufficient sample volumes available. Therefore, the characterisation experiments for optimum pH determination were repeated using the crude enzyme cocktail after it had been concentrated two-fold and buffer-exchanged. The results obtained from characterisation experiment of the crude enzyme cocktail confirmed the results obtained from the characterisation experiments of the pooled, 2 X concentrated, and buffer-exchanged HIC fraction. The temperature stability experiments could not be repeated using the 2 X concentrated and buffer-exchanged enzyme cocktail due to technical difficulties.

The pH determination experiments were pivotal in gaining a better understanding about the detection of laccase in the enzyme cocktail. Initially, as mentioned in sections above (sections 4.3 – 4.5), laccase activity could not be detected in the enzyme cocktails. It was hypothesised that the reason for this was due to low abundance of laccase in the enzyme cocktail. However, laccase activity was detected using ABTS at pH 3.0, pH 4.0, and pH 5 in the presence of citrate buffer (0.1 M). A strong colour change due to laccase activity was observed at each of these pH values. The strongest colour change was at pH 3.0 (Net A_{405} values of 1.93 for the pooled, 2 X concentrated, & buffer-exchanged HIC fractions 37, 38, & 39, and 1.61 for 2 X concentrated & buffer-exchanged 1 L bioreactor batch MBL191L054). The strong colour change due to laccase activity on ABTS was unexpected due to the hypothesis that laccase was not present in the enzyme cocktail in abundance.

In order to confirm the results obtained, the pH optimisation experiments were repeated. The results obtained remained consistent. This was not just a clear indicator of the optimum pH for laccase activity. It also depicted that citrate buffer was more suitable than potassium phosphate buffer (pH 6.4) for the storage of laccase as well as for assaying it. Previously, potassium phosphate buffer (pH 6.4) had been used in the buffer exchange process of the enzyme cocktails. However, the results from the pH optima experiments indicated that citrate buffer was a better alternative. Furthermore, these results were also useful to gain a better understanding about the stability of laccase.

It was also hypothesised that laccase was not a stable enzyme and was prone to degradation on storage. However, when the enzyme assay method was optimised and citrate buffer was added as the assay buffer, laccase activity was consistently detected in the enzyme cocktail using ABTS as the substrate. It was also interesting to find that laccase activity was detectable in enzyme cocktails that were previously buffer-exchanged in potassium phosphate buffer, pH 6.4 when citrate buffer was added as the assay buffer. It was, therefore, understood that potassium phosphate buffer was not suitable for use in both the storage and assaying of laccase. Additionally, citrate buffer, pH 3.0, was not only optimal for the storage and assay of laccase but it also seemed to have a reversing effect on the inhibition of laccase caused by storage and buffer exchange in potassium phosphate buffer, pH 6.4.

Due to time constraints, further characterisation experiments could not be carried out on laccase.

Although scientific data was not available on laccases in *T. emersonii*, it was understood from studies conducted on laccases present in other fungal strains that it preferred an acidic pH. However, the temperature optima of laccase varied between different fungal strains, ranging from 20°C to 80°C (Wang et al., 2018d). A study was conducted by More et al., (2011) on fungal laccase from *Pleurotus* sp. isolated from soil samples. The laccase enzyme was purified and its pH and temperature optima were determined. The results indicated that the optimum activity of laccase was at pH 4.5 and 65°C. Wang et al., (2018d) isolated a fungal strain belonging to the genus *Trametes*. The strain, named *Trametes* sp. MA-X01 was isolated from withered plant materials. The laccase enzyme was purified and its pH and temperature optima were determined. The purified enzyme showed better laccase activity under acidic conditions with no significant difference in the enzyme activity in the pH range of 3.0-5.0. The temperature optima of the enzyme was 60°C which indicated that it was a thermophilic enzyme.

CHAPTER 5: RESULTS & DISCUSSION - CATALASE

5.1 Introduction

Catalase was a second candidate oxidoreductase that was identified in the in-house *T. emersonii* cocktail through bioinformatics analysis.

After selection of catalase for further investigation, it was decided to purchase a commercial kit for the detection of catalase in the in-house enzyme cocktails. Two commercial catalase assay kits were initially purchased, namely, OxiSelect™ Catalase Activity Assay Kit and Megazyme Catalase Assay Kit. The Megazyme assay had a limit of detection of 0.5 U/mL and a limit of quantification of 1.8 U/mL while the detection sensitivity limit of the OxiSelect™ assay was not specified in the product manual. The assay method and assay principle were the same for both assay kits. The Megazyme assay kit provided 200 assays per kit while the OxiSelect™ provided only 96 assays per kit (Megazyme, 2019; Cell Biolabs, Inc., 2018).

However, the Megazyme Catalase Assay Kit was chosen for use in experiments thereafter as it was more cost-efficient than the OxiSelect™ kit. Although an instruction manual was provided with the catalase assay kit, it had to be optimised for use at microtitre scale. Therefore, an SOP was drafted for catalase assay of the in-house *T. emersonii* cocktail (See Methods, section 2.8.4). After optimisation of the SOP, catalase assays were carried out.

The assay was based on the degradation of hydrogen peroxide by catalase. Unlike traditional assays, catalase activity was determined by measuring the decrease in hydrogen peroxide concentration observed after the enzyme sample was incubated with a hydrogen peroxide standard solution. Two separate reactions had to be completed to determine catalase activity. Firstly, the enzyme sample of interest was incubated with a known concentration (~65 mM in assay) of hydrogen peroxide. The reaction was stopped with 15 mM sodium azide. Secondly, the exact concentration of hydrogen peroxide remaining was measured using an enzyme-linked colourimetric detection method employing 3,5-dichloro-2-hydroxy-benzenesulfonic acid, 4-aminoantipyrine and peroxidase. The resulting quinoneimine dye was measured at 520 nm (Megazyme, 2019).

5.2 Preliminary Results from the in-house *T. emersonii* cocktail

The in-house *T. emersonii* cocktail was screened for catalase activity using the Megazyme commercial assay kit. Results indicated that catalase was present in the cocktail. However, the U/mL of catalase present could not be quantified as the assay was only in the optimisation stages. The reason for this was that the incubation time for the assay was yet to be determined. The incubation time was detrimental to the accurate quantification of catalase activity. An incubation time that was shorter or longer than the optimum incubation time resulted in absorbance values that were too low or too high. This made it difficult to quantify the U/mL of Catalase present in the enzyme cocktail.

Unlike the case for laccase, catalase was detected in the crude enzyme cocktail as well as in the buffer-exchanged fractions. However, it was observed from the colour change in the reaction wells that more enzyme was detected in the buffer-exchanged fractions than in the crude enzyme fractions. This may have been a result of the removal of nonspecific production media components of low molecular weight such as salts from the enzyme cocktail after buffer-exchange. Furthermore, through buffer-exchange, the ultrapure water used to store the enzyme cocktail fractions was replaced with buffer (20 mM Potassium phosphate buffer, pH 6.4) that was more optimum for laccase storage and activity. This was also thought to have influenced the detection of the enzyme.

5.3 Preliminary Results from HIC of the in-house *T. emersonii* cocktail

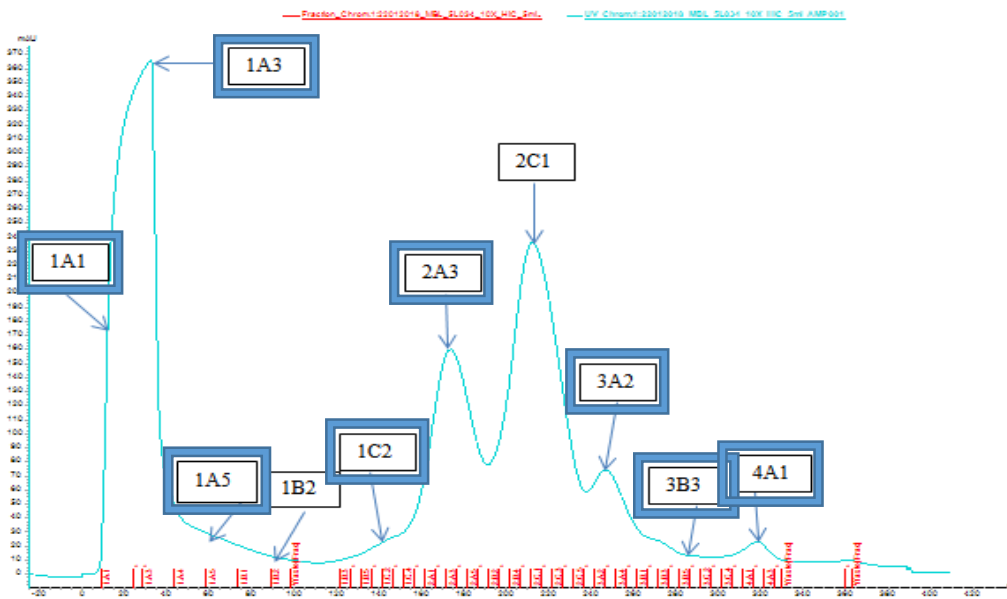


Figure 5.3. 1: An image of the HIC UV profile with linear gradient [1.2 M ammonium sulphate in 50 mM sodium phosphate, pH 7.0] for the in-house *T. emersonii* cocktail. The UV chromatogram is depicted in blue, the eluted fractions are depicted in red. The image is a screenshot from the ÄKTA Pure 25 Chromatography System software. The fractions that were selected for buffer-exchange are indicated in the figure. Fractions in which catalase activity was detected after buffer-exchange are outlined with a blue frame.

As mentioned in section 4.3, specific HIC fractions of the in-house *T. emersonii* cocktail were selected and buffer-exchanged. These fractions were also assayed for catalase activity. The assay was performed on single samples due to low sample volumes available. Fractions containing catalase are shown in Figure 5.3.1 and are highlighted with a blue frame. As the assay was still in the optimisation stages, the catalase in the buffer-exchanged HIC fractions could not be quantified. However, the results of the assay indicated that, unlike laccase, catalase was present in various peaks in the HIC profile. Therefore, it was hypothesised that more than one type of catalase was present in the in-house enzyme cocktail.

This understanding was novel as there was no data available in the scientific literature on catalase enzyme(s) present in *T. emersonii*. However, presence of catalase isoforms in other fungal strains have been found in scientific literature. The filamentous fungus *Podospora anserina* is known to contain four monofunctional catalases and one bifunctional catalase-peroxidase enzyme. These catalases are vital for the efficient utilisation of complex biomass like wood shavings to allow the fungus to grow in the presence of lignin (Bourdais et al., 2012). Another study by Kawasaki and Aguirre (2001)

identified a third catalase (CatC) in the fungus *Aspergillus nidulans*. It was already understood from previous studies that the *A. nidulans* catalase isoforms CatA has a molecular weight of ~ 84 kDa and CatB has a molecular weight of ~79 kDa. Both CatA and CatB belong to the family of large-subunit catalases whereas CatC shows similarity to small-subunit monofunctional catalases. CatC has a molecular weight of ~54 kDa. While CatA and CatB are closely related to fungal and bacterial catalases, CatC is closely related to small-subunit catalases from other fungi, *Archaea*, and animals (Kawasaki and Aguirre, 2001). It was also understood from the study by Kawasaki and Aguirre (2001) that CatA and CatB were present at different stages of the *A. nidulans* life cycle and protect different cell types from hydrogen peroxide or other types of oxidative stress and heat shock stress. However, CatC levels were found to be relatively constant. This suggested that CatC activity overlaps CatA or CatB activity.

Although no scientific data has been published regarding the presence or absence of catalase isoforms in *T. emersonii*, the knowledge of catalase isoforms in other fungal strains served as a guide to learning more about catalases in *T. emersonii*. This knowledge strengthened the hypothesis that more than one type of catalase was present in *T. emersonii*.

5.4 Shake Flask Analyses

Table 5.4. 1: A table listing the protein concentration (mg/mL), U/mL of catalase, and catalase specific activity (U/mg) in the various Shake Flask 1 batches (A, B, and D) at 120 hours. Detailed protein concentration (mg/mL) at 0, 24, 96, and 120 hours can be seen in Table 4.4.1. (Only single assays were performed, not duplicates or triplicates) (nd = not determined).

Shake Flask Batch #	1A	1B	1C	1D
Protein Concentration (mg/mL)	0.36 ± 0.01	0.39 ± 0.02	Flask broke: nd	0.39 ± 0.05
Catalase (U/mL)	95.53	93.36	nd	91.84
Catalase Specific Activity (U/mg)	265.36	239.38	nd	235.49

Table 5.4. 2: A table listing the protein concentration (mg/mL), U/mL of catalase, and catalase specific activity (U/mg) in Shake Flask 4 batches (A and D) at 120 hours. The values in italics are those obtained after 2 X concentration and buffer-exchange. Detailed protein concentrations (mg/mL) at 0, 24, 96, and 120 hours can be seen in Table 4.5.1. Catalase activity (U/mL) and catalase specific activity (U/mg) in batches 4B and 4C were not determined as the flasks with the highest protein concentration in the control and copper sulphate induced fractions were selected. (nd = not determined).

Shake Flask Batch #	4A (Control)		4B (Control)	4C (+ CuSO ₄)	4D (+ CuSO ₄)	
Protein Concentration (mg/mL)	0.34 ± 0.03	<i>0.37 ± 0.03</i>	0.24 ± 0.02	0.59 ± 0.03	0.65 ± 0.02	<i>1.56 ± 0.06</i>
Catalase (U/mL)	125.31 ± 0.08	<i>197.66 ± 0.13</i>	nd	nd	14.53 ± 0.07	<i>20.85 ± 0.03</i>
Catalase Specific Activity (U/mg)	368.56	<i>534.22</i>	nd	nd	22.35	<i>13.37</i>

Table 5.4. 3: A table listing the protein concentration (mg/mL), U/mL of catalase, and catalase specific activity (U/mg) in the Shake Flask 5 batches (A and B). The values in italics are those obtained after 2 X concentration and buffer-exchange. Detailed protein concentration (mg/mL) at 0, 24, and 120 hours can be seen in Table 4.5.2. Catalase activity (U/mL) and catalase specific activity (U/mg) was not determined for Shake Flask fraction 5C.

Shake Flask Batch #	5A (Control)		5B (+ CuSO ₄)		5C (+ CuSO ₄)
Protein Concentration (mg/mL)	0.19 ± 0.00	<i>0.24 ± 0.02</i>	0.42 ± 0.01	<i>0.49 ± 0.02</i>	0.43 ± 0.02
Catalase (U/mL)	37.31 ± 0.00	<i>73.71 ± 0.01</i>	0.00	0.00	nd
Catalase Specific Activity (U/mg)	196.37	<i>307.13</i>	0.00	0.00	nd

U/mL of catalase activity was determined using the absorbance values at 520 nm. As can be seen in Tables 5.4.1, 5.4.2, and 5.4.3, catalase was easily detectable in crude shake flask fractions as well as in 2 X concentrated and buffer-exchanged shake flask fractions. However, there are differences in catalase yields in the three batches due to batch to batch variations. This was thought to have been a result of the use of new batches of production medium components. Furthermore, parameters such as pH and temperature could not be controlled to always remain at their optimum in shake flask cultures.

Shake Flask batches 4A, 4D, 5A, and 5B were also assayed for glycosyl hydrosyl enzymes such as beta-glucosidase, endoglucanase, and cellobiohydrolase (see Table 4.5.3). The SDS-PAGE analysis of these batches can also be seen in Figures 4.5.1 and 4.5.2.

The results obtained from analysis of the shake flask fractions indicated that catalase could be detected and quantified from the crude enzyme cocktail. Another interesting finding from the shake flask experiments was that the addition of 1 mM copper sulphate had an inhibitory effect on catalase. As can be seen in Tables 5.4.2 and 5.4.3, the U/mL of catalase was higher in the control flasks, namely, Shake Flasks 4A and 5A when compared to 4D and 5B. This was consistent with findings in scientific literature which stated that metal ions such as copper are inhibitors of catalase activity as they react with the iron in the prosthetic group of the enzyme (Yordanova, 1974). Another study by Liu et al., (2008) also explains that catalase activity is inhibited by copper due to: (i) complexation of the substrate by copper, (ii) combination of copper with the protein-active group of the enzyme, or (iii) reaction of copper with the enzyme substrate complex.

Since catalase yield from shake flask batches was satisfactory, it was decided to perform characterisation experiments on catalase to determine its optimum pH and temperature. However, the results obtained for the pH characterisation experiments were not as expected. Numerous peaks of catalase activity were observed at different pH values. This was the case even with repeated assays to verify and confirm the initial results. As the patterns obtained were consistent with each repetition, it was deduced that this was due to the presence of multiple isoforms of catalase as identified through assaying the HIC fractions (see figure 5.3).

Therefore, it was decided to scale-up the culture of *T. emersonii* from shake flasks to benchtop bioreactors. This was to achieve a more controlled growth of the organism with regards to maintaining a consistent pH and temperature throughout the culture period. Consequently, a higher catalase yield may be obtained from maintaining stable growth parameters. The higher levels of catalase obtained can then be purified by hydrophobic interaction chromatography for further characterisation experiments.

5.5 Scale-up of *T. emersonii* Production

Table 5.5. 1: A table listing the protein concentration (mg/mL), catalase (U/mL), and catalase specific activity (U/mg) in the 5 L, 10 L, and 1 L bioreactor batch cultures of *T. emersonii* at 140 hours.

Bioreactor Volume and Run #	1 mM CuSO ₄ [- / +]	Protein Concentration (mg/mL)	Catalase (U/mL)	Catalase Specific Activity (U/mg)
5 L MBL195L01	-	0.92 ± 0.07	1139.27 ± 0.22	1238.34
10 L DCU1910L01	-	0.56 ± 0.02	78.32 ± 0.01	139.86
1 L MBL191L051	-	0.13 ± 0.01	34.30 ± 0.16	263.85
1 L MBL191L052	+	0.25 ± 0.00	15.52 ± 0.08	62.08
1 L MBL191L053	-	0.32 ± 0.02	271.50 ± 0.02	848.44
1 L MBL191L054	+	0.32 ± 0.02	26.32 ± 0.07	82.25

Table 5.5. 2: A table displaying the U/mL of β-Glucosidase, Endoglucanase, Cellobiohydrolase, and Xylanase as well as U/mL of catalase and catalase specific activity (U/mg) at 140 hours in the 10 L bioreactor run carried out at DCU.

Bioreactor Volume and Run #	10 L DCU1910L01
1 mM CuSO ₄ [-/+]	-
Catalase (U/mL)	78.32 ± 0.01
Catalase Specific Activity (U/mg)	139.86
β-Glucosidase (U/mL)	3.75 ± 0.03
Endoglucanase (U/mL)	198.97 ± 6.90
Cellobiohydrolase (U/mL)	0.91 ± 0.02
Xylanase (U/mL)	23.89 ± 3.47

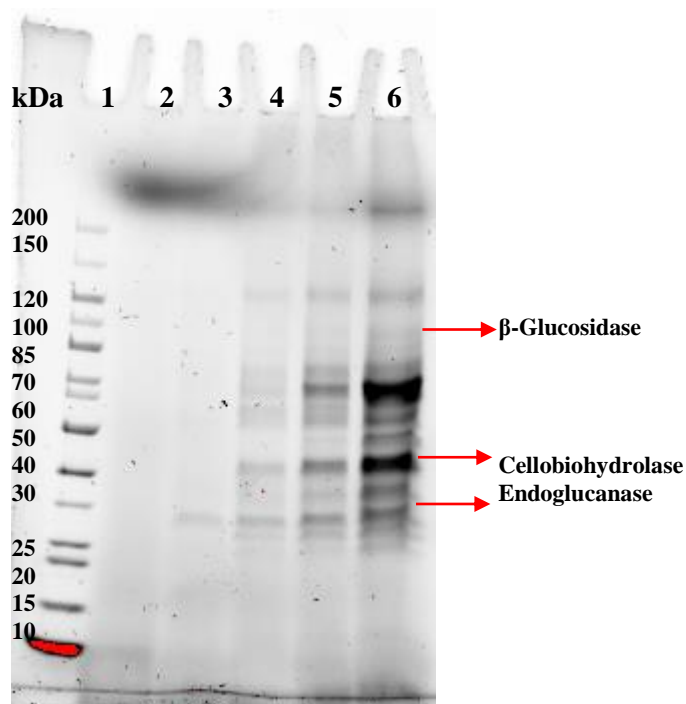


Figure 5.5. 1: SDS-PAGE analysis displaying the typical profile of *T. emersonii* proteins from 10 L fermenter fractions at 0, 24, 96, 120 and 140 hours. The arrows correspond to the protein bands formed by β -Glucosidase (~ 90 kDa), Cellobiohydrolase isoforms (~ 30 - 42 kDa), and Endoglucanase (~ 27 kDa).

(Lane 1: PageRuler™ Unstained Protein Ladder; Lanes 2-6: DCU1910L01 0 Hrs, 24 Hrs, 96 Hrs, 120 Hrs, and 140 Hrs).

T. emersonii culture was scaled up from shake flasks to bioreactors in order to achieve higher yields of catalase. Catalase was detectable in all of the scaled up bioreactor batches. The enzyme was detected in the crude fractions even without buffer exchange. The U/mL of catalase obtained in each of the batches are indicated in Table 5.5.1. As can be seen in Table 5.5.1, the highest U/mL of catalase activity was in the 5 L bioreactor batch (MBL195L01). This was followed by the 1 L bioreactor batch (MBL191L053).

Catalase activity (U/mL) was lower than expected in the 10 L batch. It was hypothesised that the 10 L batch would have the highest U/mL of catalase as it was the largest volume bioreactor run that was set up. However, this was not the case. The 10 L batch was set up in DCU due to the contamination issues described in section 4.6. As the 10 L batch was the first attempt at culturing *T. emersonii* in bioreactors outside the MBio lab, the dissolved oxygen parameter could not be optimised without prior trial runs at DCU. This could not be achieved due to time constraints. As a result, the dissolved oxygen levels during the bioreactor run were not optimal throughout the period of culture. As a result, the protein concentration as well as all enzyme yields including catalase at 140 hours was

lower than that obtained in the 5 L bioreactor run at MBio. A detailed breakdown of the protein concentration at the different time points as well as the enzymatic activity of the glycosyl hydrolase enzymes and laccase can be seen in Table 4.6.1 for all other bioreactor batches that were set up.

An SDS-PAGE analysis of the 10 L batch fractions at 0, 24, 96, 120, and 140 hours was carried out (see Figure 5.5.1). Protein bands were the thickest at 140 hours. However, protein bands were also visible at 24, 96, and 120 hours. The bands became more prominent with time. The protein bands visible were typical of the glycosyl hydrolase enzymes present in *T. emersonii*. Although the amount of catalase (U/mL) obtained was lower, it was understood from the SDS-PAGE analysis that protein production still occurred and that the protein profile obtained was similar to that obtained at MBio.

Therefore, it was decided to proceed with catalase characterisation experiments using the 5 L and 1 L batch that contained the highest catalase activity, namely, MBL195L01 and MBL191L053. However, the fermentation batches were partially purified using HIC prior to the characterisation experiments. This was because of unsuccessful attempts at catalase characterisation using shake flask fractions as mentioned above in section 5.4.

5.6 HIC of MBL195L01 and MBL191L053

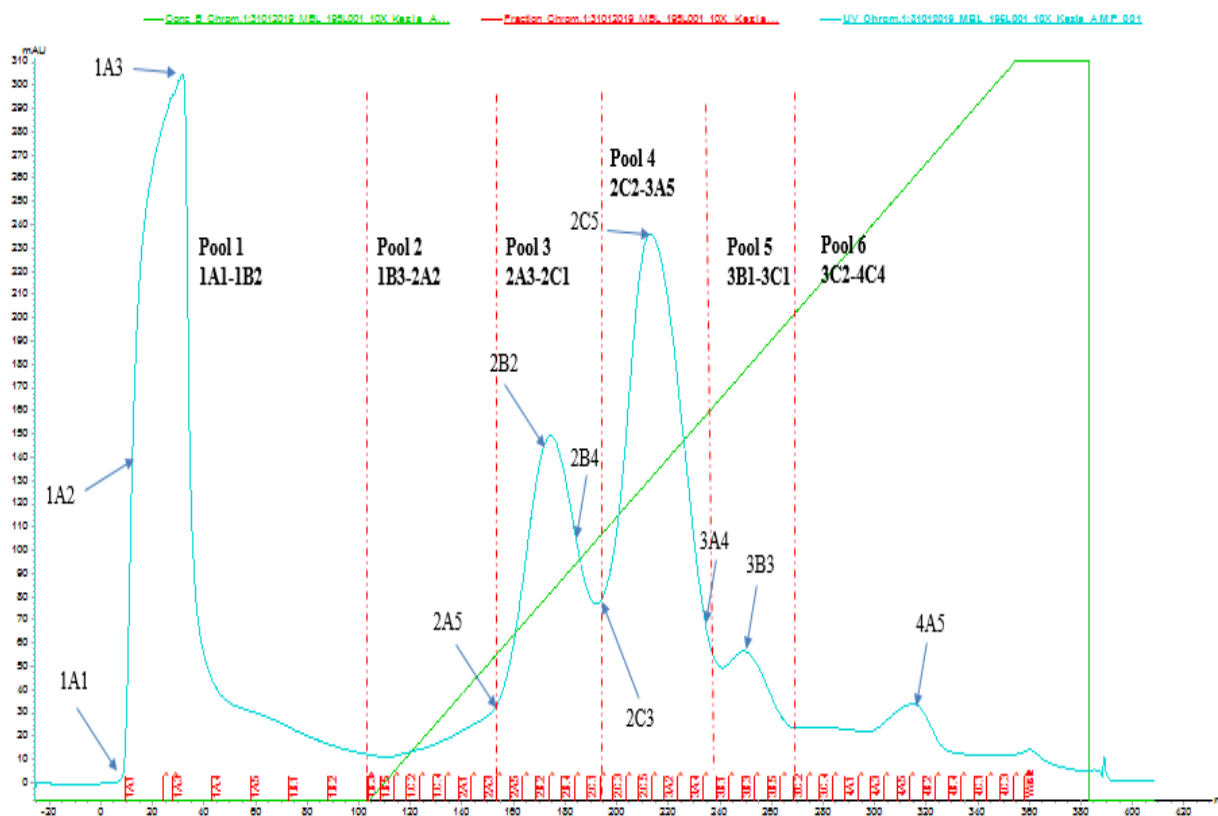


Figure 5.6. 1: An image of the HIC UV profile with linear gradient [1.2 M ammonium sulphate in 50 mM sodium phosphate, pH 7.0] in for MBL195L01 (5 L culture), 10 X concentrated. The UV chromatogram is depicted in blue, the eluted fractions are depicted in red, and the salt concentration is depicted in green. The image is a screenshot from the ÄKTA Pure 25 Chromatography System software. The fractions that were selected for buffer-exchange are indicated in the figure. The vertical dotted red lines show the boundaries between the pools (1-6) of fractions from the column.

Table 5.6. 1: A table indicating the U/mL of Catalase Activity in the buffer-exchanged HIC fractions of MBL195L01 (5 L culture) 10 X concentrated. The two columns showing values for catalase activity (U/mL) obtained were repetition of the assay (in triplicates each time) on two consecutive days.

HIC Fraction	Catalase (U/mL)	Catalase (U/mL)	HIC Pool
1A1	41.55 ± 0.06	8.66 ± 0.04	Pool 1
1A2	142.47 ± 0.17	136.64 ± 0.15	Pool 1
1A3	143.35 ± 0.11	141.06 ± 0.01	Pool 1
2A5	138.95 ± 0.06	127.59 ± 0.04	Pool 3
2B2	95.94 ± 0.07	86.61 ± 0.05	Pool 3
2B4	39.85 ± 0.05	34.31 ± 0.02	Pool 3
2C3	101.83 ± 0.21	23.95 ± 0.06	Pool 4
2C5	10.51 ± 0.07	5.89 ± 0.03	Pool 4
3A4	6.30 ± 0.08	5.95 ± 0.07	Pool 4
3B3	45.65 ± 0.02	24.66 ± 0.04	Pool 5
4A5	45.71 ± 0.07	21.68 ± 0.02	Pool 6

Table 5.6. 2: A table listing the protein concentration (mg/mL), catalase activity (U/mL), and catalase specific activity in the pooled HIC fractions of MBL195L01 (5 L culture) 10 X concentrated that had been 2 X concentrated and buffer-exchanged after pooling together.

Pooled Pool #	Protein Concentration (mg/mL)	Catalase (U/mL)	Catalase Specific Activity (U/mg)	Pooled HIC Fractions
Pooled Pool 1 (Catalase 1)	0.08 ± 0.01	283.63 ± 0.21	3545.38	1A1 + 1A2 + 1A3
Pooled Pool 3 (Catalase 3)	0.05 ± 0.00	99.69 ± 0.07	1993.80	2A5 + 2B2 + 2B4
Pooled Pool 4 (Catalase 4)	0.41 ± 0.01	35.15 ± 0.04	85.73	2C3 + 2C5 + 3A4

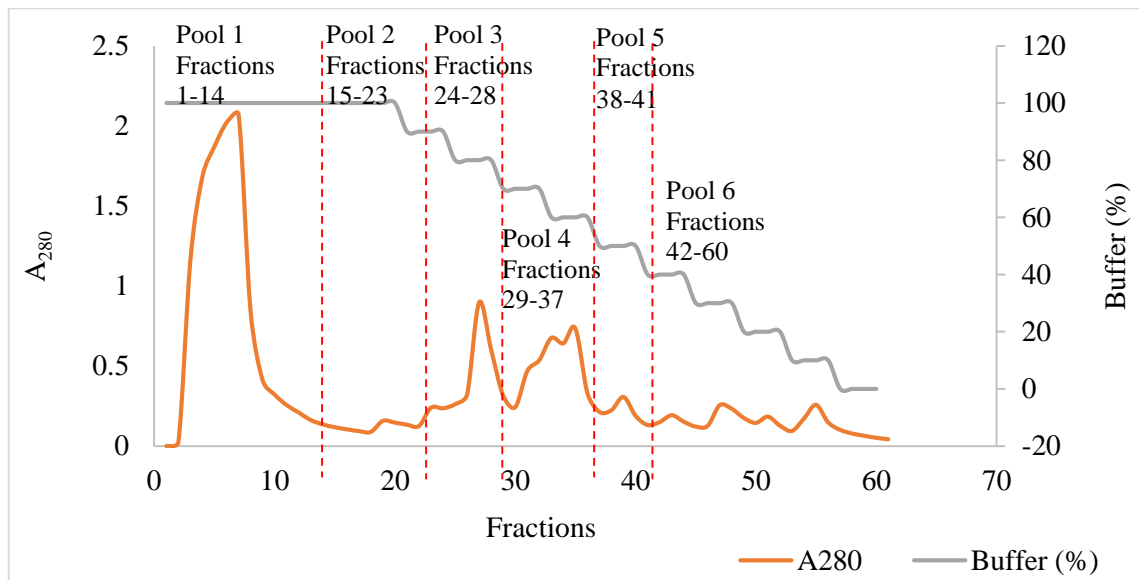


Figure 5.6. 2: An image of the HIC UV profile with linear gradient [1.2 M ammonium sulphate in 50 mM sodium phosphate, pH 7.0] for MBL191L053 (1 L culture) 20 X concentrated. The grey displays the buffer gradient and the orange displays the absorbance of the fractions at 280 nm. The vertical dotted red lines show the boundaries between the pools (1-6) of fractions from the column.

Table 5.6. 3: A table listing the catalase activity (U/mL) in the HIC fractions from MBL191L053 (1 L culture) 20 X concentrated. The assay was repeated twice (in triplicates each time) on two consecutive days.

HIC Fraction	Protein Concentration (mg/mL)	Catalase (U/mL)	Catalase (U/mL)
Fraction 1	0.03 ± 0.00	52.98 ± 0.05	41.12 ± 0.05
Fraction 5	0.02 ± 0.00	211.03 ± 0.12	41.66 ± 0.09
Fraction 6	0.02 ± 0.00	237.62 ± 0.08	66.86 ± 0.05
Fraction 25	0.03 ± 0.02	44.00 ± 0.03	35.65 ± 0.03
Fraction 26	0.06 ± 0.00	42.66 ± 0.01	25.92 ± 0.01
Fraction 28	0.02 ± 0.00	46.04 ± 0.10	29.24 ± 0.05
Fraction 29	0.01 ± 0.00	41.16 ± 0.04	21.37 ± 0.05
Fraction 34	0.19 ± 0.01	42.55 ± 0.14	20.74 ± 0.03
Fraction 36	0.04 ± 0.00	41.14 ± 0.01	27.70 ± 0.03
Fraction 38	0.06 ± 0.00	42.43 ± 0.03	15.47 ± 0.06
Fraction 46	0.06 ± 0.00	47.40 ± 0.02	16.42 ± 0.08
Fraction 54	0.01 ± 0.00	43.62 ± 0.02	15.30 ± 0.07

Table 5.6. 4: A table listing the protein concentration (mg/mL), catalase activity (U/mL), and catalase specific activity in the pooled HIC fractions of MBL191L053 (1 L culture) 20 X concentrate that had been 2 X concentrated and buffer-exchanged after pooling.

Pooled Pool #	Protein Concentration (mg/mL)	Catalase (U/mL)	Catalase Specific Activity (U/mg)	Pooled HIC Fractions
Pooled Pool 1 (Catalase 1)	0.11 ± 0.00	288.87 ± 0.07	2626.09	Fractions 1 + 5 + 6
Pooled Pool 3 (Catalase 3)	0.35 ± 0.02	90.95 ± 0.08	259.86	Fractions 25 + 26 + 28
Pooled Pool 4 (Catalase 4)	0.36 ± 0.02	45.50 ± 0.05	126.39	Fractions 29 + 30 + 34

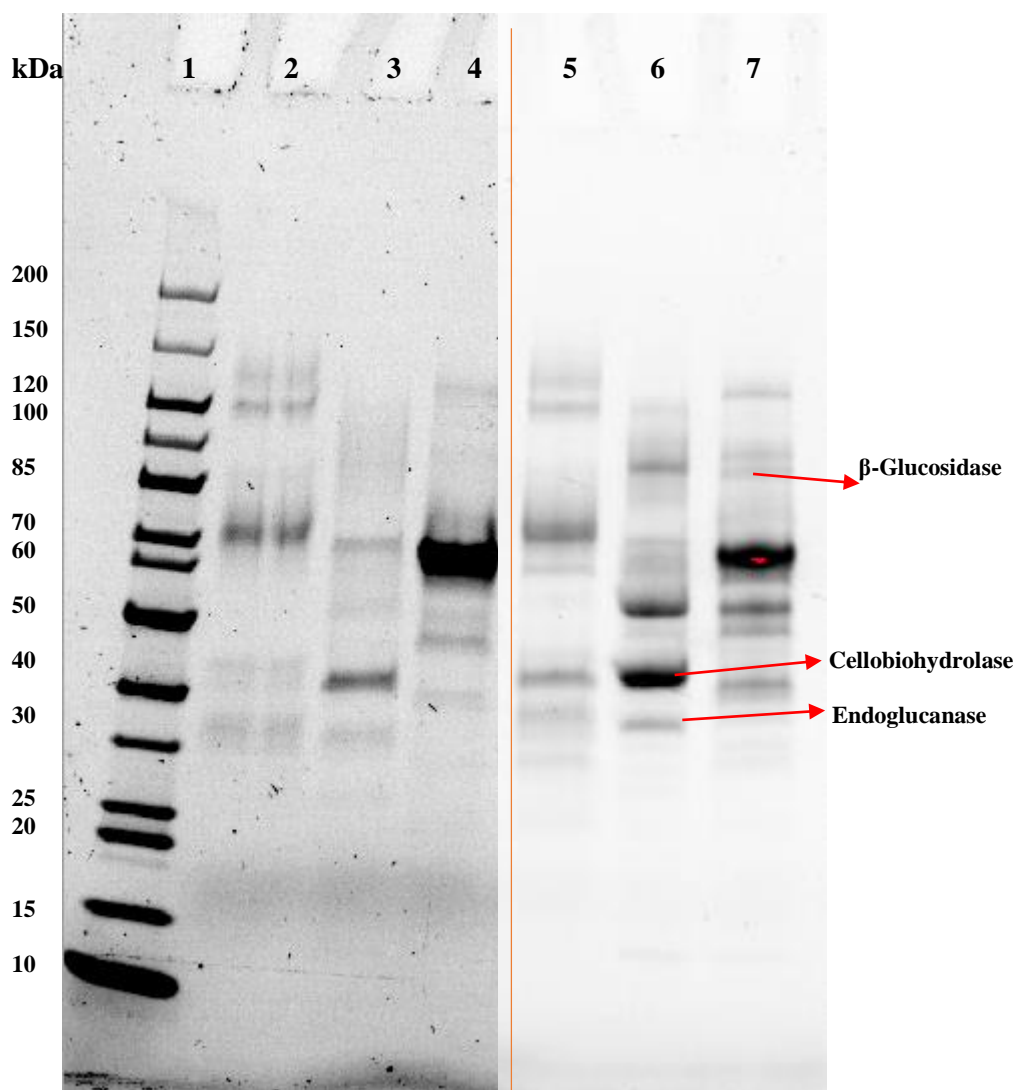


Figure 5.6. 3: SDS-PAGE analysis displaying the typical profile of *T. emersonii* proteins from the HIC Fractions. 2 X concentrated and pooled HIC fractions from MBL195L01 (5 L culture) 10 X concentrated and MBL191L053 (1 L culture) 20 X concentrated. The arrows correspond to the protein bands formed by β -Glucosidase (~90 kDa), Cellobiohydrolase isoforms (~30-42 kDa), and Endoglucanase (~27 kDa). The orange line after Lane 4 is to indicate that bands in Lanes 2, 3, and 4 come from the 5 L culture while Lanes 5, 6, and 7 come from a 1 L culture.

(Lane 1: PageRuler™ Unstained Protein Ladder; Lanes 2-4: 5 L culture 2 X Concentrated & Buffer- Exchanged Pooled Pool 1, Pooled Pool 3, and Pooled Pool 4; Lanes 5-7: 1 L culture 2 X Concentrated & Buffer Exchanged Pooled Pool 1, Pooled Pool 3, and Pooled Pool 4).

Partial purification of the in-house *T. emersonii* cocktail from two fermentation batches was carried out by HIC. The Senior Scientist at MBio undertook HIC of MBL195L01 using the ÄKTA Pure 25 Chromatography System. HIC of MBL191L053 was carried out at DCU by Dr. Andrew Dowd. Although similar overall, the slight variations in the peaks on the HIC profile in figures 5.6.1 and 5.6.2 may have been a result of the different techniques used for the enzyme cocktail purification process.

HIC fractions obtained from MBL195L01 10 X as well as MBL191L053 20 X were initially buffer-exchanged and assayed for catalase activity. It was not practical to screen all of the HIC fractions for catalase activity. Therefore, fractions were selected for screening based on the peaks observed in the HIC profile. Fractions that formed the peaks on the HIC profile as well as fractions on either sides of the peaks were screened for catalase activity. Catalase activity was detected in all fractions from the major peaks on the HIC profile. The pools in which catalase activity was detected were Pools 1, 3, 4, 5, and 6.

The fractions from each of the peaks containing catalase activity were pooled together, concentrated 2 X, and buffer-exchanged prior to re-assay for catalase activity. The results obtained indicated that the enzyme was not stable during storage following buffer exchange. This can be understood based on the results obtained in Tables 5.6.1 and 5.6.3. The buffer-exchanged HIC fractions were assayed in triplicates (each time) on two consecutive days. There was a decrease in catalase activity even after 24 hours. Consequently, it was not possible to assay all the HIC fractions that indicated catalase activity.

An SDS-PAGE analysis of the pooled HIC fractions from MBL195L01 10 X and MBL191L053 20 X was also carried out as can be seen in Figure 5.6.3. The protein bands were the thickest for pooled fractions from Pool 4 for both the bioreactor batches. The molecular weight of the band was approximately 70 kDa. Other bands observed in Pooled Pool 4 were at approximately 45 kDa for the 5 L bioreactor culture and at approximately 40, 50, 55 kDa for the 1 L bioreactor culture. The molecular weight of the prominent bands from Pooled Pool 1 were approximately 120 kDa and 70 kDa. Other bands from Pooled Pool 1 had molecular weights of approximately 40 kDa for the 1 L bioreactor batch. The molecular weights of the remaining bands from Pooled Pool 1 could not be determined as the protein bands were not well defined. The most prominent protein bands for Pooled Pool 3 were at approximately 70 kDa and 40 kDa for the 5 L bioreactor culture and 50 kDa and 40 kDa for the 1 L bioreactor culture. The protein bands observed in each of the Pooled, 2 X concentrated, and buffer-exchanged Pools 1, 3, and 4 were different from each other. Overall, the bands observed were as expected for *T. emersonii* and the prominent bands were representative of glycosyl hydrolases. Additionally, the prominent bands in each of the Pooled Pools 1, 3, and 4 were similar despite the two different HIC methods used for the 5 L and 1 L batches.

Due to time constraints and poor enzyme stability on storage, it was decided to focus on pools 1, 3, and 4 only for further characterisation experiments.

5.7 Characterisation of Catalase

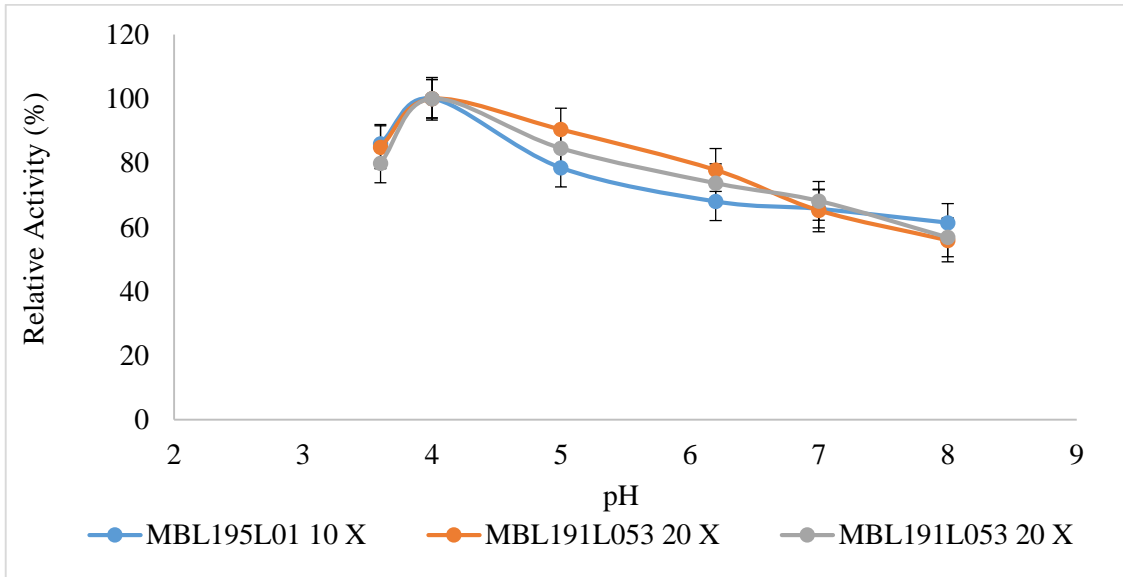


Figure 5.7. 1: A graph depicting the optimum pH of catalase in the Pooled, 2 X concentrated & Buffer-Exchanged Pool 1 (Catalase 1) fractions from MBL195L01 (5 L culture) 10 X concentrated and MBL191L053 (1 L culture) 20 X concentrated. MBL195L01 10 X was assayed once in triplicates while MBL191L053 20 X was assayed twice in triplicates each time.

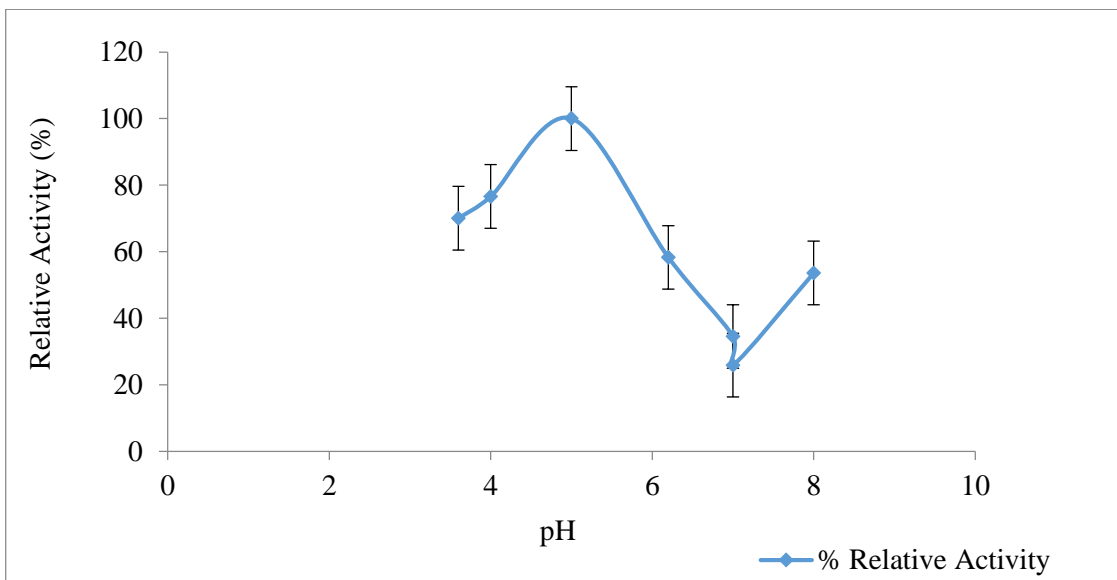


Figure 5.7. 2: A graph depicting the optimum pH of catalase in the Pooled, 2 X concentrated & Buffer-Exchanged Pool 3 (Catalase 3) fractions from MBL195L01 (5 L culture) 10 X concentrated.

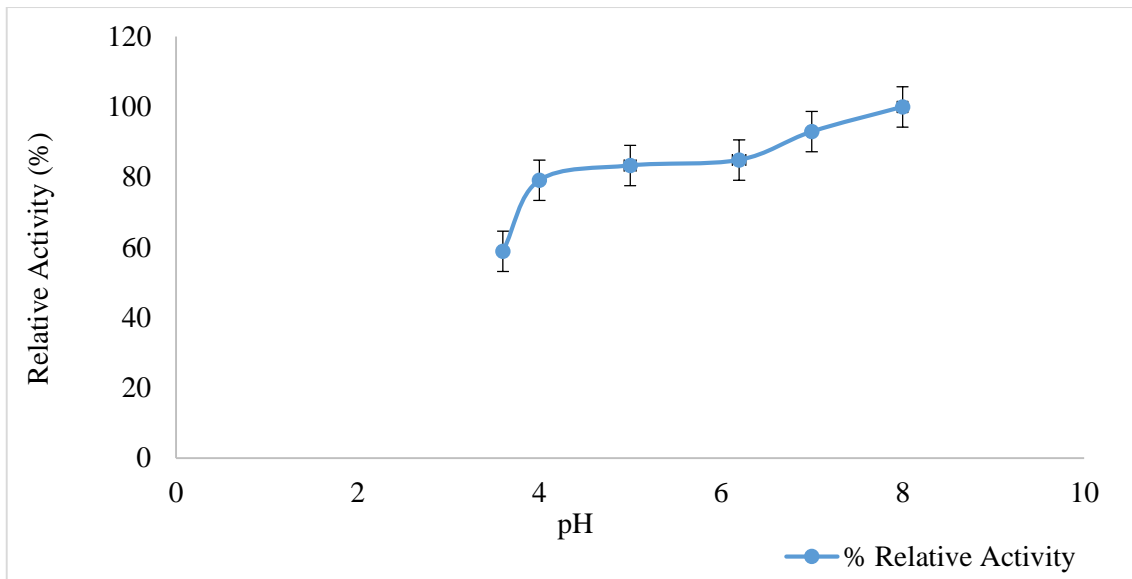


Figure 5.7. 3: A graph depicting the optimum pH of catalase in the Pooled, 2 X concentrated & Buffer-Exchanged Pool 3 (Catalase 3) fractions from MBL191L053 (1 L culture) 20 X concentrated.

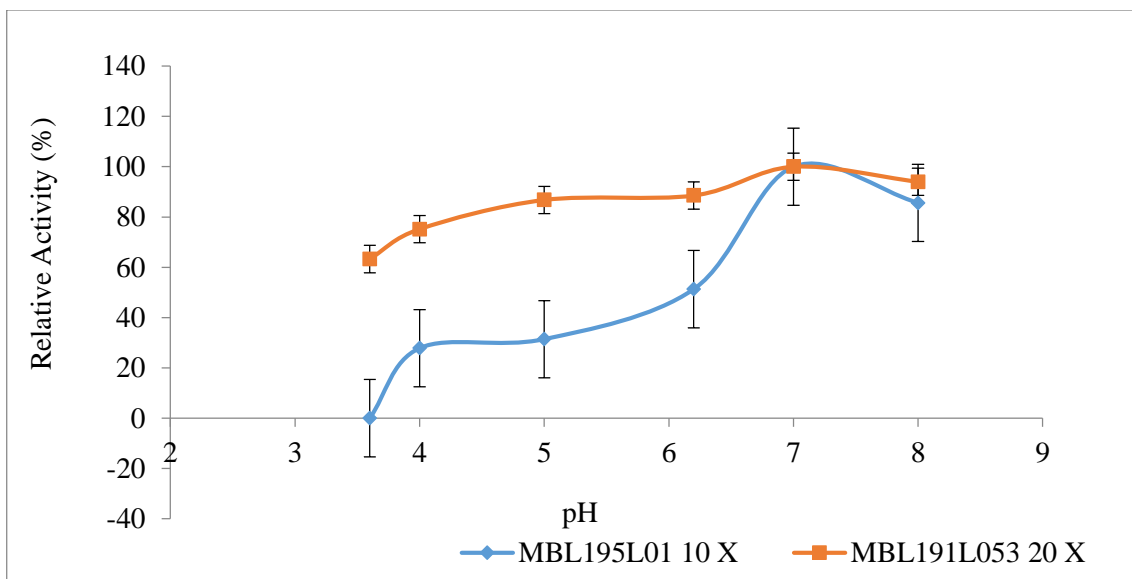


Figure 5.7. 4: A graph depicting the optimum pH of catalase in the Pooled, 2 X concentrated & Buffer-Exchanged Pool 4 fractions from MBL195L01 10 X and MBL191L053 20 X.

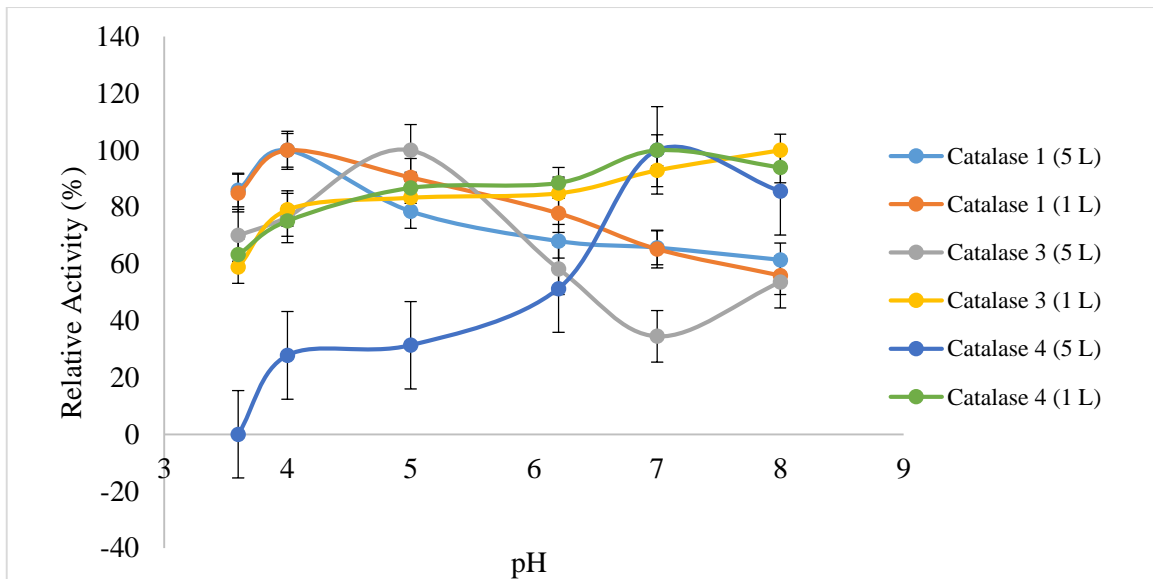


Figure 5.7. 5: A graph highlighting the different pH optima values of Catalase 1, Catalase 3, and Catalase 4 from the 5 L (MBL191L01 10 X concentrated) and 1 L (MBL191L053 20 X concentrated) fractions. The pH optimum graphs are shown individually in figures above (see figures 5.7.1 – 5.7.4).

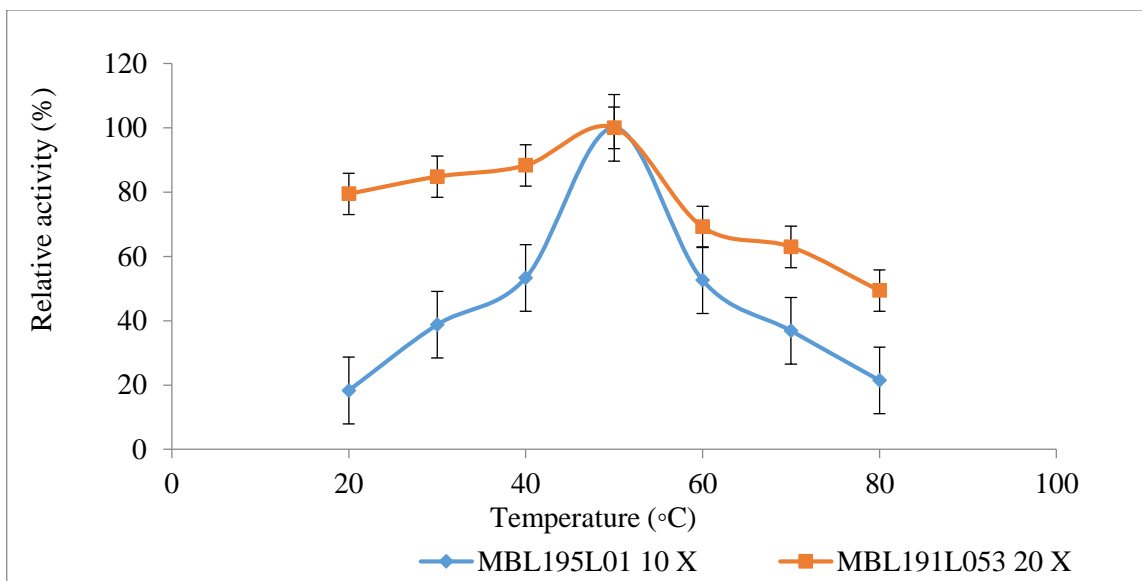


Figure 5.7. 6: A graph depicting the optimum temperature of catalase in the Pooled, 2 X concentrated & Buffer-Exchanged Pool 1 fractions from MBL195L01 (5 L culture) 10 X concentrated and MBL191L053 (1 L culture) 20 X concentrated.

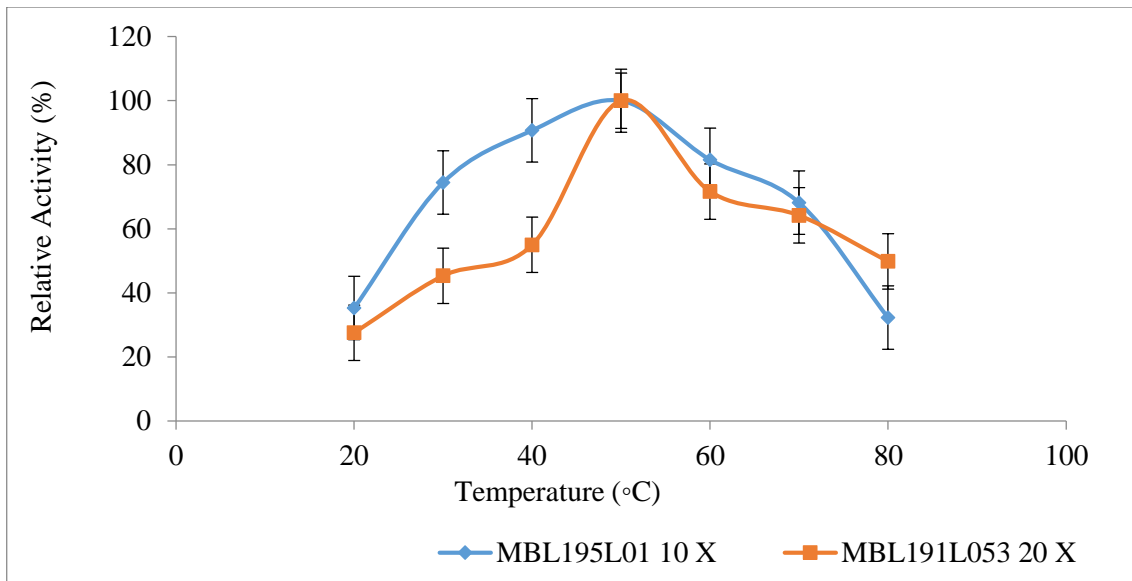


Figure 5.7. 7: A graph depicting the optimum temperature of catalase in the Pooled, 2 X concentrated & Buffer-Exchanged Pool 3 fractions from MBL195L01 (5 L culture) 10 X concentrated and MBL191L053 (1 L culture) 20 X concentrated.

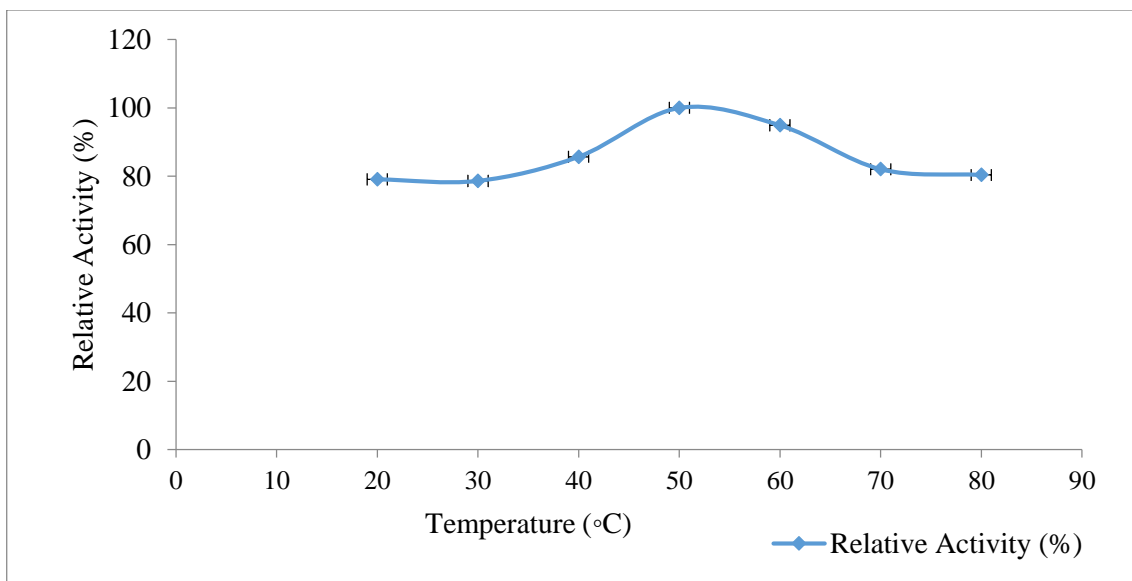


Figure 5.7. 8: A graph depicting the optimum temperature of catalase in the Pooled, 2 X concentrated & Buffer-Exchanged Pool 4 fractions from MBL191L053 (1 L culture) 20 X concentrated.

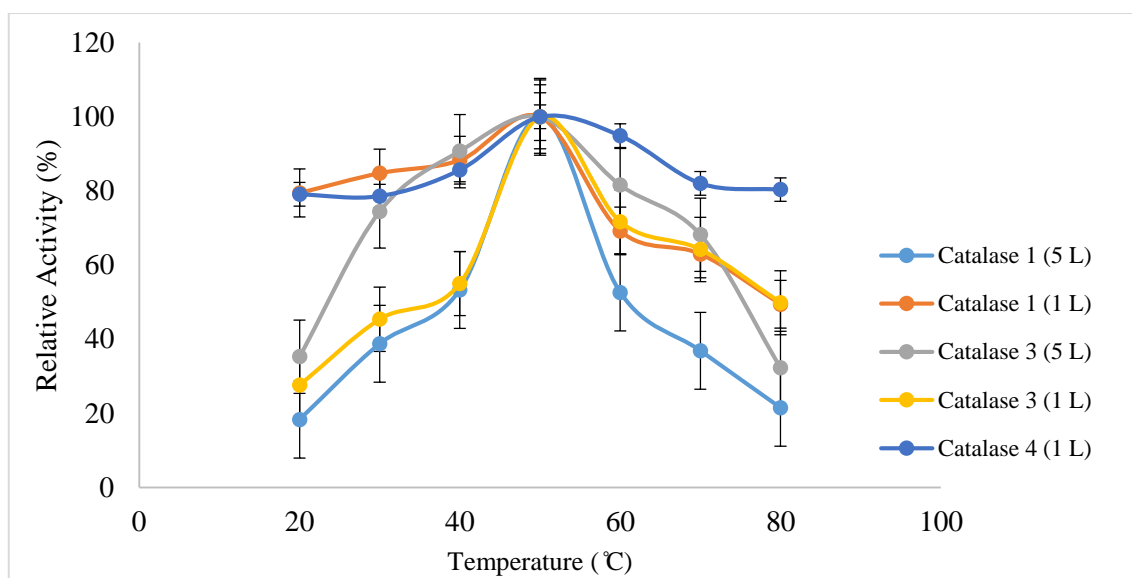


Figure 5.7. 9: A graph highlighting the different temperature optima values of Catalase 1, Catalase 3, and Catalase 4 from the 5 L (MBL191L01 10 X concentrated) and 1 L (MBL191L053 20 X concentrated) fractions. The temperature optimum graphs are shown individually in figures above (see figures 5.7.6 – 5.7.8).

Table 5.7. 1: A table summarising the pH and temperature optima values of catalase 1, catalase 3, and catalase 4 in the 5 L (MBL195L01 10 X concentrated) and 1 L (MBL191L053 20 X concentrated) fractions. The values in italics refer to the optimum pH and temperature values for the 1 L fractions.

HIC Fraction	Optimum pH		Optimum Temperature (°C)	Optimum Temperature (°C)
Catalase 1 (Pooled Pool 1)	4.0	<i>4.0</i>	50	<i>50</i>
Catalase 3 (Pooled Pool 3)	5.0	<i>8.0</i>	50	<i>50</i>
Catalase 4 (Pooled Pool 4)	7.0	<i>7.0</i>	50	<i>50</i>
Pool 5	nd	nd	nd	nd
Pool 6	nd	nd	nd	nd

Characterisation experiments were carried out using MBL195L01 10 X concentrated (Run volume: 5 L) and MBL191L053 20 X concentrated (Run volume: 1 L) fractions from 140 hours that had been purified using HIC. Characterisation experiments could only be performed to determine the optimum temperature and pH of catalase. Furthermore, as a result of limited sample volume being available, the characterisation experiments for pH and temperature could only be carried out once in triplicates for both MBL195L01 10 X concentrated and MBL191L053 20 X concentrated unless otherwise stated.

Characterisation experiments were carried out on the two different cultures (MBL195L01 10 X concentrated (Run volume: 5 L) and MBL191L053 20 X concentrated (Run volume: 1 L)). The reason for this was to investigate whether there would be differences in catalase activities and the expression of the various catalase isoforms by culturing *T. emersonii* in controlled conditions using 5 L and 1 L fermenters.

As mentioned in section 5.6, catalase was not stable on storage following buffer-exchange. The reason for this is hypothesised to be the buffer used in buffer-exchange of the HIC fractions. The buffer used for all the pooled HIC pool fractions was 20 mM Potassium Phosphate buffer at pH 6.2 as the optimum pH of the catalase isoforms was not previously known. As catalase isoforms with different optimum pH values were present in the enzyme cocktail, the potassium phosphate buffer used for buffer-exchange may have resulted in the breakdown of catalase on storage.

The presence of catalase isoforms in the enzyme cocktail was confirmed after the optimum pH determination experiments. Catalase activity was detected in fractions from all the peaks in the HIC profile (see figure 5.6.1 and 5.6.2). However, due to storage stability issues and time constraints, only three of the HIC pools from the first three peaks in the HIC profile was evaluated further for the characterisation experiments. The fractions that were buffer exchanged and assayed for catalase activity from each of the peaks were pooled together, concentrated two-fold and buffer-exchanged. The pooled fractions from each of the peaks were then assayed to determine the optimum temperature and pH.

The optimum pH of Catalase 1 from the first peak (Pooled Pool 1) was found to be pH 4.0 for both MBL195L01(5 L culture) 10 X concentrated and MBL191L053 (1 L culture) 20 X concentrated (see Figure 5.7.1). Although two different HIC methods were utilised (1- automated using the ÄKTA Pure 25 Chromatography System at MBio and 2- manually using the fraction collector at DCU), it was interesting to note that the optimum pH of Catalase 1 was the same for both the 5 L and the 1 L fraction.

The optimum pH of Catalase 3 from the second major peak (Pooled Pool 3) of HIC fractions was found to be pH 5.0 for MBL195L01 (5 L culture) 10 X concentrated (see Figure 5.7.2) and pH 8.0 for MBL191L053 (1 L culture) 20 X concentrated (see Figure

5.7.3). This result was not as expected. It was hypothesised that the two different pH optima values for Pooled Pool 3 HIC fractions may be an indicator of the need for further purification techniques to obtain more sensitive separation of the proteins present in the enzyme cocktail. As can be seen in the pH optimum graph of MBL195L01 10 X concentrated (Figure 5.7.2), there was a decrease in enzyme activity after pH 5.0. However, an increase in enzyme activity is observed again after pH 7.0, at pH 8.0. Additionally, for MBL191L053 20 X concentrated, the highest enzyme activity was found at pH 8.0. The differences in the pH optima values could also have been a result of the different HIC methods employed for partial purification of the enzyme cocktail. The graph (Figure 5.7.3) of pH optima for MBL191L053 20 X, was, however, not the typical bell curve. This may have been a result of the loss of catalase activity on storage. As a result, the catalase isoform with pH optimum of 5.0 could have been present in Pooled Pool 3 of MBL191L053 (1 L culture) 20 X concentrated but was not detected in the pH determination experiments due to loss of enzyme activity on storage. Another possibility for the differences in optimum pH values for Catalase 3 in the 1 L and 5 L culture could be the variations in the culture method. Although the culture conditions such as pH, dissolved oxygen, temperature, and agitation were kept constant in both the 1 L and 5 L fermenters, variations in vessel size may have resulted in the overexpression of one catalase isoform over the other in the different fermenters. This may also explain the increase in relative activity at pH 8.0 for the 5 L culture (see Figure 5.7.2). Two catalase isoforms may have been present in the Pooled Pool 3 fractions from the 5 L fermenter. However, the highest catalase activity may have been at pH 5.0 due to the catalase isoform with the pH optima of 5.0 being present in abundance.

The optimum pH for Catalase 4 from the third major peak in Pool 4 (Pooled Pool 4) was found to be pH 7.0 for both MBL195L01 10 X concentrated and MBL191L053 20 X concentrated. The pH curves in the graphs (see Figure 5.7.4) were not well defined and different for the two samples. It is thought to be a result of storing the samples in buffer that was not optimum for enzyme activity (enzyme storage buffer was 20 mM Potassium Phosphate Buffer, pH 6.2). The pH optima experiments could not be performed on freshly buffer-exchanged fractions. The buffer-exchanged fractions were stored at 4 °C for at least 5 days prior to experimental analyses. This may have led to the deterioration of enzyme activity on storage following buffer-exchange (for the 5 L HIC fraction). The pH profile of the 5 L HIC fraction showed lower relative activity than the 1 L HIC fraction. Catalase

4 present in the 1 L fraction is hypothesised to be stable at varying pH values as the graph was a broad bell-curve. However, the hypothesis could not be verified due to low sample volume available. Additionally, the differences in the graphs could also have resulted from culturing in two different fermenters (5 L and 1 L). Although the culture conditions such as pH, temperature, dissolved oxygen, and agitation were kept constant, variables may have arisen in the culture conditions as a result of differences in vessel sizes.

The optimum temperature of Catalase 1 and 3 was 50 °C for both MBL195L01 10 X concentrated and MBL191L053 20 X concentrated (see Figure 5.7.6 and 5.7.7). The optimum temperature for Catalase 4 for MBL191L053 20 X was also 50 °C (see Figure 5.7.8). The optimum temperature of Catalase 4 fraction from MBL195L01 10 X concentrated could not be determined as the enzyme was not stable on storage and hence, lost enzyme activity within the detectable range. For Catalase 4 from the 1 L HIC Fraction, the graph showed continued stability up to 80 °C. It was hypothesised that the enzyme was stable over varying pH and temperature values based on the graphs from Figures 5.7.4 and 5.7.8 respectively. However, as mentioned above, the hypothesis could not be verified due to low sample volumes available.

Nevertheless, this result obtained for Catalase 4 (from the 1 L HIC Fraction) was interesting as no scientific studies have been published on the catalase enzymes in *T. emersonii*. Therefore, confirmation of the hypothesis could mean the potential use of this enzyme for various industrial applications requiring higher temperatures. A similar result to Catalase 4 in *T. emersonii* was obtained in a study by Vatsyayan and Goswami (2016). In the study, experiments were conducted to determine the pH and temperature optima of *Aspergillus terreus*. The results stated that any specific temperature or pH optimum for maximum activity could not be determined for catalase in *A. terreus*. The reason for this was because the enzyme was active throughout the broad range of temperatures 25 °C to 90 °C and pH 4 to 12 (Vatsyayan and Goswami, 2016). The results of the study support the hypothesis that was drawn from the pH and temperature optima results for Catalase 4 from the 1 L HIC Fraction. However, as mentioned above, the experiment would need to be repeated to accept the hypothesis.

**CHAPTER 6: RESULTS & DISCUSSION - PROTEOMICS
ANALYSIS**

6.1 Protein Analysis

Table 6.1. 1: A table displaying the protein concentration (mg/mL) in the 12 shake flasks at 0 and 120 hours of culture.

Shake Flask #	Flask Type	Protein Concentration (mg/mL)	
		0 Hours	120 Hours
Flask 1	Control	0.18 ± 0.02	0.13 ± 0.01
Flask 2	Control	0.20 ± 0.01	0.15 ± 0.01
Flask 3	Control	0.21 ± 0.02	0.12 ± 0.00
Flask 4	Control	0.21 ± 0.03	0.17 ± 0.02
Flask 5	+ CuSO ₄	0.18 ± 0.00	0.34 ± 0.02
Flask 6	+ CuSO ₄	0.19 ± 0.01	0.29 ± 0.01
Flask 7	+ CuSO ₄	0.20 ± 0.01	0.14 ± 0.01
Flask 8	+ CuSO ₄	0.21 ± 0.01	0.12 ± 0.03
Flask 9	+ TiSiO ₄	0.18 ± 0.00	0.15 ± 0.01
Flask 10	+ TiSiO ₄	0.16 ± 0.01	0.13 ± 0.01
Flask 11	+ TiSiO ₄	0.33 ± 0.01	0.19 ± 0.02
Flask 12	+ TiSiO ₄	0.30 ± 0.01	0.14 ± 0.03

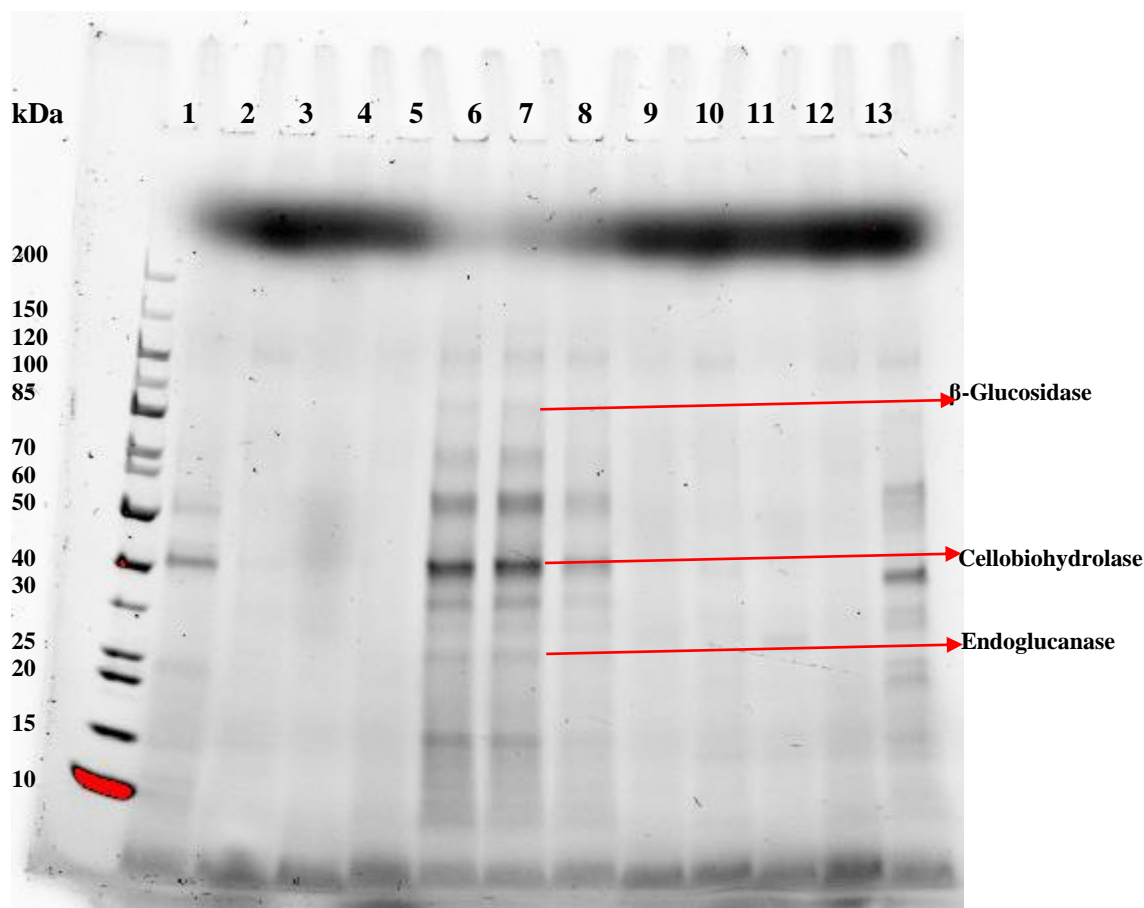


Figure 6.1. 1: SDS-PAGE analysis displaying the typical profile of *T. emersonii* proteins from the 12 Shake Flask Fractions at 120 hours. The 12 Shake Flask fractions included 4 control fractions (Lanes 2-5), Copper Sulphate induced fractions (Lanes 6-9) and Titanium Silicate induced fractions (Lanes 10-13). The arrows correspond to the protein bands formed by β -Glucosidase (~90 kDa), Cellobiohydrolase isoforms (~30-42 kDa), and Endoglucanase (~27 kDa).

(Lane 1: PageRuler Unstained™ Protein Ladder; Lanes 2-5: 120 Hours (Control) Flask 1, Flask 2, Flask 3 and Flask 4; Lanes 6-9: 120 Hours (+ CuSO₄) Flask 5, Flask 6, Flask 7, and Flask 8; Lanes 10-13: 120 Hours (+ TiSiO₄) Flask 9, Flask 10, Flask 11, and Flask 12).

Twelve shake flasks were set up for use in mass spectrometric analysis of the enzyme cocktail to identify the effect of inducers such as copper sulphate and titanium silicate (TiSiO₄) in protein expression. As mentioned above in chapter 4 (see section 4.5), copper sulphate (final concentration of 1 mM in production medium) was added to the shake flasks at 24 hours of culture. Studies had been previously carried out at MBio to investigate the effect of titanium silicate on the activity of glycosyl hydrolases. Therefore, it was decided to evaluate the effect of titanium silicate, if any, on the oxidoreductase enzymes. Unlike copper sulphate, 0.1 % titanium silicate (50 mg titanium silicate in 50 mL of primary seed culture) was added to the primary seeding flask. This method of

titanium silicate addition was carried out as it was the method used in the previous investigations at MBio.

In order to ensure that contamination risk was minimised, the shake flasks (control (flasks 1-4), and titanium silicate flasks (flasks 9-12) were only sampled at 0 and 120 hours. Copper sulphate was added to flasks 5-8 at 24 hours.

The protein concentration in each of the flasks at 0 and 120 hours were measured using the Bradford assay method (see methods, section 2.8.1). The protein concentration at 120 hours was lower than expected in all flasks (see Table 6.1.1). The highest protein concentration was in flasks 5 and 6. These flasks were induced with copper sulphate (final concentration of 1 mM in the production medium) The same was not the case for flasks 7 and 8 that were also induced with copper sulphate. A reason for the overall low protein concentration is thought to be the double-autoclaving method implemented for corn steep liquor prior to its addition in the production medium. This method was adopted in the lab at MBio to ensure that contamination risk was reduced as much as possible. Additionally, the batch to batch variation may also have been a result of shake flask culturing, as parameters such as dissolved oxygen levels and pH cannot be controlled in a shake flask environment during culture when compared to culturing in the bioreactors.

An SDS-PAGE analysis was also carried using the shake flask fractions from 120 hours. As was expected, the protein bands were not clearly visible for the control fractions and fractions containing titanium silicate. The protein bands were clearer in shake flask fractions 5, 6, and 7. This was as expected, as these flasks contained copper sulphate and copper sulphate was known to induce the activity of laccase as well as glycosyl hydrolase enzymes present in *T. emersonii*.

6.2 Proteomics Analysis – Control vs. Copper Sulphate vs. Titanium Silicate

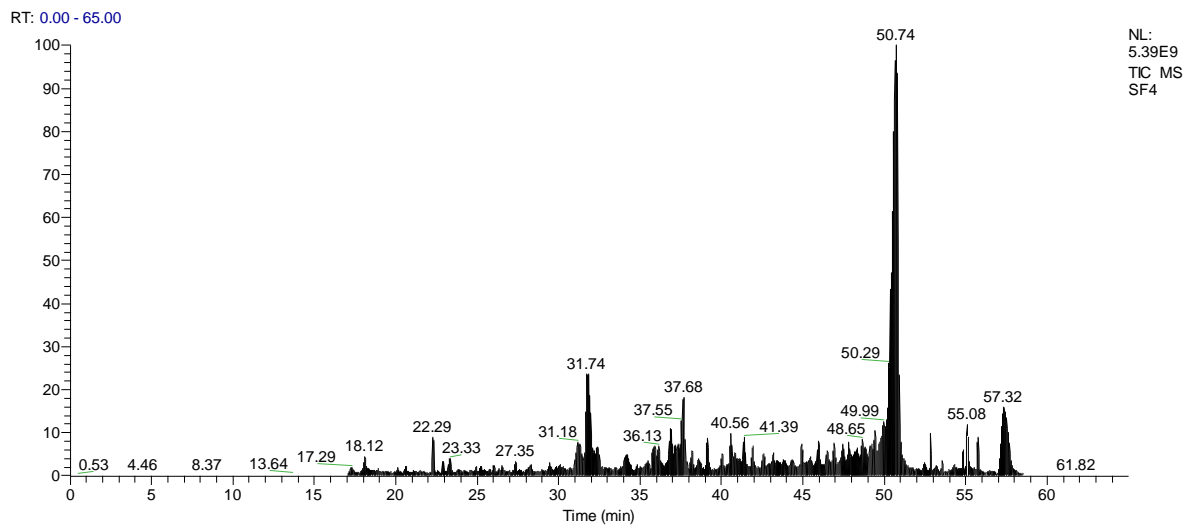


Figure 6.2. 1: Total Ion Chromatogram (TIC) trace of Shake Flask 4 (Control) at 120 hours

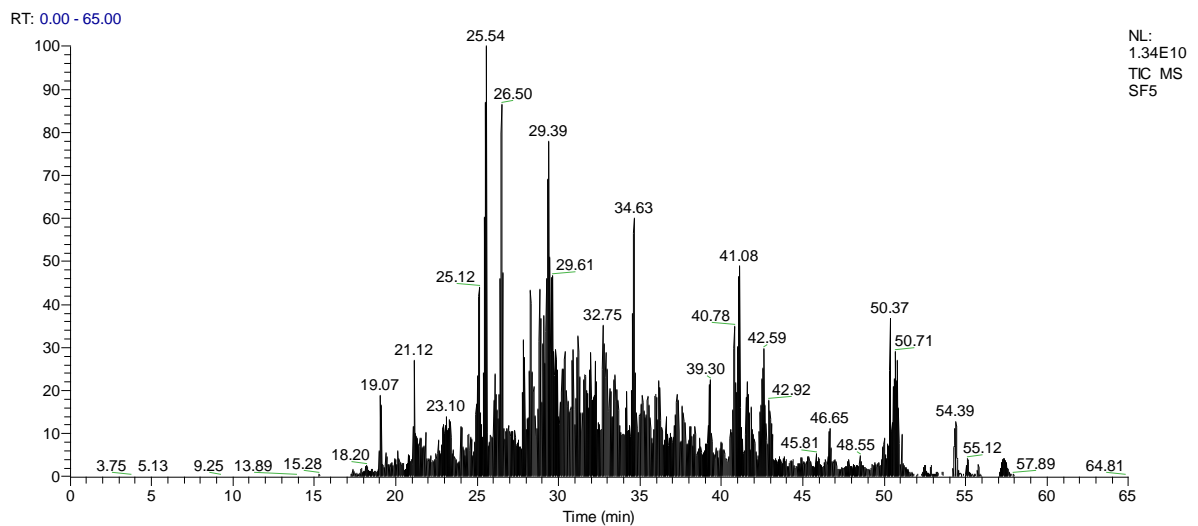


Figure 6.2. 2: TIC trace of Shake Flask 5 (copper sulphate) at 120 hours

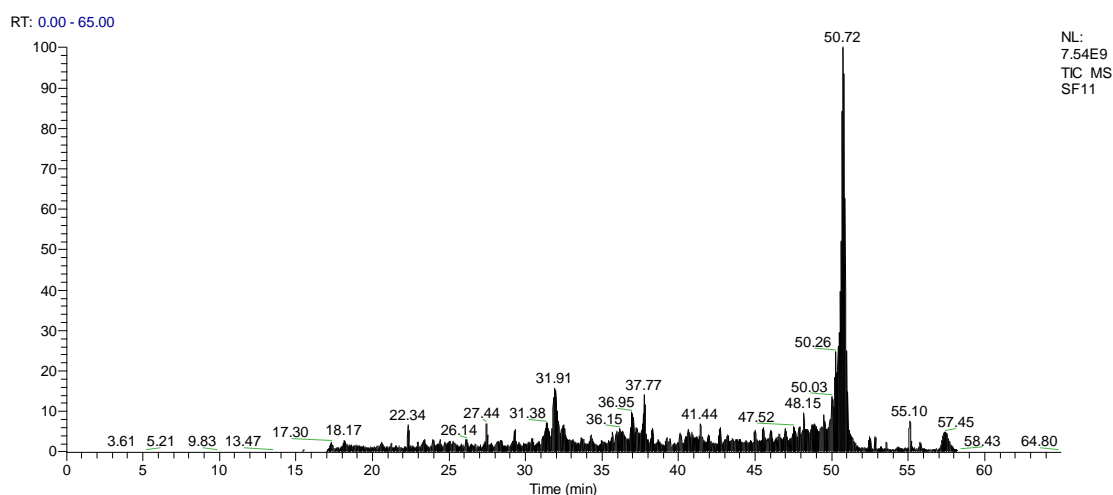


Figure 6.2. 3: TIC trace of Shake Flask 11 (titanium silicate) at 120 hours

Table 6.2. 1: A table displaying the list of proteins that were only found in the control shake flasks vs. copper sulphate induced flasks and control shake flasks vs. titanium silicate induced flasks. The proteins in italics refer to those that were upregulated in the copper sulphate and titanium silicate induced-shake flasks.

Control vs. Copper Sulphate		Control vs. Titanium Silicate	
CONTROL	COPPER SULPHATE	CONTROL	TITANIUM SILICATE
Actin	Calmodulin	Citrate Synthase	Alkaline phosphatase
Pyridoxine hydrochloride	<i>Beta-Glucosidase</i>	Nucleoside diphosphate kinase	Dipeptidyl-peptidase III
	<i>Cell wall antigenic protein</i>	Fructose-bisphosphate aldolase	Formamidase
			Phosphomannomutase
			<i>Beta-Glucosidase</i>

The mass spectrometry analyses were carried out by Dr. Paul Dowling at National University of Ireland, Maynooth.

As can be seen in figures 6.2.1 - 6.2.3, there are differences between the peaks in the TIC traces for the control, copper sulphate and titanium silicate flasks. However, as can be seen in Figures 6.2.1 and 6.2.3, the TIC traces look similar for the control and titanium silicate induced fractions. This reaffirmed the results obtained from the Bradford assay

which indicated that there was no increase in protein concentration with the addition of titanium silicate (see table 6.1.1). There was a significant difference between the TIC trace for the copper sulphate induced fraction and the control fraction (see figures 6.2.1 and 6.2.2). This supported the results obtained from the Bradford assay which indicated an increase in protein concentration for flasks 5 and 6 (see table 6.1.1). Flasks 5 and 6 were induced with copper sulphate at 24 hours of culture. As hypothesised previously, it could be confirmed from the TIC trace of copper sulphate induced fraction that induction with copper sulphate had an effect on *T. emersonii* proteins.

Two proteins were significantly upregulated in the copper sulphate-induced fractions when compared to the control. They were beta-glucosidase (ANOVA p value of 0.04) and cell wall antigenic protein (ANOVA p value of 0.02). Beta-glucosidase had a chromatographic peak of 23.86 in the control fractions and 25.72 in the copper sulphate-induced fractions with 10 unique peptides. It had a molecular weight of 92.39 kDa. Cell wall antigenic protein had a chromatographic peak of 25.70 in the control fraction and 29.89 in the copper sulphate-induced fractions with 2 unique peptides. It had a molecular weight of 28.72 kDa. It was already understood from shake flask (see table 4.5.3) and bioreactor experiments (see table 4.6.1) that copper sulphate had an inducing effect on beta-glucosidase activity. The mass spectrometry analysis confirmed this experimental observation. The effect of copper sulphate on cell wall antigenic protein was not previously known. Additionally, not much information is available on this protein(s). However, it is understood that they are heavily glycosylated.

Actin and pyridoxine hydrochloride were only present in the control fractions. This may be because copper sulphate has a negative effect on their expression.

In eukaryotes, the actin cytoskeleton is composed of polymers of actin together with actin-binding and actin-associated proteins. The actin cytoskeleton in fungi has a role in numerous cellular processes such as cell polarity, cytokinesis, endocytosis, exocytosis, bud site selection, cell wall remodelling, and cell shape determination. In filamentous fungi, actin localises to sites of cell wall deposition in growing hyphae. Specifically, actin patches accumulate at hyphal tips (Upadhyay and Shaw, 2008). The effect of copper sulphate on actin expression has not been well studied in fungi. However, a study was conducted by Kumari et al. (2018) to study the effects of heavy metals such as copper on

the health of fishes. The fish studied was *Catla catla* larvae and the effect of copper on beta-actin was investigated. The study concluded that copper sulphate was toxic to *Catla catla* larvae. Therefore, it is hypothesised that the addition of copper sulphate may have affected the morphology of *T. emersonii*, a filamentous fungus, resulting in downregulation of its expression in the copper sulphate-induced fractions.

Pyridoxine hydrochloride is a biologically interconvertible form of pyridoxine (vitamin B₆). Vitamin B₆ is an essential co-factor in numerous enzymatic reactions involved primarily in amino acid metabolism. It is required by all living organisms and must be synthesised or derived from nutrients (Bilski et al., 2000). In addition to its role as a vital co-factor, the study by Bilski et al. (2000) suggests that vitamin B₆ may function as an antioxidant by interacting with singlet molecular oxygen during photooxidative stress in the filamentous fungus *Cercospora nicotianae*. In a study by Dhawan and Kuhad (2002), laccase production was induced by pyridoxine hydrochloride in the bird's nest fungus *Cyathus bulleri*. Therefore, it is hypothesised that, in *T. emersonii*, laccase expression was also naturally induced by pyridoxine hydrochloride. However, the addition of copper sulphate may have directly induced laccase expression, thereby, reducing the expression of pyridoxine hydrochloride.

Calmodulin was only found in the copper-sulphate induced fractions. This may be due to a positive effect on its expression by copper sulphate. Calmodulin is a type of calcium-binding protein that responds to micromolar levels of Ca²⁺ by binding to certain enzymes and stimulating them. The amino acid composition of several fungal and plant calmodulins have been elucidated and found to be very similar to calmodulin from animals. Several fungal and plant enzymes have been reported to be regulated either directly or indirectly by calmodulin (Moreau, 1987). Much scientific evidence on the effect of copper sulphate on fungal calmodulins could not be found. However, in a study by González et al. (2012) on marine macroalga *Ulva compressa*, an increase in intracellular calcium was observed when cultivated with 10 µM copper. Furthermore, a study by Sakamoto et al. (2012) on *P. chrysosporium* demonstrated that transcription of the calmodulin gene was upregulated by cyclic adenosine 3',5'-monophosphate (cAMP) and isobutyl-1-methylxanthine. cAMP pathway also increases the transcription levels of most lignin peroxidase and manganese peroxidase isozyme genes through the induction of calmodulin gene transcription. Lignin peroxidase and manganese peroxidase are

thought to play an important role in the initiation of lignin degrading reaction of fungi as they can cleave lignin structures extracellularly in the first step of lignin mineralisation (Sakamoto et al., 2012). Therefore, it is hypothesised that addition of copper sulphate induced calmodulin expression which in turn results in upregulation of lignin peroxidase and manganese peroxidase gene. Consequently, this may initiate the lignin degrading reaction in *T. emersonii*.

As can be seen in figures 6.2.1 and 6.2.3, there were differences in the peaks on the TIC traces of the control fractions and the titanium silicate-induced fractions.

Only one protein was significantly upregulated in the titanium silicate-induced fractions when compared to the control. It was beta-glucosidase (ANOVA p value of 0.04). Beta-glucosidase had a chromatographic peak of 23.86 in the control fractions and 24.83 in the titanium silicate-induced fractions with 11 unique peptides. It had a molecular weight of 92.39 kDa. The effect of titanium silicate on the protein expression in *T. emersonii* was unknown. However, it was hypothesised that induction of *T. emersonii* cultures with titanium silicate may result in a slight increase in the expression of glycosyl hydrolase enzymes. However, due to time limitations, it was not possible to carry out enzyme assays to determine the effect of titanium silicate on the expression of beta-glucosidase, endoglucanase, cellobiohydrolase, and xylanase enzymes.

Citrate synthase, nucleoside diphosphate kinase, and fructose-bisphosphate aldolase were only present in the control fractions when compared to the titanium silicate-induced fractions.

Citrate synthase catalyses the condensation of acetyl-CoA with oxaloacetate to form citrate and coenzyme A. Additionally, the metabolic pathway involved in citric acid biosynthesis includes citrate synthase. Citrate synthase is also considered a 'key step' in the citric acid cycle as it may be regarded as the 'first step' of the cycle (Ruijter et al., 2000). Citrate synthase is assumed to be the rate-limiting enzyme of the cycle. The citric acid cycle regulates energy generation in mitochondrial respiration and plays a central role in carbohydrate metabolism (Chen et al., 2014). There was no scientific information available regarding the effect of titanium silicate on the expression of citrate synthase. However, based on the knowledge gained from existing scientific literature, it was

hypothesised that titanium silicate induced the expression of citrate synthase, which, in turn, affected carbohydrate metabolism by *T. emersonii*. As the enzyme was only present in the control fractions, titanium silicate may have had an inhibitory effect on its expression.

Nucleoside diphosphate kinase is a housekeeping enzyme that balances cellular nucleoside triphosphate pools by catalysing the reversible transfer of γ -phosphate from nucleoside triphosphates to nucleoside diphosphates. In addition to its role in nucleotide metabolism, nucleoside diphosphate kinase has roles in protein histidine phosphorylation, DNA cleavage/repair, and gene regulation (Yu et al., 2017). The role of nucleoside diphosphate kinase in filamentous fungi is not yet known (Wang et al., 2019). A study by Wang et al. (2019c) on *Aspergillus flavus* suggested that nucleoside diphosphate kinase regulates spore and sclerotia development. The enzyme was also found to be involved in plant virulence as understood from experiments using corn and peanut seed-based assays. Although there is no scientific evidence in the scientific literature regarding the effect of titanium silicate on nucleoside diphosphate kinase expression, it was hypothesised that the enzyme was pivotal in spore production and sclerotia formation in *T. emersonii*. As the enzyme was only found in the control fractions and not in the titanium silicate-induced fractions, it may be inhibited by titanium silicate.

Fructose-bisphosphate aldolase is an enzyme that has key roles in glycolysis and gluconeogenesis pathways. It catalyses the reversible cleavage of fructose-1,6-bisphosphate to dihydroxy-acetone phosphate and glyceraldehyde 3-phosphate. The enzyme is essential for the growth of fungus on both fermentative and non-fermentative carbon sources (Rodaki et al., 2006). The enzyme was only present in the control fractions and was thought to be pivotal for the growth of *T. emersonii* on carbon sources. Therefore, it was hypothesised that titanium silicate had an inhibitory effect on the enzyme as absence of the enzyme in titanium silicate-induced fractions may mean that the organism was not able to utilise the carbon sources present in the production medium efficiently.

Alkaline phosphatase, dipeptidyl peptidase III, formamidase, and phosphomannomutase were only present in titanium silicate-induced fractions. This may have been a result of the upregulation of the genes for each these enzymes in the presence of titanium silicate.

Alkaline phosphatase is a ubiquitous membrane-bound glycoprotein that catalyses the hydrolysis of phosphate monoesters at basic pH values (Sharma et al. 2014). A study by Eichlerová et al. (2015) stated that alkaline phosphatase levels were generally present in saprotrophic microfungi but absent in most brown-rot and white-rot fungi. However, ascomycete fungi had a higher gene copy number of alkaline phosphatase. Unfortunately, it was not understood from the available scientific research as to the role of alkaline phosphatase in filamentous fungi such as *T. emersonii*. Therefore, it was not possible to deduce whether the upregulation of alkaline phosphatase by titanium silicate was a positive effect.

Dipeptidyl peptidase III is a zinc-dependent aminopeptidase and the sole member of the M49 family of metallopeptidases. It sequentially hydrolyses dipeptides from the N-terminal of oligopeptides ranging from 3-10 amino acid residues. The precise biological function of this peptidase is still unclear (Prajapati and Chauhan, 2011; Jajčanin-Jozić et al., 2010). In mammals, this enzyme is indicated to contribute to the pain modulatory system and defence mechanisms against oxidative stress. It is also thought to have a role in normal intracellular protein catabolism (Jajčanin-Jozić et al., 2010). It was hypothesised that the expression of this enzyme may be an indicator of oxidative stress within the cells on the addition of titanium silicate. However, as scientific understanding of the enzyme in filamentous fungi is currently limited, it cannot be known for sure whether the presence of this enzyme in titanium silicate-induced fractions is a positive or negative effect.

Formamidase enzymes hydrolyse formamide and play a role in fungal nitrogen metabolism (Borges et al., 2010). Nitrogen is an essential requirement for growth and the ability to metabolise a wide variety of nitrogen sources enables fungi to colonise different environmental niches and survive nutrient limitations (Tudzynski, 2014). Therefore, it was hypothesised that the expression of formamidase in the fractions upon induction with titanium silicate was a positive effect.

Phosphomannomutase catalyses the interconversion of mannose-6-phosphate and mannose-1-phosphate. Mannose-1-phosphate is the substrate for the synthesis of GDP-mannose, an essential intermediate for protein glycosylation, protein sorting and secretion, and maintaining a functional endomembrane system in eukaryotic cells. In

Saccharomyces cerevisiae, phosphomannomutase is essential for viability (Qian et al., 2007). It was, therefore, assumed that the presence of phosphomannomutase in titanium silicate-induced fractions may have a positive effect as it has a role in protein glycosylation. The reason for this was because protein glycosylation was crucial in ensuring proper confirmation of membrane proteins.

From the proteomics analysis, it was evident that copper sulphate had an impact on protein activity in *T. emersonii*. This confirmed the experimental results obtained in chapter 4 (see tables 4.5.3 and 4.6.1) with regards to the effect of copper on protein concentration and its ability to upregulate the activity of the three main glycosyl hydrolase enzymes namely, beta glucosidase, endoglucanase, and cellobiohydrolase. From the results obtained in chapter 4 (see tables 4.5.3 and 4.6.1), it was also understood that the greatest impact of copper sulphate was on the activity of betaglucosidase. This was also confirmed from the proteomics analysis. The effect of titanium silicate on protein activity was investigated as experiments were conducted by the Scientists at MBio regarding its influence on glycosyl hydrolase activity. Therefore, it was interesting to investigate further to see if it had an influence on oxidoreductase activity. As scientific evidence on the effect of Titanium silicate was not widely available, it was hypothesised that it did not affect protein activity in *T. emersonii*. The only protein whose activity was upregulated by titanium silicate was beta-glucosidase. As the TIC traces for the control and titanium silicate was almost similar, the hypothesis that titanium silicate did not influence protein activity was supported.

CHAPTER 7: DISCUSSION & CONCLUSION

7.1 Bioinformatics Analyses

Mass spectrometry analysis of HIC pools of *T. emersonii* cocktail generated short peptide sequences of the proteins present in the organism. Through bioinformatics analyses of the mass spectrometric data, complete amino acid sequences of the proteins present in *T. emersonii* were obtained. As a result, it was possible to identify and name the proteins present in *T. emersonii*. This enabled screening and selection of the four oxidoreductase enzymes of interest for use in further studies. Those selected were laccase, catalase, dehydrogenase, and lytic polysaccharide monooxygenase.

7.2 Laccase

Initially, laccase could not be detected in the in-house enzyme cocktail using the ABTS assay method. Therefore, it was decided to look into more sensitive assay methods for the detection of laccase. As a result, the Amplex Red assay method was identified through survey of scientific literature. This method was adopted and an SOP was drafted for use at MBio. It was understood that Amplex Red method (a fluorimetric method) was more sensitive than the ABTS method (a spectrophotometric method).

Although laccase was detected by the Amplex Red method, activity was lower in the shake flask fractions. Therefore, it was decided to use copper sulphate as an inducer of laccase activity in the shake flask fractions. A study by Viswanath et al. (2014) stated that copper was a strong laccase inducer in several fungal species such as *Neurospora crassa*, *Trametes versicolor*, *Phanerochaete chrysosporium*, *Panus osteratus*, *Pleurotus sajor-caju*, *Trametes trogii*, *Volvariella volvacea*, *Lentinula edodes*, and *Grifola frondosa*. The promoter regions of the genes encoding for laccase contain various recognition sites that are specific for xenobiotics and heavy metals. These can bind to the recognition sites of the gene when present in the medium and induce laccase production. The induction of laccase gene transcription by copper is suggested to be related to a defence mechanism against oxidative stress caused by free copper ions (Viswanath et al., 2014).

Following experimental analyses, it was understood that copper sulphate had a positive effect on the activity of laccase as well as the glycosyl hydrolase enzymes, namely beta-glucosidase, endoglucanase, cellobiohydrolase, and xylanase. Furthermore, even though

laccase was detectable in the shake flask fractions after the addition of copper sulphate, the enzymatic activity (U/mL) detected was low. Therefore, it was decided to scale-up *T. emersonii* culture from shake flasks to benchtop bioreactors to obtain higher yields of the enzyme for successful characterisation of the enzyme. After set-up of several benchtop bioreactor batches, fractions obtained from a 1 L benchtop bioreactor run at 140 hours were selected for use in the laccase characterisation experiments.

Although partial purification of the enzyme cocktail was achieved by HIC, several purification steps are required to obtain pure laccase free from other contaminant proteins. Multiple steps like ultrafiltration, precipitation using ammonium sulphate or organic solvents, and ion exchange and size exclusion chromatography have been used in various studies for the purification of laccases from the culture filtrate (Viswanath et al., 2014). Typical fungal laccase is a protein of approximately 60-70 kDa with acidic isoelectric point around pH 4.0 (Viswanath et al., 2014; Baldrian, 2006).

The 1 L bioreactor fraction from 140 hours was first purified by HIC. The HIC fractions were screened for laccase activity. Screening of the HIC fractions indicated that there was only one laccase present in the *T. emersonii* cocktail. Characterisation experiments indicated that laccase had an acidic pH optimum of 3 and a temperature optimum of 40 C. By performing the pH determination experiments on laccase using the ABTS assay method, it was observed that the enzyme was easily detectable in the presence of 0.1 M citrate buffer (pH 3.0). Therefore, it was used as the assay buffer in all further assays of laccase using both ABTS and Amplex Red as the substrate.

The pH optimum of *T. emersonii* laccase (pH 3.0) indicates that it can function optimally under conditions that are not favourable to growth.

However, natural fungal hosts produce very low yields of laccases, too low for commercial purposes. Therefore, cloning of laccase genes and heterologous expression are employed to improve laccase production. Although laccase production has often been significantly improved by expression in heterologous hosts, the reported levels have still been rather low for industrial applications. This is due to incorrect folding and inefficient codon usage of expression organisms that in turn results in non-functional or low yields of laccase (Viswanath et al., 2014).

Nevertheless, fungal laccases are of particular interest with regard to potential industrial applications because of their capability to oxidise a wide range of industrially relevant substrates. Additionally, oxidation reactions are comprehensively used in industrial processes such as textile, food, wood processing, and pharmaceutical and chemical industries. Enzymatic oxidation is preferred to chemical methods since enzymes are very specific and efficient catalysts and are ecologically sustainable. Currently, laccases are already used on a large scale in the textile industry. Together with low molecular weight redox-mediator compounds, laccases can generate a desired worn appearance on denim by bleaching indigo dye. There are also esoteric suggestions for the usage of laccase in the presence of hydroxyl stilbenes as hair dyes. Another potential environmental application of laccases is the bioremediation of contaminated soils, as laccases are able to oxidise toxic organic pollutants such as polycyclic aromatic hydrocarbons and chlorophenols. The most useful method for this application would be to inoculate the soil with fungi that are efficient laccase producers because the use of isolated enzymes is not economically feasible for soil remediation in large-scale (Viswanath et al., 2014).

7.3 Catalase

Catalase was the second *T. emersonii* oxidoreductase that was selected for further studies.

Catalase was easily detectable in the in-house cocktail in both shake flask fractions and benchtop bioreactor fractions. However, it was also clear that the addition of copper sulphate had an inhibitory effect on catalase activity. Shake flask fractions were assayed for catalase activity. Although attempts at characterisation of catalase were made using the shake flask fractions, they were not successful. It was hypothesised that more than one isoform of catalase was present in the *T. emersonii* cocktail. As a result, it was decided to scale-up *T. emersonii* culture from shake flasks to benchtop bioreactors to obtain higher yields of catalase for use in further purification experiments. Several benchtop bioreactor batches were set up. Two of the batches, namely, MBL195L01 (5 L) and MBL191L053 (1 L) were partially purified using HIC prior to catalase characterisation.

In order to achieve purification of catalase from the enzyme cocktail, multiple chromatography steps are required such as anion exchange chromatography, hydrophobic

interaction chromatography, and gel filtration chromatography (Mina et al., 2015). However, only partial purification using HIC was carried out at MBio. Following HIC, fractions forming peaks as well as fractions on either sides of the peaks were selected to screen for catalase activity. Through screening of the HIC fractions, the hypothesis that more than one isoforms of catalase were present in the *T. emersonii* cocktail was confirmed. Although catalase was present in all of the fractions that formed the peaks on the HIC profile, due to time constraints and loss of enzymatic activity on storage following buffer-exchange, it was decided to perform characterisation experiments on only three of the catalases. The fractions forming the first three peaks were each pooled together, concentrated 2 X, and buffer-exchanged. The fractions were labelled Pooled Pool 1, Pooled Pool 3, and Pooled Pool 4 respectively. The optimum pH and temperature of catalase in each of the pooled pools 1, 3, and 4 were determined experimentally. The optimum temperature of catalase in each of the pools was 50°C. However, catalase present in each of the three pools had different pH optima, namely, pH 4.0 (Pooled Pool 1), 5.0 (Pooled Pool 3), and 8.0 (Pooled Pool 4). The pH profile of Pooled Pool 4 indicated that further purification may be needed to obtain pure catalase from Pooled Pool 4 fractions. The reason for this was the increase in relative activity of catalase at pH 8.0 following the drop in pH at pH 6.0 and 7.0.

It was also observed that, following buffer-exchange, there was a loss of enzyme activity on storage. Due to time limitations, it was not possible to perform stability studies to investigate methods to improve enzyme stability on storage. If time had permitted, the pooled pools 1, 3, and 4 would be buffer-exchanged in buffers that had pH values similar to their optimum pH values. The enzyme activity would have been detected every day for a week to evaluate the change in activity on storage. Additionally, the effect of stabilising components such as glycerol, ammonium sulphate, and polyethylene glycol as well as the effect of various storage temperatures would also have been investigated. Currently, catalase has industrial applications in the fabric and food processing industries. In the fabric industry, catalase is used for removing excess hydrogen peroxide from fabric. Catalase is also used along with other enzymes in the food processing industry. Catalase is often used with glucose oxidases for food preservation (Raveendran et al., 2018). Glucose oxidase and catalase enzymes work together. Glucose oxidase has antioxidant, preservative, and stabiliser properties. Catalase assists in the breakdown of hydrogen peroxide produced by glucose oxidase. Consequently, inhibition and

deactivation by hydrogen peroxide is reduced (Wong et al., 2008). Catalase is also used to eliminate peroxide from milk in the milk processing industry. Hydrogen peroxide is used for the cold-sterilisation of milk. However, the hydrogen peroxide must be removed from the product by appropriate chemical or physical means. Hence, catalase is used for the removal of hydrogen peroxide as it is cost-effective and more environmentally friendly than chemical methods for reducing hydrogen peroxide. Additionally, in the baking industry, catalase is used to remove glucose from egg white. The enzyme is also used in food wrappers to prevent oxidation and to control perishability of food. Furthermore, catalase also has limited use in cheese production (Raveendran et al., 2018). The catalases present in *T. emersonii* could (if obtainable in pure form and in high yield) be utilised for these above-mentioned industrial applications as they have an optimum temperature of 50 °C and pH optima ranging between acidic and basic in the different pooled pool fractions 1, 3, and 4.

7.4 Proteomics Analysis

The mass spectrometry analyses were useful to gain an understanding of the differences in protein expression between the control shake flasks as well the shake flasks induced with copper sulphate and titanium silicate.

The mass spectrometry results of the control vs. copper sulphate-induced fractions were not as expected. The reason for this was because the expression of laccase as well as glycosyl hydrolases (such as endoglucanase, cellobiohydrolase, and xylanase) also showed slight increase in enzyme activity when assayed. However, the mass spectrometry analyses only showed a significant effect of copper induction for betaglucosidase. It was expected that copper sulphate induction would have an effect on betaglucosidase as it showed the greatest increase in enzyme activity when assayed. Additionally, it was also surprising to note that actin and pyridoxine biosynthesis protein were only present in the control fractions and not in the copper sulphate-induced fractions. The reason for this was because the final concentration of copper sulphate in the production medium was only 1 mM. Therefore, it was not expected that it would have potential inhibitory effects on proteins present in *T. emersonii*. Furthermore, it was also slightly disappointing to note that laccase activity was not significantly upregulated in

the mass spectrometry results. The aim behind the addition of copper sulphate to the fractions was primarily to induce laccase expression.

The results of the control vs. titanium silicate-induced fractions was not as expected. It was interesting to note that more proteins were identified in control vs. titanium silicate induced-fractions than in the control vs. copper sulphate-induced fractions. Furthermore, when surveying the literature for understanding the effect of titanium silicate on each of the identified proteins, it was positive to learn that research-based evidence in this area was rare. Therefore, it opens the door to further experimental investigations that will provide better insights into the effect of titanium silicate on protein expression in *T. emersonii*.

7.5 Conclusion

Although four candidate oxidoreductases were selected for further studies, experimental analyses could be conducted only on two of the four enzymes. This was primarily due to the contamination issue faced during the project. *T. emersonii* cultures could not progress further without identifying the root cause of contamination. Although the cause of the contamination was identified, several weeks were required for the troubleshooting process. As a result, time available was limited and studies could not be carried out on the two remaining oxidoreductase enzymes that were selected. However, the project enabled an in-depth study of laccase and catalases present in *T. emersonii*. and has fulfilled its intended objective, the “Discovery of industrially relevant oxidoreductase enzymes”. Had time not been a limiting factor, similar studies to those described in Chapters 2, 4 and 5 could also be conducted on dehydrogenase and lytic polysaccharide monooxygenases. Furthermore, experiments would also be carried out to increase the amounts of laccase produced by cloning and expression of the laccase gene from *T. emersonii* in other eukaryotic hosts such as *Pichia pastoris*, *Pichia methanolica*, *Saccharomyces cerevisiae*, and *Aspergillus niger*. Additionally, methods such as directed evolution and recombinant DNA technology could be utilised to select for functional laccase gene variants.

8.0 References

- Amorim, A. M., Gasques, M. D. G., Andreaus, J. and Scharf, M. 2002. 'The application of catalase for the elimination of hydrogen peroxide residues after bleaching of cotton fabrics', *Anais da Academia Brasileira de Ciências*, 74(3), pp. 433-436.
- Baldrian, P. 2006. 'Fungal laccases-occurrence and properties', *FEMS Microbiology Reviews*, 30(2), pp. 215-242.
- Baminger, U., Nidetzky, B., Kulbe, K. D. and Haltrich, D. 1999. 'A simple assay for measuring cellobiose dehydrogenase activity in the presence of laccase', *Journal of Microbiological Methods*, 35(3), pp. 253-259.
- Beers, R. F. and Sizer, I. W. 1952. 'A Spectrophotometric method for measuring the breakdown of hydrogen peroxide by catalase', *The Journal of Biological Chemistry*, 195(1), pp.133-140.
- Bilski, P., Li, M. Y., Ehrenshaft, M., Daub, M. E. and Chignell, C. F. 2000. 'Vitamin B₆ and its derivatives are efficient singlet oxygen quenchers and potential fungal antioxidants', *Photochemistry and Photobiology*, 71(2), pp. 129-134.
- Bollenbach, T. J., Schuster, G. and Stern, D. B. 2004. 'Cooperation of endo- and exoribonucleases in chloroplast mRNA turnover', *Progress in Nucleic Acid Research and Molecular Biology*, 78, pp.305-337.
- Borges, C. L., Parente, J. A., Barbosa, M. S., Santana, J. M., Báo, S. N., De Sousa, M. V. and De Almeida Soares, C. M. 2010. 'Detection of a homotetrameric structure and protein-protein interactions of *Paracoccidioides brasiliensis* formamidase lead to new functional insights', *FEMS Yeast Research*, 10(1), pp. 104-113.
- Bourdais, A., Bidard, F., Zickler, D., Berteaux-Lecellier, V., Silar, P. and Espagne, E. 2012. 'Wood utilization is dependent on catalase activities in the filamentous fungus *Podospora anserina*', *PLOS ONE*, 7(4), pp. e29820.
- Bradford, M. M. 1976. 'A rapid and sensitive method for the quantitation of microgram quantities of protein utilizing the principle of protein-dye binding', *Analytical Biochemistry*, 72, pp. 248-254.
- Brenelli, L., Squina, F. M., Felby, C. and Cannella, D. 2018. 'Laccase-derived lignin compounds boost cellulose oxidative enzymes AA9', *Biotechnology for Biofuels*, 11(1), pp. 10.
- Brijwani, K., Rigdon, A. and Vadlani, V. 2010. 'Fungal laccases: production, function, and applications in food processing', *Enzyme Research*, 2010, pp.1-10.
- Brugger, D., Krondorfer, I., Zahma, K., Stoisser, T., Bolivar, J. M., Nidetzky, B., Peterbauer, C. K. and Haltrich, D. 2014. 'Convenient microtiter plate-based, oxygen-independent activity assays for flavin-dependent oxidoreductases based on different redox dyes', *Biotechnology Journal*, 9(4), pp. 474-482.
- Cell Biolabs, Inc. (2019). *OxiSelect™ Catalase Activity Assay Kit, Fluorometric*. [Online] USA: Cell Biolabs, Inc. pp. 1-7. Available at: <https://www.cellbiolabs.com/sites/default/files/STA-341-T-catalase-activity-assay.pdf> [Accessed: 05 Dec. 2019].

- Center for Cancer Research (no date) *Geneious R11*. Available at: <https://ostr.ccr.cancer.gov/bioinformatics/software/geneious/> (Accessed: 16 September 2019).
- Chefetz, B., Chen, Y. and Hadar, Y. 1998. 'Purification and Characterization of Laccase from *Chaetomium thermophilum* and Its Role in Humification', *Applied and Environmental Microbiology*, 64(9), pp. 3175-3179.
- Chen, L., Liu, T., Zhou, J., Wang, Y., Wang, X., Di, W. and Zhang, S. 2014. 'Citrate synthase expression affects tumor phenotype and drug resistance in human ovarian carcinoma', *PLOS ONE*, 9(12), pp. e115708.
- Christopher, L. P., Yao, B. and Ji, Y. 2014. 'Lignin biodegradation with laccase-mediator systems', *Frontiers in Energy Research*, doi: 10.3389/fenrg.2014.00012. Available at: <https://www.frontiersin.org/articles/10.3389/fenrg.2014.00012/full>. (Accessed: 16 Apr 2020).
- Ciullini, I., Tilli, S., Scozzafava, A. and Briganti, F. 2008. 'Fungal laccase, cellobiose dehydrogenase, and chemical mediators: Combined actions for the decolorization of different classes of textile dyes,' *Bioresource Technology*, 99(15), pp. 7003-7010.
- Couto, S. R. and Toca, J. L. 2006. 'Inhibitors of Laccases: A Review', *Current Enzyme Inhibitors*, 2, pp. 343-352.
- Dashtban, M., Schraft, H., Syed, T. A. and Qin, W. 2010. 'Fungal biodegradation and enzymatic modification of lignin', *International Journal of Biochemistry and Molecular Biology*, 1(1), pp. 36-50.
- Dekker, R. F. H. 1980. 'Induction and characterization of a cellobiose dehydrogenase produced by a species of *Monilia*', *Journal of General Microbiology*, 120 (2), pp. 309-316.
- Dhawan, S. and Kuhad, R. C. 2002. 'Effect of amino acids and vitamins on laccase production by the bird's nest fungus *Cyathus bulleri*', *Bioresource Technology*, 84(1), pp. 35-38.
- Dias, A. A., Matos, A. J. S., Fraga, I., Sampaio, A. and Bezerra, R. M. F. 2017. 'An easy method for screening and detection of laccase activity', *The Open Biotechnology Journal*, 11(1), pp.89-93.
- Doshi, R. and Shelke, V. 2001. 'Enzymes in textile industry-An environment-friendly approach', *Indian Journal of Fibre & Textile Research*, 26, pp. 202-205.
- Duarte, J. C., Costa-Ferreira, M. and Sena-Martins, G. 1999. 'Cellobiose dehydrogenase. Possible roles and importance for pulp and paper biotechnology', *Bioresource Technology*, 68(1), pp.43-48.
- Eichlerová, I., Homolka, L., Žifčáková, Lisá, L., Dobiášová, P. and Baldrian, P. 2015. 'Enzymatic systems involved in decomposition reflects the ecology and taxonomy of saprotrophic fungi', *Fungal Ecology*, 13, pp. 10-22.
- [Enzyme Consultancy Company] (2010) [Enzyme Consultancy Company] *Proposal for the Manufacture of an Enzyme Preparation Comprising Heat Stable Beta-Glucanase by the Submerged Fermentation of Talaromyces emersonii*. Spain: [Enzyme Consultancy Company]. Unpublished.
- Evguenieva-Hackenberg, E., Schiltz, E. and Klug, G. 2002. 'Dehydrogenases from all three domains of life cleave RNA', *The Journal of Biological Chemistry*, 277, pp. 46145-46150.

- Frandsen, K. E. H. and Lo Leggio, L. 2016. 'Lytic polysaccharide monooxygenases: a crystallographer's view on a new class of biomass-degrading enzymes', *IUCrJ*, 3(6), pp 448-467.
- Fu, K., Fu, S., Zhan, H., Zhou, P., Liu, M. and Liu, H. 2013. 'A newly Isolated Wood-rot Fungus for Laccase Production in Submerged Cultures', *BioResources*, 8(1), pp. 1385-1397.
- Gadda, G. and McAllister-Wilkins, E. E. 2003. 'Cloning, Expression, and Purification of Choline Dehydrogenase from the Moderate Halophile *Halomonas elongata*', *Applied and Environmental Microbiology*, 69(4), pp. 2126-2132.
- Gomma, O. M. and Momtaz, O. A. 2015. 'Copper induction and differential expression of laccase in *Aspergillus flavus*', *Brazilian Journal of Microbiology*, 46(1), pp. 285-292.
- González, A., Cabrera, M. d. l. A., Henríquez, M. J., Contreras, R. A., Morales, B. and Moenne, A. 2012. 'Cross talk among calcium, hydrogen peroxide, and nitric oxide and activation of gene expression involving calmodulins and calcium-dependent protein kinases in *Ulva compressa* exposed to copper excess', *Plant Physiology*, 158(3), pp. 1451-1462.
- Goodell, B., Qian, Y. and Jellison, J. (2008) *Development of Commercial Wood Preservatives*. Edited by Tor P. Schultz, Holger Miltz, Michael H. Freeman, Barry Goodell and Darrel D. Nicholas. Washington DC: American Chemical Society. ACS Symposium Series, volume 982, pp. 9-31.
- Hansberg, W., Salas-Lizana, R. and Domínguez, L. 2012. 'Fungal catalases: Function, phylogenetic origin and structure', *Archives of Biochemistry and Biophysics*, 525(2), pp. 170-180.
- Hanukoglu, I. 2015. 'Proteopedia: Rossmann fold: a beta-alpha-beta fold at dinucleotide binding sites', *Biochemistry and Molecular Biology Education*, 43(3), pp. 206-209.
- Hemsworth, G. R., Johnston, E. M., Davies, G. J. and Walton, P. H. 2015. 'Lytic polysaccharide monooxygenases in biomass conversion', *Trends in Biotechnology*, 33(12), pp. 747-761.
- Huang, S. and Lin, Q. 2003. 'Functional expression and processing of rat choline dehydrogenase precursor', *Biochemical and Biophysical Research Communications*, 309(2), pp. 344-350.
- Huijbers, M. M. E., Martínez-Júlvez, M., Westphal, A. H., Delgado-Arciniega, E., Medina, M. and van Berkel, W. J. H. 2017. 'Proline dehydrogenase from *Thermus thermophilus* does not discriminate between FAD and FMN as cofactor', *Scientific Reports*, 7, pp. 43880-43893.
- IHC World (2018) *ABC of Safety in the Biological Sciences*. Available at: <http://www.ihcworld.com/royellis/ABCsafe/chemicals/pararosanine.htm> (Accessed: 10 July 2018).
- Isobe, K., Inoue, N., Takamatsu, Y., Kamada, K. and Wakao, N. 2006. 'Production of catalase by fungi growing at low pH and high temperature', *Journal of Bioscience and Bioengineering*, 101(1), pp. 73-76.
- Jaber, S. M., Md Shah, U. K., Asa'ari, A. Z. M. and Ariff, A. B. 2017. 'Optimisation of laccase production by locally isolated *Trichoderma muroiana* IS1037 using rubber wood dust as substrate', *BioResources*, 12(2), pp. 3834-3849.

- Jain, J. L., Jain, S. and Jain, N. (2005). 'Chapter 16 Enzymes-I Nomenclature and Classification', *Fundamentals of Biochemistry*. New Delhi: S. Chand & Company Ltd., pp. 333-348.
- Jajčanin-Jozić, N., Deller, S., Pavkov, T., Macheroux, P. and Abramić, M. 2010. 'Identification of the reactive cysteine residues in yeast dipeptidyl peptidase III', *Biochimie*, 92(1), pp. 89-96.
- Jiang, J., Wu, X. and Chen, Y. 2012. 'Strategy to solve cofactor issues in oxidoreductase catalysed biocatalytic applications', *Sheng Wu Gong Cheng Xue Bao*, 28(4), pp. 410-419.
- Johannes, T. W., Woodyer, R. D. and Zhao, H. (2006) 'High-throughput Screening Methods Developed for Oxidoreductases', in Reymond, J. L. (ed.) *Enzyme Assays: High-Throughput Screening, Genetic Selection and Fingerprinting*. Weinheim: Wiley-VCH Verlag GmbH & Co. KGaA, pp.77-93.
- Johansen, K. S. 2016. 'Discovery and industrial applications of lytic polysaccharide mono-oxygenases', *Biochemical Society Transactions*, 44(1), pp. 143-149.
- Kameshwar, A. K. S. and Qin, W. 2017. 'Qualitative and Quantitative Methods for Isolation and Characterization of Lignin-Modifying Enzymes Secreted by Microorganisms', *BioEnergy Research*, 10(1), pp. 248-266.
- Karigar, C. S. and Rao, S. S. 2011. 'Role of microbial enzymes in the bioremediation of pollutants: a review', *Enzyme Research*, 2011, pp.1-11.
- Kawasaki, L. and Aguirre, J. 2001. 'Multiple catalase genes are differentially regulated in *Aspergillus nidulans*', *Journal of Bacteriology*, 183(4), pp. 1434-1440.
- Khatoun, N., Jamal, A. and Ali, M. I. 2017. 'Polymeric pollutant biodegradation through microbial oxidoreductase: A better strategy to safe environment', *International Journal of Biological Macromolecules*, 105, pp.9-16.
- Kirkman, H. N. and Gaetani, G. F. 1984. 'Catalase: A tetrameric enzyme with four tightly bound molecules of NADPH', *Proceedings of the National Academy of Sciences of the United States of America*, 81(14), pp. 4343-4347.
- Kittl, R., Kracher, D., Burgstaller, D., Haltrich, D. and Ludwig, R. 2012. 'Production of four *Neurospora crassa* lytic polysaccharide mono-oxygenases in *Pichia pastoris* monitored by a fluorimetric assay', *Biotechnology for Biofuels*, 5(1), p. 79.
- Kumar, V. V., Kirupha, S. D., Periyaraman, P. and Sivanesan, S. 2011. 'Screening and induction of laccase activity in fungal species and its application in dye decolorization', *African Journal of Microbiology*, 5(11), pp. 1261-1267.
- Kumari, K., Krishna, G., Pathakota, G. B., Annam, P. K. and Kumar, S. 2018. 'Acute toxicity of copper sulphate on *Catla catla* larvae and its effect of expression of three commonly used housekeeping genes', *Indian Journal of Biochemistry & Biophysics*, 55, pp. 12-16.
- Lackie, J. M. (2013). *The Dictionary of Cell and Molecular Biology*. Fifth Edition. Edited by J. G. Coote and C. W. Lloyd. Boston: Academic Press. p.168.
- Lambou, K., Pennati, A., Valsecchi, I., Tada, R., Sherman, S., Sato, H., Beau, R., Gadda, G. and Latgé, J-P. 2013. 'Pathway of Glycine Betaine Biosynthesis in *Aspergillus fumigatus*', *Eukaryotic Cell*, 12(6), pp. 853-863.

- Laurinavicius, V., Razumiene, J., Ramanavicius, A. and Ryabov, A. D. 2004. 'Wiring of PQQ-dehydrogenases', *Biosensors and Bioelectronics*, 20(6), pp. 1217-1222.
- Leech, D., Pellissier, M. and Barrière, F. (2008). 'Chapter 12 Powering fuel cells through biocatalysis', in Zhang, X. (ed.), Ju, H. (ed.) and Wang, J. (ed.) *Electrochemical Sensors, Biosensors and Their Biomedical Applications*. United States of America: Academic Press, pp. 385-410.
- Liu, J., Xie, J., Chu, Y., Sun, C., Chen, C. and Wang, Q. 2008. 'Combined effect of cypermethrin and copper on catalase activity in soil', *J Soils Sediments*, 8, pp. 327-332.
- Liu, X. and Kokare, C. (2017). 'Chapter 11 – Microbial Enzymes of use in Industry', in Brahmachari, G. (ed.) *Biotechnology of Microbial Enzymes*. Academic Press, pp. 267-298.
- Loginov, D. S., Vavilova, E. A., Savinova, O. S., Abyanova, A. R., Chulkin, A. M., Vasina, D. V., Zherdev, A. V. and Koroleva, O. V. 2014. 'Immunoassays of fungal laccases for screening of natural enzymes and control of recombinant enzyme production: Immunoassays of fungal laccases', *Biotechnology and Applied Biochemistry*, 61(2), pp. 230-236.
- Lo Leggio, L., Simmons, T. J., Poulsen, J. N., Frandsen, K. E. H., Hemsworth, G. R., Stringer, M. A., von Freiesleben, P., Tovborg, M., Johansen, K. S., De Maria, L., Harris, P. V., Soong, C., Dupree, P., Tryfona, T., Lenfant, N., Henriissat, B., Davies, G. J. and Walton, P. H. 2015. 'Structure and boosting activity of a starch-degrading lytic polysaccharide monooxygenase', *Nature Communications*, 6, p. 5961.
- Loose, J. S. M., Forsberg, Z., Fraaije, M. W., Eijsink, V. G. H. and Vaaje-Kolstad, G. 2014. 'A rapid quantitative activity assay shows that the *Vibrio cholera* colonization factor GbpA is an active lytic polysaccharide monooxygenase', *FEBS Letters*, 588(18), pp. 3435-3440.
- Martínez, A. T, Ruiz-Dueñas, F. J., Camarero, S., Serrano, A., Linde, D., Lund, H., Vind, J., Tovborg, M., Herold-Majumdar, O. M., Hofrichter, M., Liers, C., Ullrich, R., Scheibner, K., Sannia, G., Piscitelli, A., Pezzella, C., Sener, M. E., Kılıç, S., van Berkel, W. J. H., Guallar, V., Lucas, M. F., Zuhse, R., Ludwig, R., Hollmann, F., Fernández-Fueyo, E., Record, E., Faulds, C. B., Tortajada, M., Winkelmann, I., Rasmussen, J., Gelo-Pujic, M., Gutiérrez, A., del Río, J., Rencoret, J. and Alcalde, M. 2017. 'Oxidoreductases on their way to industrial biotransformations', *Biotechnology Advances*, 35(6), pp.815-831.
- Martins, D. and English, A. M. 2014. 'Catalase activity is stimulated by H₂O₂ in rich culture Medium and is required for H₂O₂ resistance and adaptation in yeast', *Redox Biology*, 2, pp. 308-313.
- May, S. W. and Padgett, S. R. 1983. 'Oxidoreductase enzymes in biotechnology: current status and future potential', *Nature Biotechnology*, 1(8), pp.677-686.
- Mayer, K. M. and Arnold, F. H. 2002. 'A colorimetric assay to quantify dehydrogenase activity in crude cell lysates', *Journal of Biomolecular Screening*, 7(2), pp. 135-140.
- Moreau, R. A. 1987. 'Calcium-binding proteins in fungi and higher plants', *Journal of Dairy Science*, 70(7), pp. 1504-1512.
- Nakamura, K. and Go, N. 2005. 'Function and molecular evolution of multicopper blue proteins', *Cellular and Molecular Life Sciences*, 62(18), pp. 2050-2066.

Megazyme (2019). *Catalase Assay Procedure*. [Online] Bray: Megazyme, pp. 1-2. Available at: https://www.megazyme.com/documents/Booklet/K-CATAL_DATA.pdf [Accessed 05 Dec. 2019].

Mina, S., Marot-Leblond, A., Cimon, B., Fleury, M. J. J., Larcher, G., Bouchara, J-P. and Robert, R. 2015. 'Purification and Characterisation of a Mycelial Catalase from *Scedosporium boydii*, a Useful Tool for Specific Antibody Detection in Patients with Cystic Fibrosis', *Clinical and Vaccine Immunology*, 22(1), pp. 37-45.

More, S. S., P. S. R., K. P., M. S., Malini, S. and S. M. V. 2011. 'Isolation, purification, and characterisation of fungal laccase from *Pleurotus* sp.', *Enzyme Research*, 2011, pp. 248735-248742.

Nekiunaite, L., Arntzen, M. O., Svensson, B., Vaaje-Kolstad, G. and Hagem, M. A. 2016. 'Lytic polysaccharide monooxygenases and other oxidative enzymes are abundantly secreted by *Aspergillus nidulans* grown on different starches', *Biotechnology for Biofuels*, 9(1), p. 187.

Nicholls, P., Fita, I. and Loewen, P. C. 2000. 'Enzymology and Structure of Catalases', *Advances in Inorganic Chemistry*, 51, pp. 51-106.

Nomenclature Committee of the International Union of Biochemistry and Molecular Biology (NC-IUBMB), 2010, *The Enzyme List Class 1 – Oxidoreductases*. Available at: <http://www.enzymedatabase.org/downloads/ec1.pdf> (Accessed: 01 January 2018).

Pardo, I., Chanagá, X., Vicente, A. I., Alcade, M. and Carero, S. 2013. 'New colorimetric screening assays for the directed evolution of fungal laccases to improve the conversion of plant biomass', *BMC Biotechnology*, 13(1), pp. 90-103.

Prajapati, S. C. and Chauhan, S. S. 2011. 'Dipeptidyl peptidase III: a multifaceted oligopeptide N-end cutter', *The FEBS Journal*, 278(18), pp. 3256-3276.

Qian, W., Yu, C., Qin, H., Liu, X., Zhang, A., Johansen, I. E. and Wang, D. 'Molecular and functional analysis of phosphomannomutase (PMM) from higher plants and genetic evidence for the involvement of PMM in ascorbic acid biosynthesis in *Arabidopsis* and *Nicotiana benthamiana*', *The Plant Journal*, 49(3), pp. 339-413.

Raveendran, S., Parameswaran, B., Ummalya, S. B., Abraham, A., Mathew, A. K., Madhavan, A., Rebello, S. and Pandey, A. 2018. 'Applications of microbial enzymes in food industry', *Food Technology & Biotechnology*, 56(1), pp. 16-30.

Richardson, G. H. (1975) 'Chapter 13 Dairy Industry', in Reed, G. (ed.) *Food Science and Technology A Series of Monographs*. 2nd edn. New York: Academic Press, Inc., pp. 361-396.

Riviera-Hoyos, C. M., Morales-Álvarez, E. D., Poutou-Piñales, R. A., Pedroza-Rodríguez, A. M., Rodríguez-Vázquez, R. and Delgado-Boada, J. M. 2013. 'Fungal laccases', *Fungal Biology Reviews*, 27(3-4), pp. 67-82.

Robinson, P. K. 2015. 'Enzymes: principles and biotechnological applications', *Essays in Biochemistry*, 59(0), pp.1-41.

Rodaki, A., Young, T. and Brown, A. J. P. 2006. 'Effects of depleting the essential central metabolic enzyme fructose-1,6-bisphosphate aldolase on the growth and viability of *Candida albicans*: Implications for antifungal drug target discovery', *Eukaryotic Cell*, 5(8), pp. 1371-1377.

Rodríguez-Delgado, M. M., Alemán-Nava, G. S., Rodríguez-Delgado, J. M., Dieck-Assad, G., Martínez-Chapa, S. O., Barceló, D. and Parra, R. 2015. 'Laccase-based biosensors for detection of phenolic compounds', *Trends in Analytical Chemistry*, 74, pp. 21-45.

Ruijter, G. J. G., Panneman, H., Xu, D-B. and Visser, J. 2000. 'Properties of *Aspergillus niger* citrate synthase and effects of *citA* overexpression on citric acid production', *FEMS Microbiology Letters*, 184(2000), pp. 35-40.

Sahay, R., Yadav, R. S. S. and Yadav, K. D. S. 2008. 'Purification and characterisation of extracellular laccase secreted by *Pleurotus sajor-caju* MTCC 141', *Chinese Journal of Biotechnology*, 24(12), pp. 2068-2073.

Sakamoto, T., Yao, Y., Hida, Y., Honda, Y., Watanabe, T., Hashigaya, W., Suzuki, K. and Irie, T. 2012. 'A calmodulin inhibitor, W-7 influences the effect of cyclic adenosine 3',5'-monophosphate signalling on ligninolytic enzyme gene expression in *Phanerochaete chrysosporium*', *AMB Express*, 2(7), pp. 1-9.

Shah, V., Jain, K., Desai, C. and Madamwar, D. (2012) 'Molecular analyses of microbial activities involved in bioremediation', in Satyanarayana, T. (ed.), Johri, B. N. (ed.), and Prakash, A. (ed.) *Microorganisms in Environmental Management: Microbes and Environment*. Springer Science and Business Media: India, pp. 221-247.

Sharma, I. and Ahmad, P. (2014). 'Chapter 4 - Catalase: A Versatile Antioxidant in Plants', in Ahmad, P. (ed.) *Oxidative Damage to Plants: Antioxidant Networks and Signaling*. San Diego: Academic Press, pp. 131-148.

Sharma, U., Pal, D. and Prasad, R. 2014. 'Alkaline phosphatase: An overview', *Indian Journal of Clinical Biochemistry*, 29(3), pp. 269-278.

Sigma-Aldrich, 2018. Available at:

https://www.sigmaaldrich.com/catalog/product/sigma/c7752?lang=en®ion=US&gclid=EA1aIQobChMIwuqAn_mt3AIVSrfCh1iGAiZEAMYASAAEgIyvvd_BwE (Accessed: 21 December 2018).

Sygmund, C., Santner, P., Krondorfer, I., Peterbauer, C. K., Alcalde, M., Nyanhongo, G. S., Guebitz, G. M. and Ludwig, R. 2013. 'Semi-rational engineering of cellobiose dehydrogenase for improved hydrogen peroxide production', *Microbial Cell Factories*, 12(1), p.38.

The Enzyme List Class 1 – Oxidoreductases (2010) Available at: <http://www.enzyme-database.org/downloads/ec1.pdf> (Accessed: 10 July 2018).

Trawczyńska, I. and Wójcik, M. 2015. 'Optimization of permeabilization process of yeast cells for catalase activity using response surface methodology', *Biotechnology, Biotechnological Equipment*, 29(1), pp. 72-77.

Tudzynski, B. 2014. 'Nitrogen regulation of fungal secondary metabolism in fungi', *Front Microbiology*, 5, pp.1-15.

Upadhyay, S. and Shaw, B. D. 2008. 'The role of actin, fimbrin and endocytosis in growth of hyphae in *Aspergillus nidulans*', *Molecular Microbiology*, 68(3), pp. 690-705.

Upadhyay, P., Shrivastava, R. and Agrawal, P. K. 2016. 'Bioprospecting and biotechnological applications of fungal laccases', *3 Biotech*, 6(1), p.15.

- Vaaje-Kolstad, G., Westereng, B., Horn, S. J., Liu, Z., Zhai, H., Sørli, M. and Eijsink, V. G. H. 2010. 'An oxidative enzyme boosting the enzymatic conversion of recalcitrant polysaccharides', *Science*, 330(6001), pp. 219-222.
- Valle, J. S., Vandenberghe, L. P. S., Santana, T. T., Almeida, P. H., Pereira, A. M., Linde, G. A., Colauto, N. B. and Soccol, C. R. 2014. 'Optimum conditions for inducing laccase production in *Lentinus crinitus*', *Genetics and Molecular Research*, 13(4), pp.8544-8551.
- VanderJagt, D. J., Garry, P. J. and Hunt, W. C. 1986. 'Ascorbate in plasma measured by liquid chromatography and by dichlorophenolindophenol colorimetry', *Clinical Chemistry*, 32(6), pp. 1004-1006.
- Vatsyayan, P. and Goswami, P. 2016. 'Highly active and stable large catalase isolated from a hydrocarbon degrading *Aspergillus terreus* MTCC 6324', *Enzyme Research*, 2016, pp. 1-8.
- Vemuluri, V. R., Shaw, S., Autenrieth, C. and Ghosh, R. 2017. 'A rapid procedure for the *in situ* assay of periplasmic, PQQ-dependent methanol dehydrogenase in intact single bacterial colonies', *Journal of Microbiological Methods*, 137, pp. 46-49.
- Villares, A., Moreau, C., Bennati-Granier, C., Garajova, S., Foucat, L., Falourd, X., Saake, B., Berrin, J. and Cathala, B. 2017. 'Lytic polysaccharide monooxygenases disrupt the cellulose fibers structure', *Scientific Reports*, 7, p.40262.
- Viswanath, B., Rajesh, B., Janardhan, A., Kumar, A. P. and Narasimha, G. 2014. 'Fungal laccases and their applications in bioremediation', *Enzyme Research*, 2014, pp. 1-21.
- Vrsanska, M., Voberkova, S., Langer, V., Palovcikova, D., Moulick, A., Adam, V. and Kopel, P. 2016. 'Induction of laccase lignin peroxidase and manganese peroxidase activities in white-rot fungi using copper complexes', *Molecules*, 21(11), pp. 1553.
- Wang, Q., Ding, L. and Zhu, C. 2018d. 'Characterization of laccase from a novel isolated white-rot fungi *Trametes* sp. MA-X01 and its potential application in dye decolorization', *Biotechnology & Biotechnological Equipment*, 32(6), pp. 1477-1485.
- Wang, T., Xiang, Y., Liu, X., Chen, W. and Hu, Y. 2017a. 'A novel fluorimetric method for laccase activities measurement using Amplex Red as substrate', *Talanta*, 162, pp. 143-150.
- Wang, X., Saba, T., Yiu, H. H. P., Howe, R. F., Anderson, J. A. and Shi, J. 2017b. 'Cofactor NAD(P)H regeneration inspired by heterogeneous pathways', *Chem*, 2(5), pp. 621-654.
- Wang, Y., Wang, S., Nie, X., Yang, K., Xu, P., Wang, X., Liu, M., Yang, Y., Chen, Z. and Wang, S. 2019c. 'Molecular and structural basis of nucleoside diphosphate kinase-mediated regulation of spore and sclerotia development in the fungus *Aspergillus flavus*', *The Journal of Biological Chemistry*, 294(33), pp. 12415-12431.
- Wierenga, R. K. 2001. 'The TIM-barrel fold: a versatile framework for efficient enzymes', *FEBS Letters*, 492(3), pp. 193-198.
- Wong, C. M., Wong, K. H. and Chen, X. D. 'Glucose oxidase: natural occurrence, function, properties and industrial applications', *Applied Microbiology and Biotechnology*, 78(6), pp. 927-938.
- Yordanova, E. 1974. 'In vitro and In vivo inhibitory effect of copper sulphate upon the activity of blood catalase', *Scripta Scientifica Medica*, 11, pp. 97-103.

Yu, H., Rao, X. and Zhang, K. 2017. 'Nucleoside diphosphate kinase (Ndk): A pleiotropic effector manipulating bacterial virulence and adaptive responses', *Microbiological Research*, 205, pp. 125-134.

Zhang, M., Smith, A. and Gorski, W. 2004. 'Carbon nanotube-chitosan system for electrochemical sensing based on dehydrogenase enzymes', *Analytical Chemistry*, 76(17), pp.5045-5050.

9.0 Appendix

Table 9. 1: A Table showing the raw data for the protein concentration at 0 hours for Shake Flasks 1A, 1B, 1C, and 1D (Table 4.4.1)

Original Plate Data	1	2	3	4	5	6	7	8	9	10	11	12
A	0.77	0.77	0.74	0.80	0.05	0.05	0.05	0.05	0.39	0.39	0.39	0.39
B	0.74	0.76	0.74	0.77	0.05	0.05	0.05	0.05	0.51	0.53	0.52	0.51
C	0.75	0.76	0.76	0.80	0.05	0.05	0.05	0.05	0.62	0.62	0.62	0.60
D	0.74	0.74	0.73	0.77	0.05	0.05	0.05	0.05	0.76	0.78	0.79	0.76
E	0.05	0.05	0.05	0.05	0.05	0.05	0.65	0.99	0.90	0.97	0.97	0.97
F	0.05	0.05	0.05	0.05	0.05	0.05	0.63	0.98	1.15	1.17	1.20	1.15
G	0.05	0.05	0.05	0.05	0.05	0.05	0.62	0.95	0.05	0.05	0.05	0.05
H	0.05	0.05	0.05	0.05	0.05	0.05	0.62	0.94	0.05	0.05	0.05	0.05

Table 9. 2: A Table showing the raw data for the protein concentration at 24 hours for Shake Flasks 1A, 1B, 1C, and 1D (Table 4.4.1)

Original Plate Data	1	2	3	4	5	6	7	8	9	10	11	12
A	0.59	0.73	0.66	0.63	0.05	0.05	0.05	0.05	0.37	0.38	0.38	0.38
B	0.62	0.71	0.67	0.64	0.05	0.05	0.05	0.05	0.49	0.51	0.50	0.50
C	0.61	0.70	0.65	0.63	0.05	0.05	0.05	0.05	0.57	0.59	0.58	0.56
D	0.61	0.67	0.66	0.62	0.05	0.05	0.05	0.05	0.68	0.75	0.73	0.69
E	0.05	0.05	0.05	0.05	0.05	0.05	0.60	0.99	0.90	0.96	0.96	0.88
F	0.05	0.05	0.05	0.05	0.05	0.05	0.61	1.01	1.11	1.16	1.16	1.12
G	0.05	0.05	0.05	0.05	0.05	0.05	0.61	0.98	0.05	0.05	0.05	0.05
H	0.05	0.05	0.05	0.05	0.05	0.05	0.60	1.00	0.05	0.05	0.05	0.05

Table 9. 3: A Table showing the raw data for the protein concentration at 96 hours for Shake Flasks 1A, 1B, 1C, and 1D (Table 4.4.1)

Original Plate Data	1	2	3	4	5	6	7	8	9	10	11	12
A	0.64	0.62	0.67	0.60	0.05	0.05	0.05	0.05	0.40	0.40	0.40	0.40
B	0.65	0.61	0.66	0.62	0.05	0.05	0.05	0.05	0.51	0.52	0.51	0.50
C	0.65	0.62	0.67	0.61	0.05	0.05	0.05	0.05	0.61	0.61	0.60	0.61
D	0.64	0.60	0.66	0.60	0.05	0.05	0.05	0.05	0.73	0.77	0.76	0.74
E	0.05	0.05	0.05	0.05	0.05	0.05	0.65	1.03	0.98	0.95	0.93	0.96
F	0.05	0.05	0.05	0.05	0.05	0.05	0.64	1.00	1.07	1.16	1.16	1.15
G	0.05	0.05	0.05	0.05	0.05	0.05	0.62	0.98	0.05	0.05	0.05	0.05
H	0.05	0.05	0.05	0.05	0.05	0.05	0.65	0.96	0.05	0.05	0.05	0.05

Table 9. 4: A Table showing the raw data for the protein concentration at 120 hours for Shake Flasks 1A, 1B, and 1D (Table 4.4.1)

Original Plate Data	1	2	3	4	5	6	7	8	9	10	11	12
A	0.66	0.68	0.69	0.05	0.05	0.05	0.05	0.05	0.39	0.39	0.39	0.39
B	0.69	0.71	0.73	0.05	0.05	0.05	0.05	0.05	0.51	0.51	0.52	0.51
C	0.67	0.68	0.70	0.05	0.05	0.05	0.05	0.05	0.60	0.60	0.60	0.59
D	0.66	0.70	0.65	0.05	0.05	0.05	0.05	0.05	0.78	0.75	0.75	0.71
E	0.05	0.05	0.05	0.05	0.05	0.05	0.61	1.03	0.99	0.97	0.96	0.87
F	0.05	0.05	0.05	0.05	0.05	0.05	0.62	1.01	1.05	1.17	1.12	1.14
G	0.05	0.05	0.05	0.05	0.05	0.05	0.61	0.95	0.05	0.05	0.05	0.05
H	0.05	0.05	0.05	0.05	0.06	0.05	0.60	0.94	0.05	0.05	0.05	0.05

Table 9. 5: A Table showing the raw data for the protein concentration at 0 hours for Shake Flasks 2A, 2B, 2C, and 2D (Table 4.4.2)

Original Plate Data	1	2	3	4	5	6	7	8	9	10	11	12
A	0.05	0.76	0.65	0.65	0.65	0.05	0.05	0.05	0.38	0.38	0.38	0.38
B	0.05	0.71	0.66	0.62	0.64	0.05	0.05	0.05	0.51	0.51	0.51	0.50
C	0.05	0.70	0.67	0.63	0.64	0.05	0.05	0.05	0.58	0.62	0.60	0.61
D	0.05	0.67	0.64	0.58	0.59	0.05	0.05	0.05	0.80	0.79	0.77	0.74
E	0.05	0.05	0.05	0.05	0.05	0.05	0.66	1.09	0.99	0.97	0.99	0.97
F	0.05	0.05	0.05	0.05	0.05	0.05	0.65	1.03	0.92	1.19	1.18	1.15
G	0.05	0.05	0.05	0.05	0.05	0.05	0.66	1.03	0.05	0.05	0.05	0.05
H	0.05	0.05	0.05	0.05	0.05	0.05	0.63	0.98	0.05	0.05	0.05	0.05

Table 9. 6: A Table showing the raw data for the protein concentration at 96 hours and 120 hours for Shake Flasks 2A, 2B, 2C, and 2D (Table 4.4.2)

Original Plate Data	1	2	3	4	5	6	7	8	9	10	11	12
A	0.05	0.59	0.51	0.60	0.63	0.05	0.05	0.05	0.39	0.39	0.39	0.38
B	0.05	0.58	0.50	0.56	0.64	0.05	0.05	0.05	0.49	0.50	0.50	0.49
C	0.05	0.59	0.50	0.56	0.64	0.05	0.05	0.05	0.57	0.59	0.60	0.57
D	0.05	0.58	0.50	0.60	0.63	0.05	0.05	0.05	0.68	0.73	0.74	0.71
E	0.05	0.57	0.48	0.64	0.66	0.05	0.62	0.98	0.85	0.94	0.94	0.93
F	0.05	0.60	0.48	0.62	0.66	0.05	0.60	1.00	1.25	1.17	1.23	1.12
G	0.05	0.59	0.47	0.64	0.65	0.05	0.61	0.98	0.05	0.05	0.05	0.05
H	0.05	0.58	0.47	0.63	0.64	0.05	0.61	0.95	0.05	0.05	0.05	0.05

Table 9. 7: A Table showing the raw data for the protein concentration at 144 hours for Shake Flasks 2A, 2B, 2C, and 2D (Table 4.4.2)

Original Plate Data	1	2	3	4	5	6	7	8	9	10	11	12
A	0.05	0.57	0.44	0.65	0.66	0.06	0.05	0.05	0.39	0.38	0.39	0.39
B	0.05	0.59	0.46	0.64	0.66	0.05	0.05	0.05	0.51	0.51	0.50	0.50
C	0.05	0.57	0.46	0.63	0.66	0.05	0.05	0.05	0.60	0.60	0.59	0.57
D	0.05	0.56	0.45	0.62	0.63	0.05	0.05	0.05	0.73	0.77	0.76	0.71
E	0.05	0.05	0.05	0.05	0.05	0.05	0.66	0.82	0.93	0.98	0.98	0.91
F	0.05	0.05	0.05	0.05	0.05	0.05	0.64	1.03	1.10	1.17	1.16	1.15
G	0.05	0.05	0.05	0.05	0.05	0.05	0.65	1.02	0.05	0.05	0.05	0.05
H	0.05	0.05	0.05	0.05	0.05	0.05	0.61	1.02	0.05	0.05	0.05	0.05

Table 9. 8: A Table showing the raw data for the protein concentration at 0 hours and 96 hours for Shake Flasks 3A, 3B, 3C, 3D, and 3E (Table 4.4.3)

Original Plate Data	1	2	3	4	5	6	7	8	9	10	11	12
A	0.62	0.63	0.66	0.63	0.62	0.64	0.37	0.37	0.38	0.38	0.37	0.38
B	0.63	0.62	0.64	0.62	0.61	0.67	0.37	0.37	0.50	0.51	0.51	0.50
C	0.62	0.62	0.64	0.62	0.61	0.64	0.37	0.37	0.61	0.61	0.60	0.60
D	0.61	0.61	0.63	0.62	0.61	0.63	0.37	0.37	0.75	0.77	0.76	0.77
E	0.64	0.58	0.59	0.58	0.58	0.37	0.67	1.14	0.97	0.97	0.96	0.96
F	0.63	0.56	0.56	0.56	0.57	0.37	0.62	1.04	1.14	1.19	1.18	1.15
G	0.62	0.58	0.58	0.57	0.57	0.36	0.62	1.00	0.36	0.37	0.37	0.37
H	0.62	0.57	0.58	0.56	0.58	0.36	0.60	0.97	0.37	0.38	0.37	0.37

Table 9. 9: A Table showing the raw data for the protein concentration at 120 hours for Shake Flasks 3A, 3B, 3C, 3D, and 3E (Table 4.4.3)

Original Plate Data	1	2	3	4	5	6	7	8	9	10	11	12
A	0.72	0.67	0.70	0.70	0.67	0.05	0.05	0.05	0.39	0.38	0.38	0.39
B	0.69	0.66	0.69	0.67	0.68	0.05	0.05	0.05	0.51	0.52	0.51	0.51
C	0.67	0.68	0.69	0.68	0.67	0.05	0.05	0.05	0.59	0.60	0.61	0.60
D	0.67	0.65	0.69	0.69	0.66	0.05	0.05	0.05	0.78	0.77	0.78	0.72
E	0.05	0.05	0.05	0.05	0.05	0.05	0.63	1.00	0.93	0.96	0.98	0.94
F	0.05	0.05	0.05	0.05	0.05	0.05	0.63	1.02	1.06	1.19	1.16	1.11
G	0.05	0.05	0.05	0.05	0.05	0.05	0.62	1.02	0.05	0.05	0.05	0.05
H	0.05	0.05	0.05	0.05	0.05	0.05	0.61	1.00	0.05	0.05	0.05	0.05

Table 9. 10: A Table showing the raw data for the protein concentration at 144 hours for Shake Flasks 3A, 3B, 3C, 3C, and 3E (Table 4.4.3)

Original Plate Data	1	2	3	4	5	6	7	8	9	10	11	12
A	0.56	0.56	0.57	0.58	0.53	0.05	0.05	0.05	0.37	0.37	0.37	0.38
B	0.57	0.56	0.59	0.57	0.53	0.05	0.05	0.05	0.50	0.51	0.51	0.49
C	0.57	0.55	0.57	0.56	0.52	0.05	0.05	0.05	0.59	0.59	0.60	0.59
D	0.57	0.54	0.58	0.57	0.52	0.05	0.05	0.05	0.75	0.77	0.79	0.74
E	0.05	0.05	0.05	0.05	0.05	0.05	0.63	1.01	0.99	0.99	0.97	0.96
F	0.05	0.05	0.05	0.05	0.05	0.05	0.65	1.02	1.02	1.15	1.16	1.16
G	0.05	0.05	0.05	0.05	0.05	0.05	0.63	1.02	0.05	0.05	0.05	0.05
H	0.05	0.05	0.05	0.05	0.05	0.05	0.61	0.98	0.05	0.05	0.05	0.05